Natural Resources Canada | Ressources naturelles Canada

GEOLOGICAL SURVEY OF CANADA
OPEN FILE 8615

Geochronology of the Klaza River area, Yukon

N.L. Joyce, P. Iraheta Muniz, D.A. Kellett, N.M. Rayner, and J.J. Ryan

2022

Canada

GEOLOGICAL SURVEY OF CANADA
OPEN FILE 8615

Geochronology of the Klaza River area, Yukon

N.L. Joyce[1], P. Iraheta Muniz[2], D.A. Kellett[3], N.M. Rayner[1], and J.J. Ryan[4]

[1]Geological Survey of Canada, 601 Booth Street, Ottawa, Ontario
[2]McIntosh Perry Consulting Engineers Ltd., 115 Walgreen Road, Carp, Ontario
[3]Geological Survey of Canada, 1 Challenger Drive, P.O. Box 1006, Dartmouth, Nova Scotia
[4]Geological Survey of Canada, 1500-605 Robson Street, Vancouver, British Columbia

2022

Permanent link: https://doi.org/10.4095/321893

This publication is available for free download through GEOSCAN (https://geoscan.nrcan.gc.ca/).

Recommended citation
Joyce, N.L., Iraheta Muniz, P., Kellett, D.A., Rayner, N.M., and Ryan, J.J., 2022. Geochronology of the Klaza River area, Yukon; Geological Survey of Canada, Open File 8615, 1 .zip file. https://doi.org/10.4095/321893

Publications in this series have not been edited; they are released as submitted by the author.

CONTENTS

INTRODUCTION

This multicomponent Open File presents zircon U-Pb results for 10 rock samples and hornblende, muscovite and biotite $^{40}Ar/^{39}Ar$ results for 16 rock samples from select units in west central Yukon, Canada (Figure 1). Most samples come from the Klaza River area, with an additional few samples from along the Yukon River and Ladue River to the northwest of the Klaza area (Table 1, Figures 1 and 2). This analytical work was conducted as part of the Crustal Blocks activity of the Geomapping for Energy and Minerals (GEM) Cordillera Project of the Geological Survey of Canada, in large part to support the geological mapping in the Klaza River area, and enhance our understanding of the tectonic and metamorphic evolution of Yukon-Tanana terrane (YTT), mafic-ultramafic complexes, and the younger successor rocks built upon them in west-central Yukon. Bedrock geology of the Klaza River area consists primarily of a central domain of metamorphosed and poly-deformed Paleozoic basement that was intruded and overlain by relatively little-deformed Mesozoic and Cenozoic intrusive rocks and sedimentary successions. More detailed information on the geology of the area can be found in Ryan et al. (2018). The Klaza River mapping and geochronology complements the neighbouring study in the Mount Nansen-Nisling River area (Ryan et al., 2016; Joyce et al., 2020).

In this report, a one-page (in most cases) summary for each sample is provided, including sample information, representative transmitted light and back-scattered electron (BSE)/cathodoluminescence (CL) images of zircon (for U-Pb samples), U-Pb or $^{40}Ar/^{39}Ar$ results, data plots, and data interpretations are shown for each zircon sample. U-Pb detrital zircon results are plotted on Concordia and combined histogram/probability density diagrams, whereas U-Pb igneous/metamorphic zircon results are plotted only using Concordia diagrams. $^{40}Ar/^{39}Ar$ hornblende, muscovite and biotite data are presented in step heat spectrum plots, and inverse isochron diagrams where appropriate. The results and age interpretations for all samples presented are summarized in Table 1 (of8615_Table 1.xlsx). The full U-Pb and $^{40}Ar/^{39}Ar$ datasets are provided as separate Microsoft Excel files in Appendices A and B, respectively. Adobe PDF files for each U-Pb zircon sample containing BSE and CL images for all mounted zircon grains are provided in Appendix C. Grains are numbered and correspond to analysis spot names; the locations of SHRIMP (Sensitive High Resolution Ion Microprobe) analytical spots are depicted by ellipses.

REGIONAL GEOLOGICAL FRAMEWORK

Yukon-Tanana Terrane

The central part of the Klaza River area (Figure 2) is dominantly underlain by the polydeformed and metamorphosed rocks of YTT, dominated by Snowcap assemblage, which is constrained to upper Devonian to lower Paleozoic. The Snowcap assemblage is characterized by amphibolite-facies quartzite, micaceous quartzite, and psammitic quartz-muscovite-biotite (±garnet) schist, large domains of amphibolite, and rare, decametre-thick lenses of marble. The amphibolite units, with lesser garnet amphibolite, are commonly massive, and are interpreted as metamorphosed mafic sills and dykes. In the neighbouring Mount Nansen–Nisling River area to the east, Ryan et al. (2016) attributed most amphibolite units there, which had apparent spatial association with the Devono-Mississippian Simpson Range intrusive suite, to the Devono-Mississippian Finlayson assemblage. However, no Simpson Range suite intrusions were identified in the Klaza River map area, and all amphibolite units there are attributed to the Snowcap assemblage.

The westernmost side of the Klaza River study area (Figure 2) hosts quartzite, psammite, and phyllite of the Stevenson Ridge schist of Ryan et al. (2014). This unit is regionally correlated with a carbonaceous siliciclastic member of the upper Devonian-Mississippian Finlayson assemblage. In the east-central part of the area, Snowcap assemblage rocks are intruded by scattered bodies of variably foliated K-feldspar-porphyritic to porphyroclastic augen granite. Medium-grained, non-porphyritic monzogranite to syenogranite that are similar in appearance to the Mississippian Simpson Range suite intrude the Snowcap assemblage, however these are demonstrated in this study to be part of the Permian Sulphur Creek suite, the plutonic portion of the Middle to Late Permian (269-253 Ma) Klondike assemblage (e.g. Mortensen, 1992).

Mafic-ultramafic complexes

The Schist Creek mafic-ultramafic complex occurs in the southeast part of the map area and is dominated by serpentinite and peridotite with minor metagabbro. The complex appears to be in structural contact with the surrounding Snowcap assemblage. The serpentinite has a predominantly harzburgitic protolith, indicated by high-temperature deformed orthopyroxene porphyroclasts and aligned olivine, suggesting that it originated as lithospheric mantle (Dubman, 2016). The serpentinite is intruded by plagioclase-porphyritic metagabbro dykes that yield Late Permian ages (W. McClelland, unpublished data, 2016). Other minor lenses (10 to 100 m wide) of serpentinite, talc-tremolite schist, and listwaenite may be related to the Schist Creek complex, and occur along the trace of the Schist Creek fault (Figure 2). The above mentioned Permian Sulphur Creek suite occurs on the northwest side of the fault, whereas the Mississippian Simpson Range suite occurs only on the southeast side of the fault (Ryan et al., 2016).

Mesozoic-Cenozoic rocks

Middle Cretaceous to Eocene magmatic rocks are common in the study area. The northern part of the map area is underlain by numerous occurrences of well-preserved mid-Cretaceous aphyric and feldspar-hornblende phyric andesite to dacite breccias, flows, and tuffaceous rocks of the Mount Nansen group, which has yielded U-Pb ages ranging between 110 and 105 Ma (Klocking et al., 2016). Heterolithic quartz and feldspar-phyric felsic lapilli tuff, and rare flow-banded quartz-phyric rhyolite are less abundant.

The middle Cretaceous Whitehorse plutonic suite is represented by two distinct phases in the map area. The voluminous Dawson Range phase, which has yielded U-Pb ages ranging between 108–105 Ma (Mortensen et al., 2003, 2016; Klocking et al., 2016), dominates the northern part of the map area, and is composed of white to beige, hornblende-biotite granodiorite and lesser granite, tonalite, quartz diorite, and diorite. The unit characteristically has blocky hornblende phenocrysts, is medium to coarse grained, and weakly foliated to unfoliated. The southern portion of the map hosts the easternmost occurrences of the Maloney Creek phase of the Whitehorse plutonic suite, and comprises grey to beige biotite-hornblende monzogranite to granodiorite. This phase is medium to coarse grained, unfoliated, and smoky quartz-bearing. The Maloney Creek phase has yielded U-Pb and $^{40}Ar/^{39}Ar$ ages of ca. 105 Ma (W. McClelland, unpublished data 2016), indicating that the suite is the same age as the Dawson Range phase. Similar crystallization ages presented in this study demonstrate that the Mount Nansen volcanic rocks and the Whitehorse plutonic suite are comagmatic.

The Late Cretaceous Casino suite is represented in the southeast part of the area by small scattered occurrences of porphyritic dacite to rhyolite. It is generally fine to medium grained, and alkali-feldspar-, plagioclase-, biotite- and quartz-porphyritic, with local flow banding. A sample from the Casino suite just to the east of the Klaza River map area yielded a U-Pb crystallization age of ca. 74 +/- 0.7 Ma (Joyce et al., 2020).

The Late Cretaceous Carmacks group (71 to 68 Ma; Grond et al., 1984) is prevalent in the northern third of the map area. It comprises a mafic, flow-dominated upper sequence, and an intermediate to mafic volcanic and volcaniclastic lower sequence. The Carmacks group has a strong aeromagnetic expression. No samples were collected for dating in this study.

The Paleogene Rhyolite Creek complex (57 to 54 Ma; J. Crowley, unpublished data 2011) occurs as small erosional remnants of felsic and intermediate volcanic and hypabyssal rocks sparsely dotted across the map area. The felsic rocks are predominant and comprise smoky quartz ± feldspar porphyritic, and locally flow-banded tan to cream rhyolite to rhyodacite dykes, flows, sills, and crystal and ash tuff. The dykes generally form a north-trending swarm.

The Ruby Range suite (ca. 64 to 57 Ma; Israel et al., 2011) is characterized by fine- to medium-grained, unfoliated light grey to pinkish biotite ± hornblende granodiorite with typical smoky grey quartz, and partly overlaps in age with the Rhyolite Creek complex. Hypabyssal varieties of this suite dominate the Mount Pattison complex in the western part of the map area, where they exhibit common miarolitic cavities with vuggy grey quartz, and are transitional in composition with the Rhyolite Creek complex.

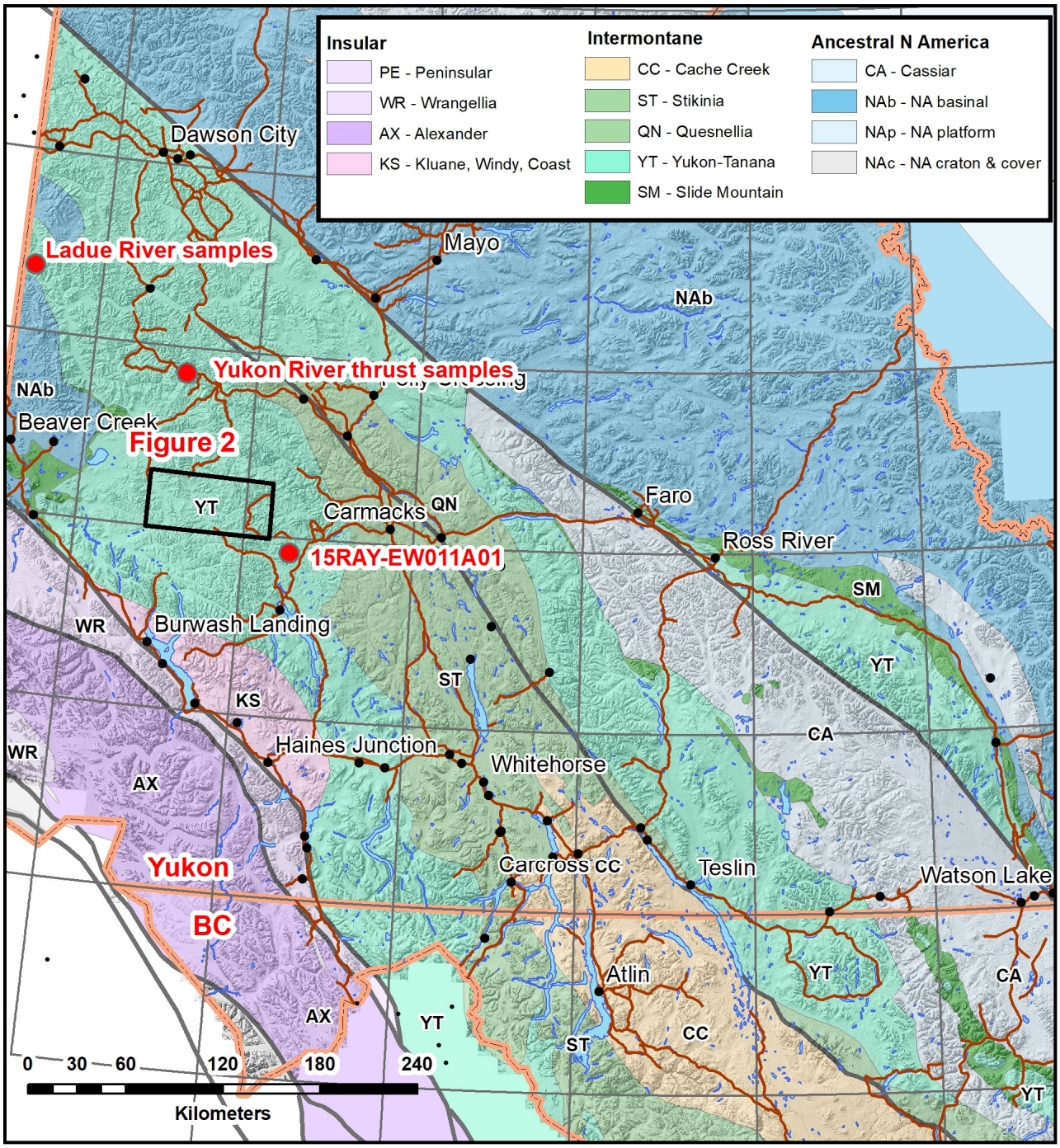

Figure 1: *A simplified terrane map of the Northern Canadian Cordillera (modified from Colpron and Nelson, 2011) showing the location of the Klaza River map area (black outline, labelled Figure 2). Also shown with red dots are the locations of the Ladue River and Yukon River thrust samples, as well as sample 15RAY-EW011A01.*

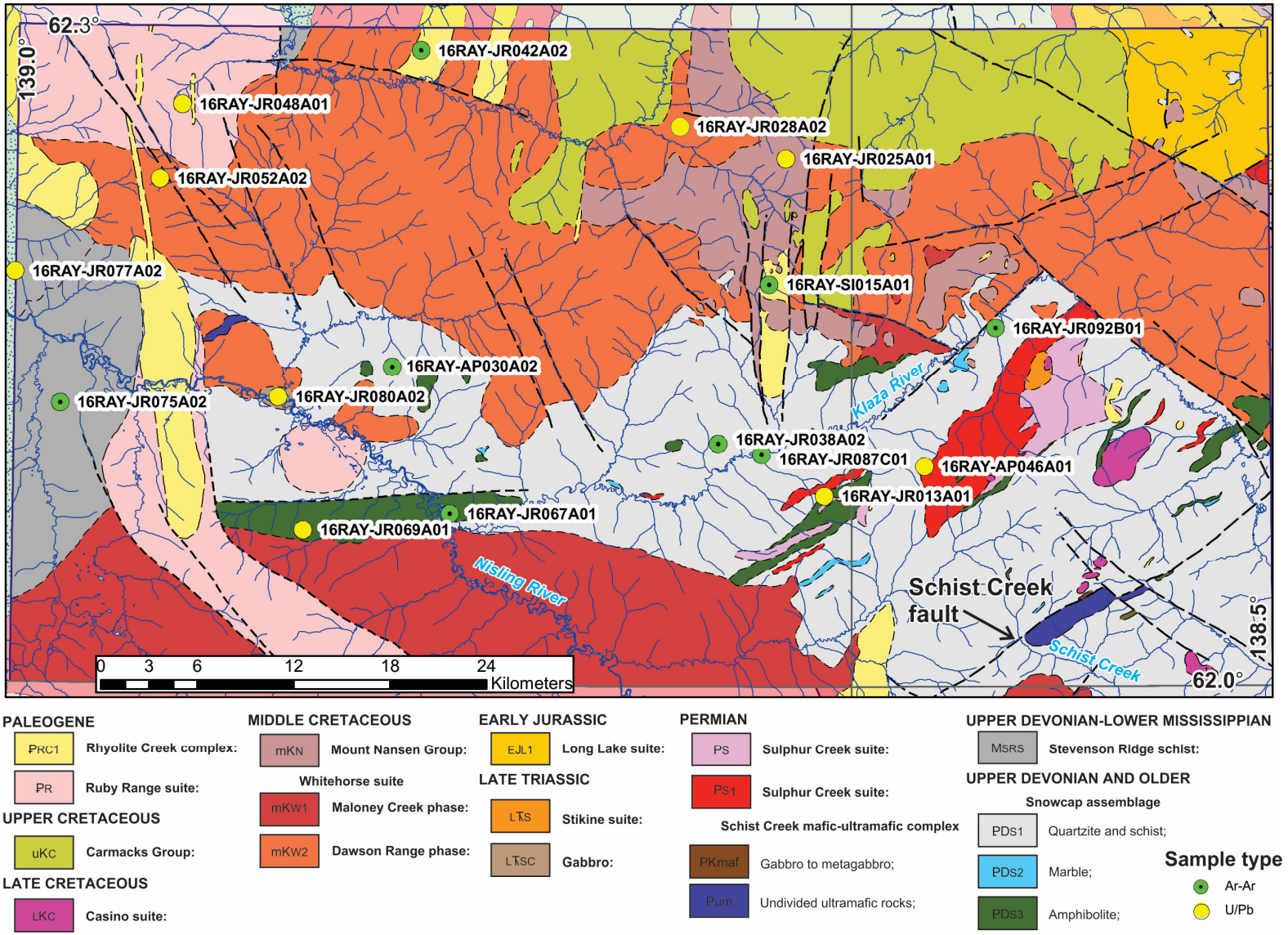

Figure 2: *Geology map of the Klaza River area modified from Ryan et al. (2018), with the location of geochronology samples (green and yellow dots).*

U-Pb ANALYTICAL METHODS

All samples were disaggregated using standard crushing/pulverizing techniques followed by density separation using a Wilfley table and heavy liquids. A Frantz™ Magnetic Separator was used to isolate a zircon-rich non-magnetic separate.

SHRIMP analytical procedures followed those described by Stern (1997), with standards and U-Pb calibration methods following Stern and Amelin (2003). Briefly, zircon grains were cast in 2.5 cm diameter epoxy mounts (GSC #844, 859, 871, 906, and 908) along with fragments of GSC laboratory reference zircon (z6266, with $^{206}Pb/^{238}U$ age = 559 Ma or z10493 with $^{206}Pb/^{238}U$ age = 416.8 ± 0.33 Ma (Temora2 zircon, Black et al., 2004)). The mid-sections of the zircon grains were exposed using 9, 6, and 1 μm diamond compound, and the internal features of the grains (such as zoning, structures, alteration, etc.) were characterized in back-scattered electron mode (BSE) and/or cathodoluminescence mode (CL) utilizing a Zeiss Evo 50 scanning electron microscope (Appendix D). On the mass spectrometer, eleven masses including background were sequentially measured with a single electron multiplier. Off-line data processing was accomplished using SQUID2 (version 2.50.11.10.15, rev. 15 Oct 2011). The 1σ external errors of $^{206}Pb/^{238}U$ ratios reported in Appendix A incorporate the ±1% error the standard zircon (see Stern and Amelin, 2003). Common Pb correction utilized the Pb composition of the surface blank (Stern, 1997). Details of each analytical session, including spot size, number of scans, primary reference material used, and calibration error, are given in the footnotes of Appendix A.

Analyses of secondary zircon reference materials were interspersed between sample analyses to verify the accuracy of the U-Pb calibration. The measured $^{206}Pb/^{238}U$ ages of the secondary reference materials are reported for each session in the footnote of Appendix A for comparison against their published, accepted ages.

Isoplot v. 4.15 (Ludwig, 2003) was used to calculate weighted mean ages and Concordia ages (including its 2σ error, MSWD, and probability of concordance), as well as to generate Concordia plots, histogram/probability density plots, and weighted average plots. The error ellipses on the Concordia diagrams and the weighted mean errors are reported at the 95% confidence level. All weighted mean U-Pb ages reported are corrected for common Pb by the ^{204}Pb method. An evaluation of the long term reproducibility of $^{206}Pb/^{238}U$ age of secondary standard 9910 indicates that the minimum reproducibility precision of SHRIMP ion probe weighted mean results is 1% (2σ, based on 51 analytical sessions, B. Davis pers. comm). In cases where the precision of the weighted mean age calculation for individual samples falls below this threshold, the weighted mean 2σ error is augmented to 1%.

There are many ways to determine the maximum depositional age of a sample based on a population of detrital zircon U-Pb ages (e.g. Dickinson and Gehrels, 2009). For the purpose of this report we utilize the youngest population mode (Dickinson and Gehrels 2009).

$^{40}Ar/^{39}Ar$ ANALYTICAL METHODS

Each sample was crushed using a ceramic mortar and pestle. The highest quality mineral grains were picked under the optical microscope from the 250-500 μm fraction and then packed into aluminum foil packets and arranged in 35 mm-long vertical tubes. Several flux monitor grains of Fish Canyon tuff sanidine (FCT-SAN) (28.201 ±0.023 Ma; 1σ, Kuiper et al., 2008)) were loaded into each sample packet. J values were interpolated for samples situated between the spaced FCT-SAN monitor grains. GA 1550 biotite (99.77 ± 0.11 1σ Ma, normalized to FCT-SAN at 28.201 ± 0.023 1σ Ma) was used as a secondary reference material to confirm the accuracy of the interpolations (Renne et al., 2010). The prepared can

was irradiated for 160 MWH in medium flux position 8B at the research nuclear reactor of McMaster University (MNR) in Hamilton, Ontario, Canada. Neutron fluence was ~0.9 x 10^{13} neutrons/cm^2 operating at a 2.5 MW power level. Correction factors for interference species produced by thermal neutrons during irradiation are included in the footnote of Appendix B.

The $^{40}Ar/^{39}Ar$ analyses were conducted at the Noble Gas Laboratory at the Geological Survey of Canada in Ottawa (Canada). Individual grains were loaded into a copper sample holder placed into a CO_2 laser source chamber under ultrahigh vacuum. A Photon Machines, Inc. Fusions 10.6 55 W CO_2 laser equipped with a beam-homogenizing lens was used to heat each grain for at least 30 seconds per step, and laser power was increased incrementally for each subsequent step. Heating schedules ranged from 0.1 to 7 W and were adjusted with the aim of releasing near equal volumes of ^{39}Ar among heating steps.

The gas released during each incremental heating step was cleaned for 1-4 minutes using two SAES™ NP-10 getters held at ~400°C, and a room temperature getter containing HY-STOR® 201 calcium-nickel alloy pellets. The gas was then admitted to a Nu Instruments Limited Noblesse magnetic sector multicollector noble gas mass spectrometer. The Nu Noblesse is a single-focusing, Nier-source, magnetic sector multicollector noble gas spectrometer equipped with two quadrupole lens arrays. Ar ions were measured with a fixed array of three ETP® discrete dynode ion-counting multipliers. Data collection followed the measurement scheme 'MC-Y' detailed in Kellett and Joyce (2014). Blanks were run every 5th analysis, in an identical manner to unknowns. Air shots were analyzed every 10th analysis to monitor efficiency and mass fractionation. Full results including background measurements are included in Appendix B. Sensitivity of the Nu Noblesse at the time of analyses was 7.1-7.5 Amps/mol. Data collection, reduction, error propagation, age calculation and plotting were performed using the software MassSpec (version 7.93) (Deino, 2001). Thorough descriptions of laboratory procedures, instrument specifications, data collection, and correction factors are provided in Kellett and Joyce (2014).

All ages presented here (with the exception of inverse isochron ages with free-floating intercepts) were calculated using an assumed $^{40}Ar/^{36}Ar$ ratio of 298.56 for atmospheric Ar (Lee et al., 2006). Decay constants are after Steiger and Jäger (1977), with recalculated ages using the decay constants recommended in Min et al. (2000) shown in Table 1 for comparison. Plateau ages met the following criteria: at least three consecutive heating steps that are of equivalent age at the 2σ level, and together comprising at least 50% of ^{39}Ar released. For some samples, the age spectra did not meet the plateau criteria, but the spectra are still considered to provide geologically meaningful information. For these samples, integrated ages for the flattest portions of the step heat spectrum are provided (equivalent to weighted mean ages). In the past, such ages would have been referred to as 'pseudoplateau ages', but this term is being abandoned (see Schaen et al., 2020). Total gas ages represent an integration of all heating steps. All ages are reported with 2σ uncertainty. In the $^{40}Ar/^{39}Ar$ plots below, all error bars and ellipses are at the 2σ level. The following abbreviations are also used in the plots: PL = plateau; IA = integrated age, and TGA = total gas age. For clarity, heating steps comprising <1% of total ^{39}Ar released are not plotted. A confidence level is reported for each interpreted $^{40}Ar/^{39}Ar$ age, with high = highly homogeneous results, e.g. plateau age, intermediate = relatively homogeneous results, e.g. integrated age of a relatively flat portion of the spectrum, and low = heterogeneous results. Justifications for the confidence levels are provided in the text. It is recommended that low confidence-level results are treated with appropriate caution in constructing geological interpretations.

U-Pb RESULTS (listed in order by GSC lab number)

Sample: 16RAY-JR013A01
Geological unit: Sulphur Creek suite
Sample description: Foliated medium grained, homogeneous granodiorite
GSC lab number: z11875
SHRIMP mount: 844

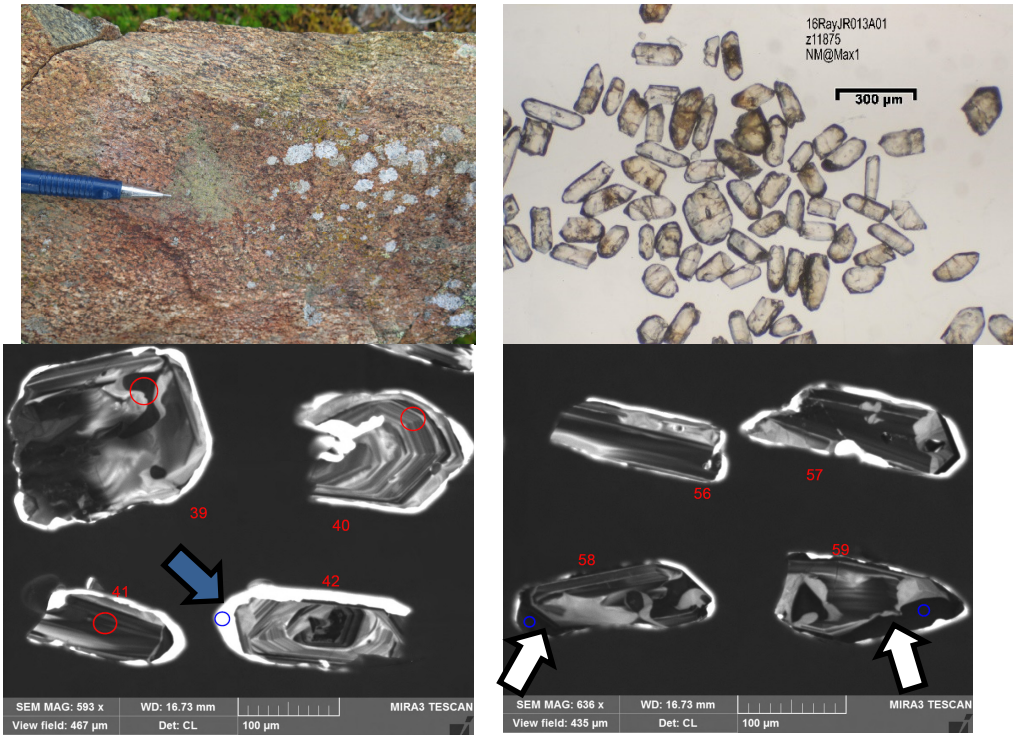

***Figure 3**: Upper left – outcrop weathered surface showing hornblende phenocrysts. Photograph by J.J. Ryan. NRCan photo 2021-529; Upper Right - Photomicrograph of zircon from the non-magnetic fraction at 1 degree side slope; Lower left - CL image of zircon showing oscillatory growth zoning, and bright low U mantles of zircon growth on outer parts of the grains (e.g. blue arrow); Lower right – CL image of zircon showing areas of unzoned zircon (white arrows).*

Zircon Description

Zircon grains recovered from this sample range from clear to opaque, and from colourless to brown (Fig. 3, upper right); fractures and inclusions are common. Grains vary between sub-equant to elongated prisms/prism fragments primarily displaying convoluted to parallel zoning under CL (Fig. 3 lower left and right: grains 39, 58, 59 and grain 56, respectively); some prism fragments display complex or simple oscillatory zoning (grains 40, 42), or areas of unzoned zircon (grain 58 and 59, white arrows, dark in CL). Bright (under CL) unzoned patches or rims of various thicknesses are observed in all grains.

U-Pb Results and Interpretation

Thirty-six analyses were carried out on 32 individual zircon grains over two separate sessions: *session 844_1* used a 19µm spot size to target prism/fragments with convoluted/parallel/oscillatory zoning, and *session 844_2* used an 11µm spot size to target areas of unzoned dark zircon or bright patches/rims (under CL).

Analyses targeting areas of convoluted, parallel, or oscillatory zoning, or areas of dark unzoned zircon have U concentrations greater than 245 ppm and yield a $^{206}Pb/^{238}U$ weighted mean age of 262.3±1.5 Ma (MSWD=1.7, n=28). As this calculated uncertainty falls below the long term reproducibility threshold, this result is more appropriately reported as 262.3±2.6 Ma. One analysis targeting an area of convoluted zircon is excluded from the weighted mean calculation as its significantly younger age may reflect Pb loss or potential mixing related to the ca. 178 Ma event described below.

Analyses targeting bright patches/rims display lower U concentrations ranging between 4-65 ppm, with Th/U ratios < 0.07. These analyses yield a $^{206}Pb/^{238}U$ weighted mean age of 177.6±9.8 Ma (MSWD=1.0, n=7).

We interpret the 262.3±2.6 Ma age as the igneous crystallization age of the granodiorite. The low Th/U ratios of the bright rim analyses may be an indication that the 177.6±9.8 Ma zircon growth is metamorphic in origin.

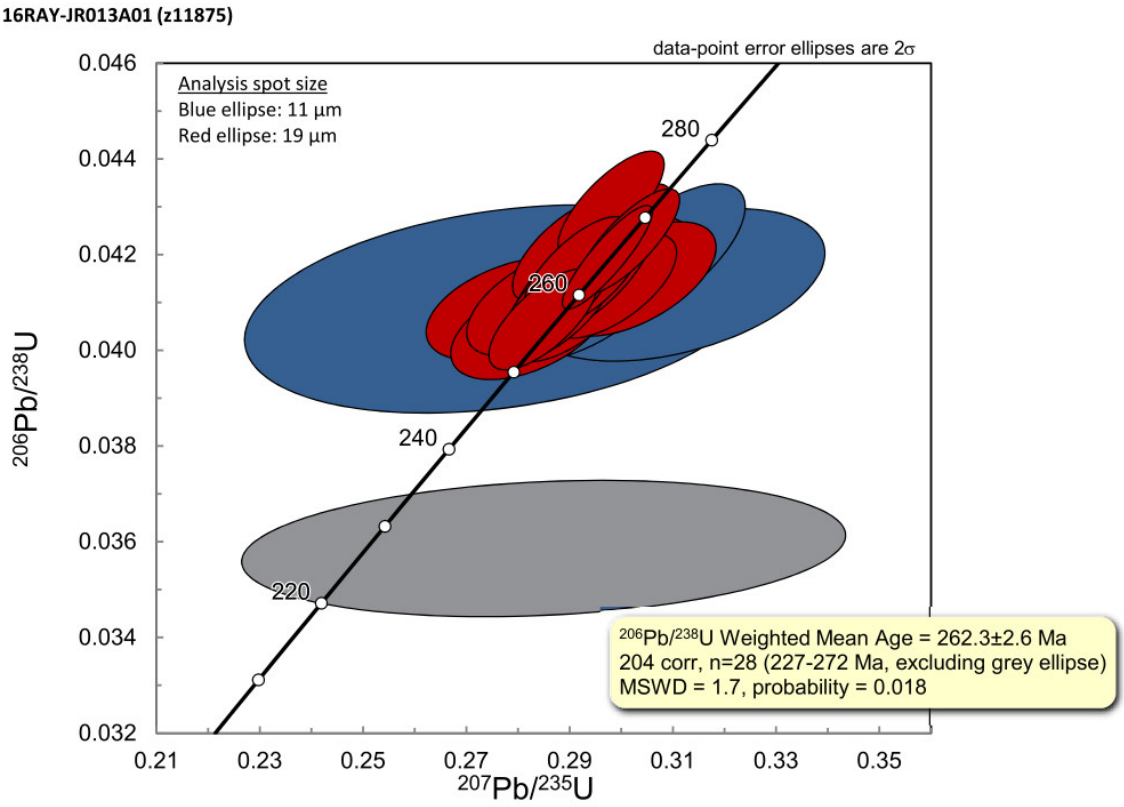

***Figure 4**: Concordia diagram for older analyses targeting prism/fragments or areas of dark unzoned zircon*

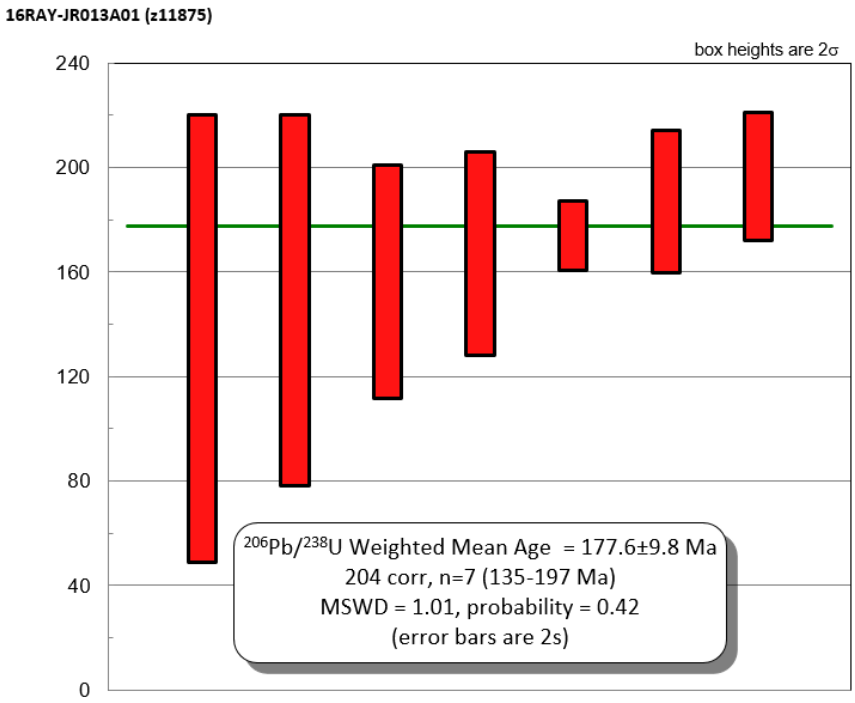

Figure 5: *Weighted average diagram for younger analyses targeting bright patches/rims*

Sample: 16RAY-JR025A01
Geological unit: Mount Nansen group
Sample description: Hornblende-quartz porphyritic dacite; is volcanic or hypabyssal, with abundant volcanic fragments; irregular jointing, flaggy
GSC lab number: z11876
SHRIMP mount: 844

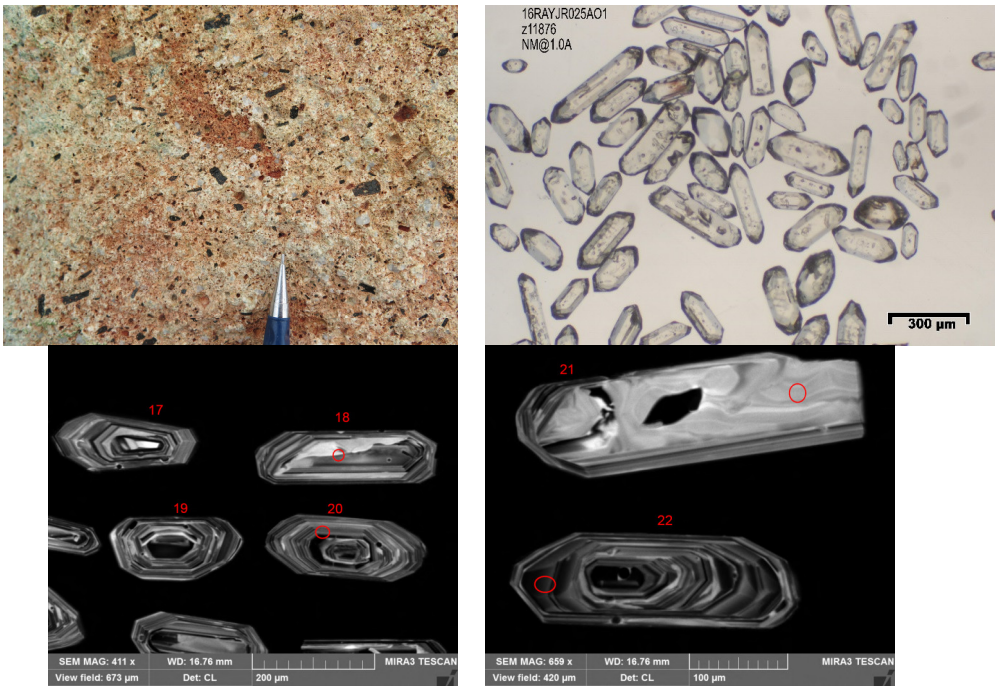

***Figure 6**: Upper left - outcrop weathered surface showing hornblende phenocrysts. Photograph by J.J. Ryan. NRCan photo 2021-530. Upper Right - Photomicrograph of zircon from the non-magnetic fraction at 1.0A, 10° side slope; Lower left - CL image of zircon showing oscillatory growth zoning; Lower right - CL image showing convoluted zoning in grain 21.*

Zircon Description

Zircon grains recovered from this dacite are clear and colourless, sub-equant to elongated well-faceted prisms, commonly displaying opaque inclusions (top right image). Under CL (bottom images) grains primarily display simple oscillatory zoning (grains 17, 19, 20, 22); rare grains have areas of convoluted zoning (grains 18 and 21).

U-Pb Results and Interpretation

Eighteen analyses were performed on 18 separate zircon grains, targeting areas with oscillatory and/or convoluted zoning. These yield a weighted mean $^{206}Pb/^{238}U$ age of 104.7±0.7 Ma (MSWD=1.3). There is no distinguishable age difference between the oscillatory-zoned and convolutedly-zoned zircon. As this calculated error falls below the long term reproducibility threshold, this result is more appropriately reported as 104.7±1.0 Ma, interpreted as the igneous crystallization age of this dacite.

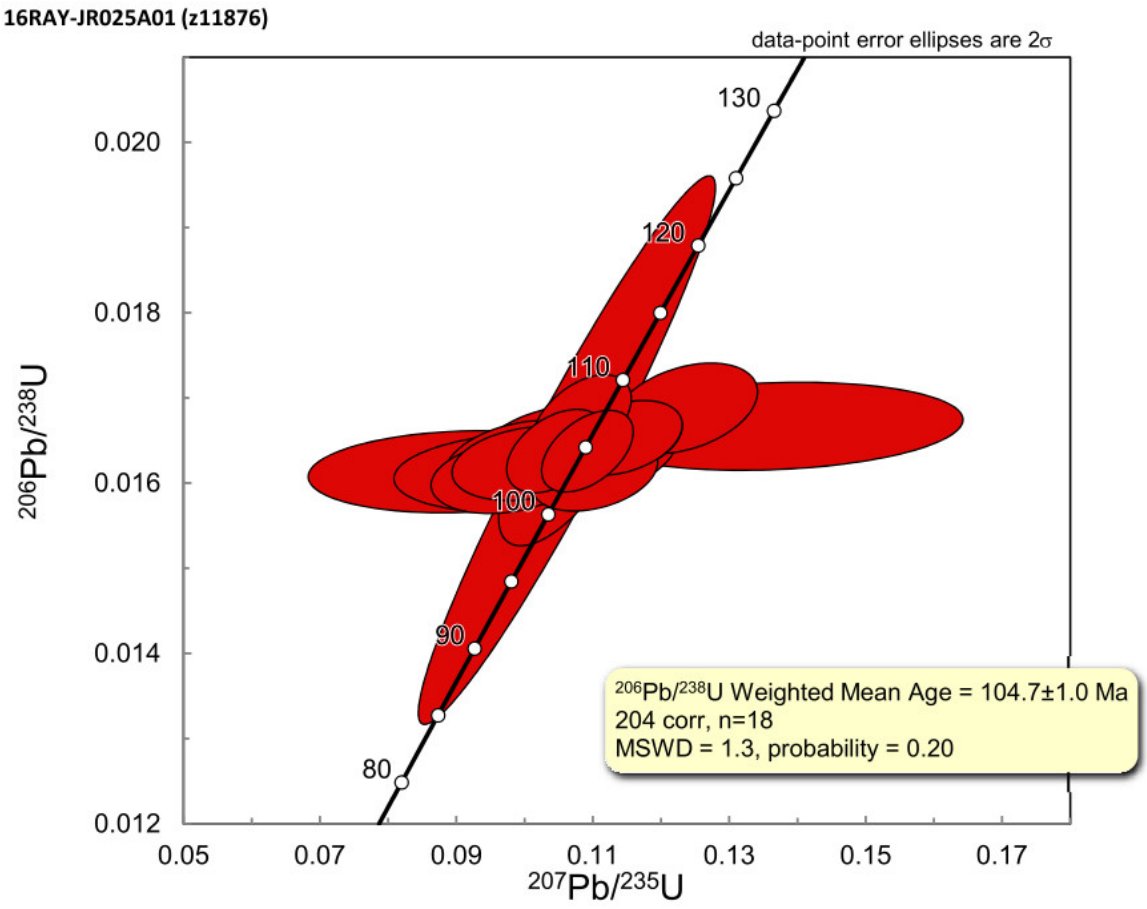

***Figure 7**: Concordia diagram for sample 16RAY-JR025A01. There is no distinguishable age difference between oscillatory- and convolutedly-zoned zircon*

Sample: 16RAY-JR028A02
Geological unit: Whitehorse suite (Dawson Range phase)
Sample description: Hornblende porphyritic, homogeneous massive granodiorite
GSC lab number: z11877
SHRIMP mount: 844

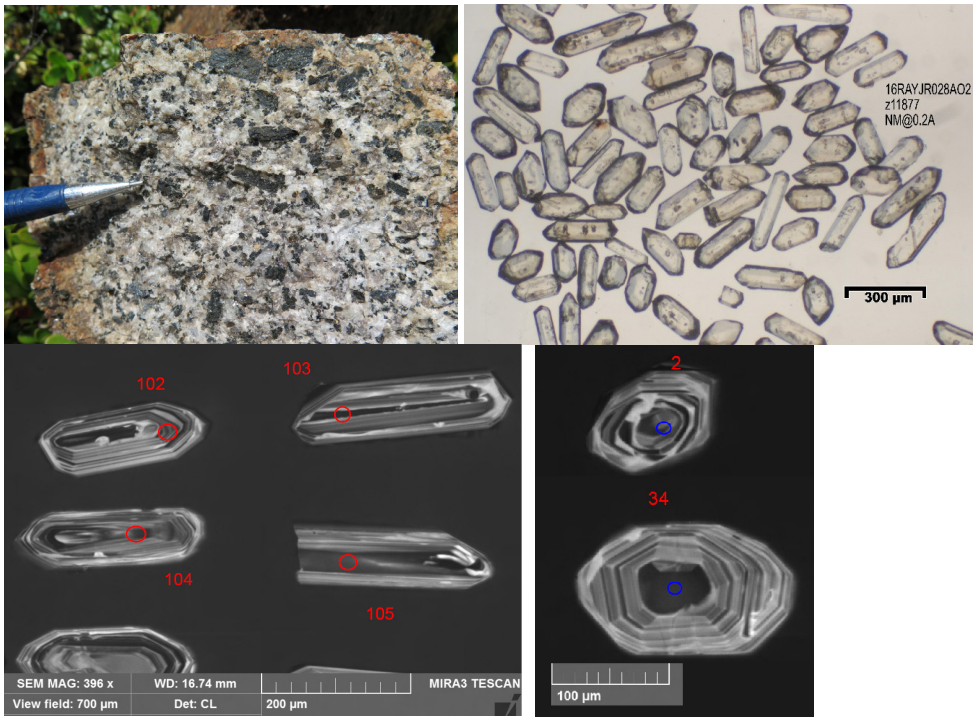

***Figure 8**: Clockwise from upper left: typical hand sample fresh surface. Photograph by J.J. Ryan. NRCan photo 2021-531; photomicrograph of zircon showing euhedral, prismatic habit; CL image of grains showing oscillatory or planer growth zoning; CL image of grains with unzoned core regions mantled by oscillatory-zoned zircon.*

Zircon Description

Zircon grains recovered from this granodiorite are clear and colourless, sub-equant to elongated well-faceted prisms (Fig. 8, top right). Under CL (Fig. 8, bottom images) grains display complex or simple oscillatory zoning (grain 2, and grains 102-105, respectively), or an unzoned inner portion surrounded by an oscillatory zoned outer portion (grain 34). Zoning is commonly disturbed by opaque inclusions.

U-Pb Results and Interpretation

Twenty-one analyses were conducted on 21 separate zircon grains over two separate sessions: *session 844_1* used a 19 µm spot size to target simple oscillatory zoned zircon, and *session 844_2* used an 11µm spot size to target zircon with complex oscillatory zoning or unzoned inner portions of grains. A weighted mean $^{206}Pb/^{238}U$ age of 17 analyses from *session 844_1* is 105.8±1.0 Ma, and that of the 4 analyses from *session 844_2* is 108.8±1.7 Ma. The unzoned inner regions of the grains are, therefore, slightly older than the oscillatory-zoned regions, but the ages are very nearly overlapping. There is no distinguishable difference in the U, Th, Yb or Hf content between the two populations, except for grain 116 which has a Th/U ratio of 3.06 compared to the average value of 0.49 for the other 20 analyses. Excluding grain 116 from the calculation on this basis, the weighted mean $^{206}Pb/^{238}U$ age for the other

20 analyses is 106.0±0.7 Ma (MSWD=1.5). As this calculated error falls below the long term reproducibility threshold, this result is more appropriately reported as 106.0±1.1 Ma, and is interpreted as the igneous crystallization age of this granodiorite.

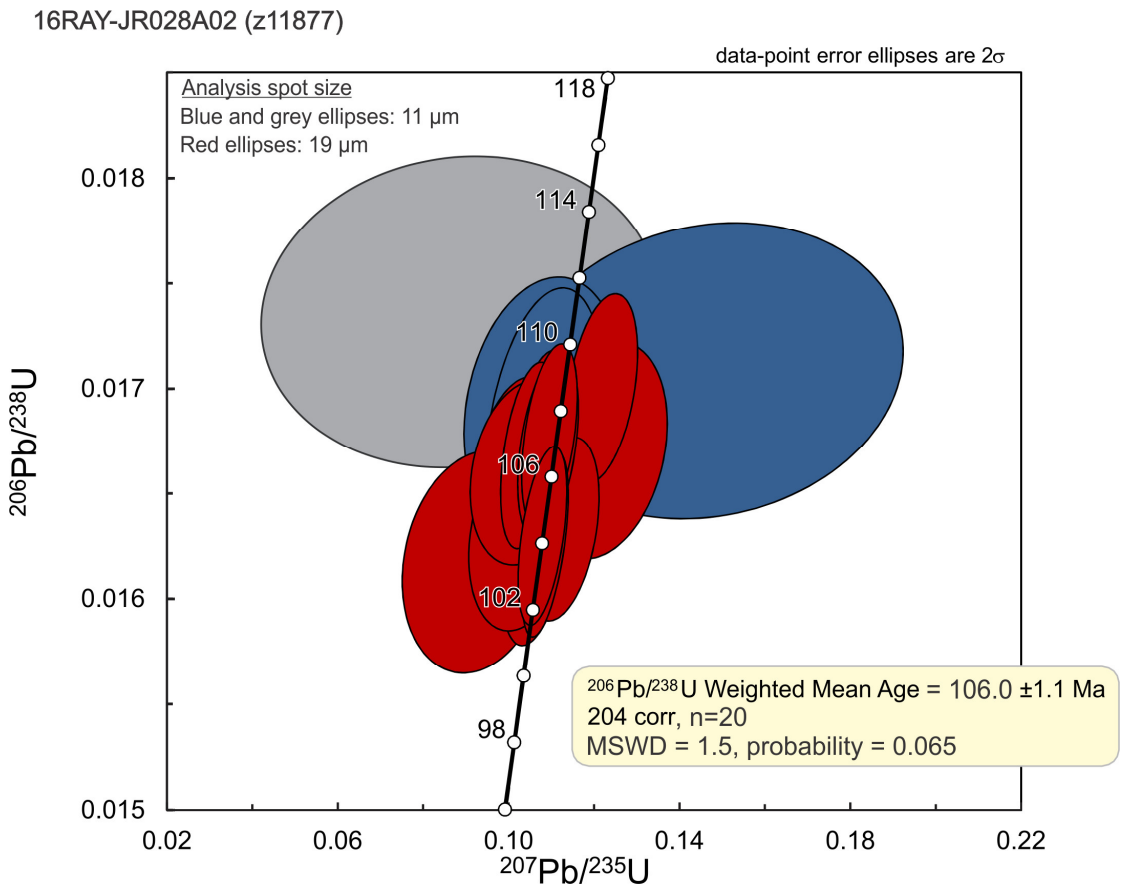

Figure 9: *U-Pb Concordia diagram for sample 16RAY-JR028A02. Red ellipses are from an analytical session using a 19µm spot size, and the blue and grey ellipses are from a session using an 11µm spot size. The weighted mean age is based on all analyses except the grey ellipse for grain 116, which had a much higher Th/U composition and slightly older age than the other grains.*

Sample: 16RAY-JR052A02
Geological unit: Whitehorse suite (Dawson Range phase)
Sample description: Massive equigranular, medium grained granodiorite
GSC lab number: z11878
SHRIMP mount: 871

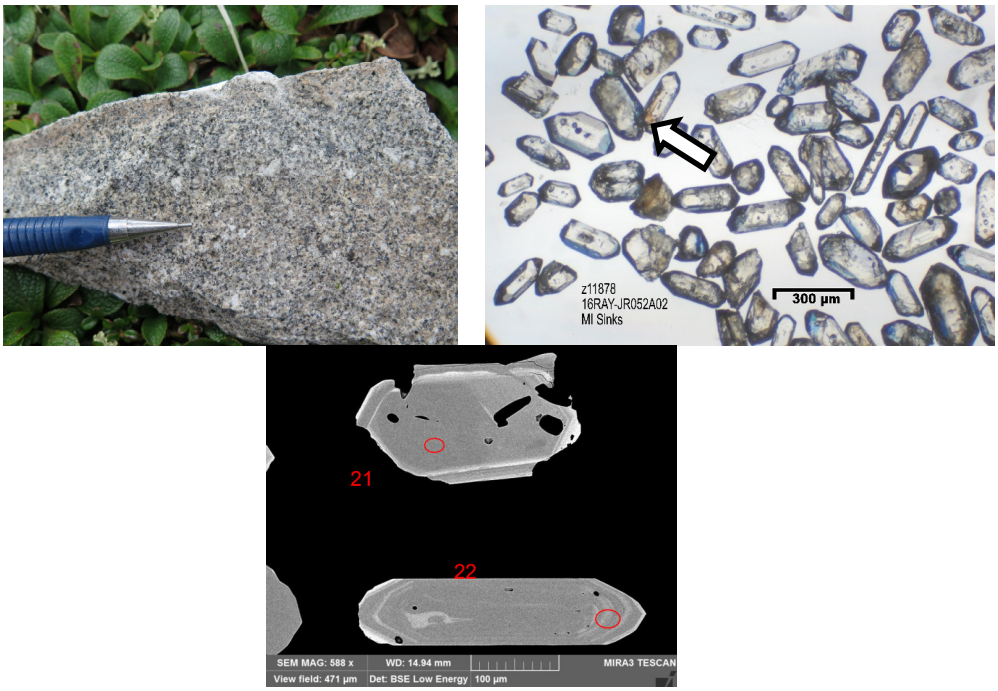

***Figure 10**: Upper left is a hand sample of 16RAY-JR052A02. Photograph by J.J. Ryan. NRCan photo 2021-532; Upper right is a photomicrograph of zircon grains from the sample. There were very few zircons obtained from the crushing and mineral separation processes so grains were picked directly from the methylene iodide sinks without any magnetic separation steps undertaken; Bottom image is the SEM BSE image of grains 21 and 22 showing homogeneous zircon texture and simple oscillatory zoning.*

Zircon Description

This sample yielded clear to turbid, colourless zircon grains often displaying iron oxide staining around opaque inclusions (Fig. 10, upper right, white arrow). Grains range between sub-equant to elongated prisms, with some grains displaying irregular grain boundaries due to the presence of inclusions (Fig 10, bottom image, grain 21). Under BSE (Fig. 10) grains either display simple oscillatory zoning (grains 21 and 22) or no zoning.

U-Pb Results and Interpretation

Twenty-two analyses were carried out on 22 individual zircon grains. The three oldest analyses (not shown on plot below) yield $^{206}Pb/^{238}U$ ages of 328±16 Ma (concordant), 234±10 Ma (discordant), and 194±10 Ma (discordant), all derived from unzoned prisms. Analysis of 18 sub-equant to elongate oscillatory zoned prisms yield a weighted mean $^{206}Pb/^{238}U$ age of 104.4±1.2 Ma (MSWD=1.9, POF=0.013, 1 rejection); these analyses have U concentrations ranging between 227-1554 ppm. One analysis (11878-002.1) was manually excluded from the weighted mean calculation due to its extremely high U content (3849 ppm)

We interpret the ca. 328-194 Ma ages as inherited, and the 104.4±1.2 Ma age as the igneous crystallization age of this granodiorite. The data scatter reflected by a slightly elevated MSWD of 1.9 may be due to possible lead loss and/or presence of antecrysts.

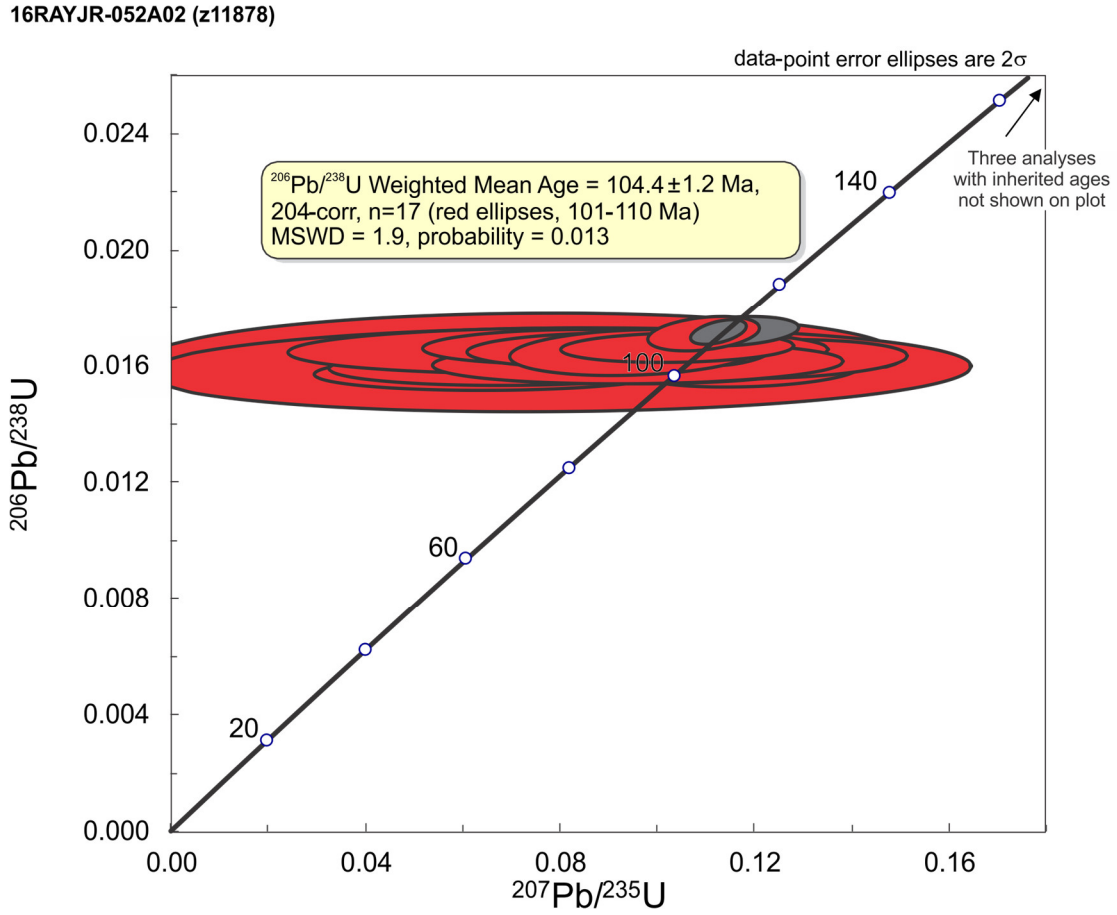

***Figure 11**: U-Pb Concordia diagram for sample 16RAY-JR052A02. The weighted mean age is based on all analyses except the 2 grey ellipses; one was statistically rejected by Isoplot in the weighted mean calculation, the other was manually excluded due to its high U content (3849 ppm).*

Sample: 16RAY-JR069A01
Geological unit: Snowcap assemblage amphibolite
Sample description: Layered amphibolite orthogneiss; possibly mafic metaplutonic
GSC lab number: z11879
SHRIMP mount: -

No zircon grains were recovered from this sample.

Sample: 16RAY-JR077A02
Geological unit: Stevenson Ridge schist
Sample description: Metaquartzite, siliciclastic, granoblastic, sheared orthoquartzite beds in some quartz-feldspathic beds, cut by quartz veins, grey colour
GSC lab number: z11881
SHRIMP mount: 859

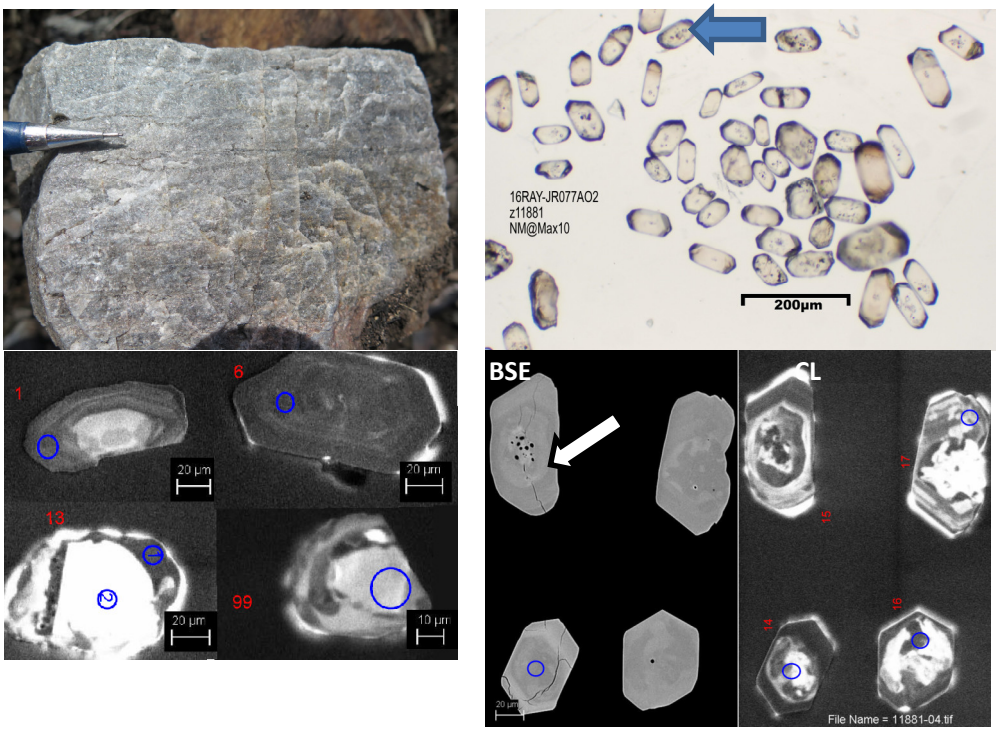

***Figure 12**: Upper left shows the hand specimen of sample 16RAYJR-077A02. Photograph by J.J. Ryan. NRCan photo 2021-533. Upper right is a photomicrograph of the zircon grains selected from the Frantz™ non-magnetic fraction at 10° side slope. Lower left shows CL images of grains with oscillatory zoning (grains 1 and 6) and grains 13 and 99 that have anhedral cores mantled by zircon growth showing convoluted zoning. Lower right shows zircon grains in CL that have spongy textures at their cores with mantles of oscillatory-zoned or homogeneous textures.*

Zircon Description

This detrital sample is composed of clear, colourless to light brown zircon grains ranging between stubby to regular prisms. Opaque inclusions are common in the center (Fig. 12; top right, blue arrow) giving grains a spongy appearance under BSE (Fig. 12; bottom images, grain 15, white arrow). Under CL, approximately 10% of grains display simple oscillatory zoning (Fig. 12; grain 6). The remaining grains either display convoluted zoning or a convoluted center surrounded by darker oscillatory zoned/unzoned zircon (Fig 12; grains 14-17). Approximately 20% of these convoluted-textured grains display a bright anhedral core (grains 13 and 99). One grain displays a sector zoned core surrounded by a simple oscillatory zoned rim (grain 1).

U-Pb Results and Interpretation

Forty-one analyses were conducted on 35 separate zircon grains. See Figure 13 for the Concordia diagram. The five oldest concordant analyses in this detrital sample yield $^{207}Pb/^{206}Pb$ ages of 2730±16 Ma (grain 1, described above), 2646±32 Ma and 1121±84 Ma (both from anhedral cores), and Concordia

ages of 334±11 Ma and 302±9 Ma (both from convoluted areas of grains). An additional six analyses have very discordant ages and are not collinear.

A dominant cluster, targeting unzoned zircon or areas with oscillatory or convoluted zoning, yields Concordia ages ranging between ca. 256-266 Ma, with a dominant mode at ca. 262 Ma (Fig. 14; n=30). These results require some careful interpretation in the regional geologic context, because this sample was collected from a unit that correlates with the Finlayson assemblage, and is thought to be Late Devonian in age (Ryan et al., 2018). If these oscillatory zoned grains with Permian results are detrital grains of igneous origin, then ca. 262 Ma could be interpreted as defining the maximum age of deposition for this detrital sample; and consequently would negate the unit as being part of the Finlayson assemblage. However, these grains have very low (ca. 0.01) Th/U ratios, more typical or metamorphic origin as either new zircon growth or resetting/recrystallizing of older zircon. If this is the case, all we can conclude is that the protolith was deposited prior to the ca. 262 Ma metamorphic episode. Regionally, these Yukon-Tanana terrane rocks are known to have experienced pervasive mid-Permian tectonometamorphism (Berman at al., 2007). Another sample (16RAY-JR077A01; see below) was crushed, to further investigate this problem, but the sample did not yield zircon.

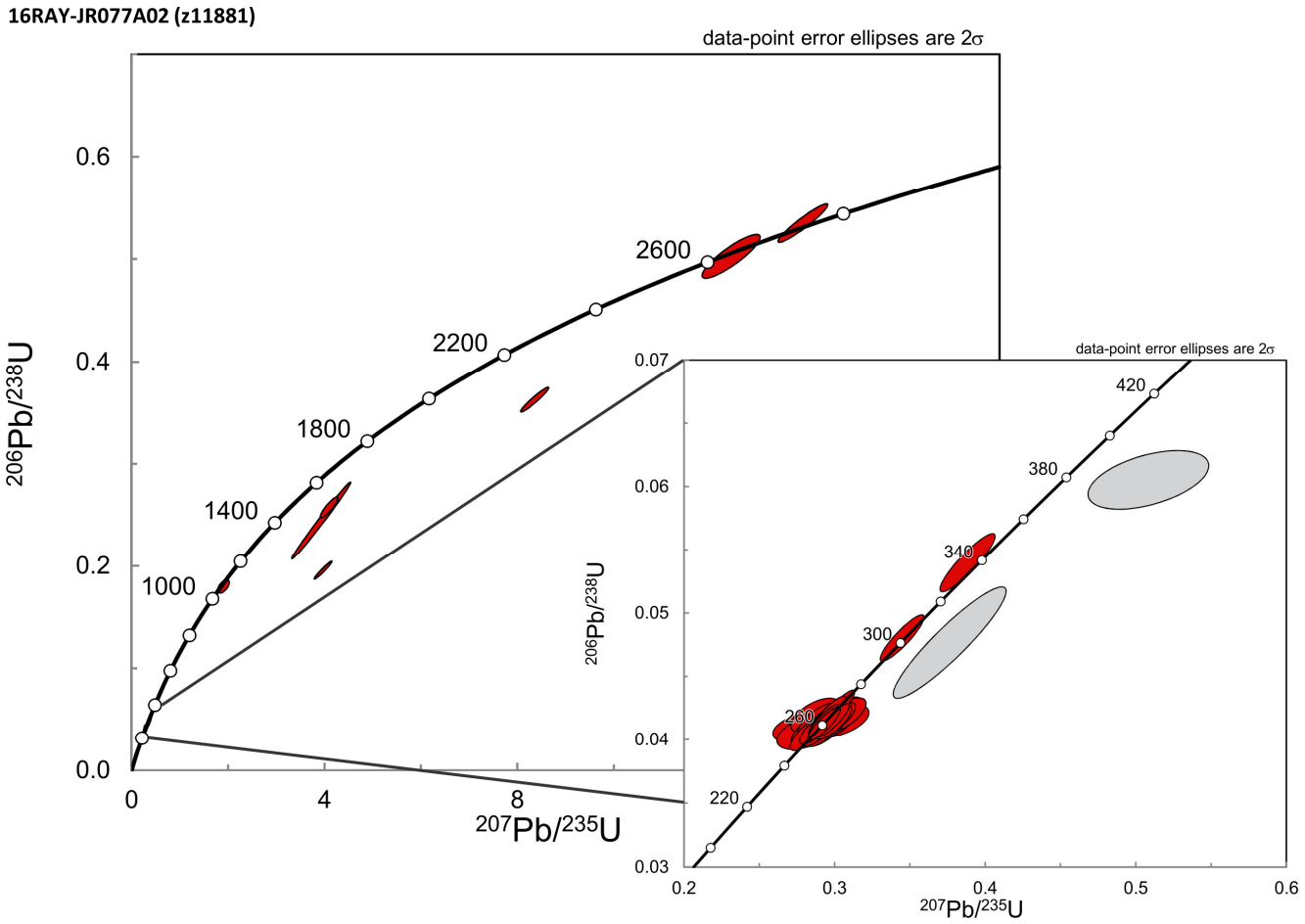

***Figure 13**: U-Pb Concordia diagram for sample 16RAY-JR077A02. The rightmost image is zoomed in to the Devonian to Triassic portion of the Concordia diagram to show where the majority of analyses plot.*

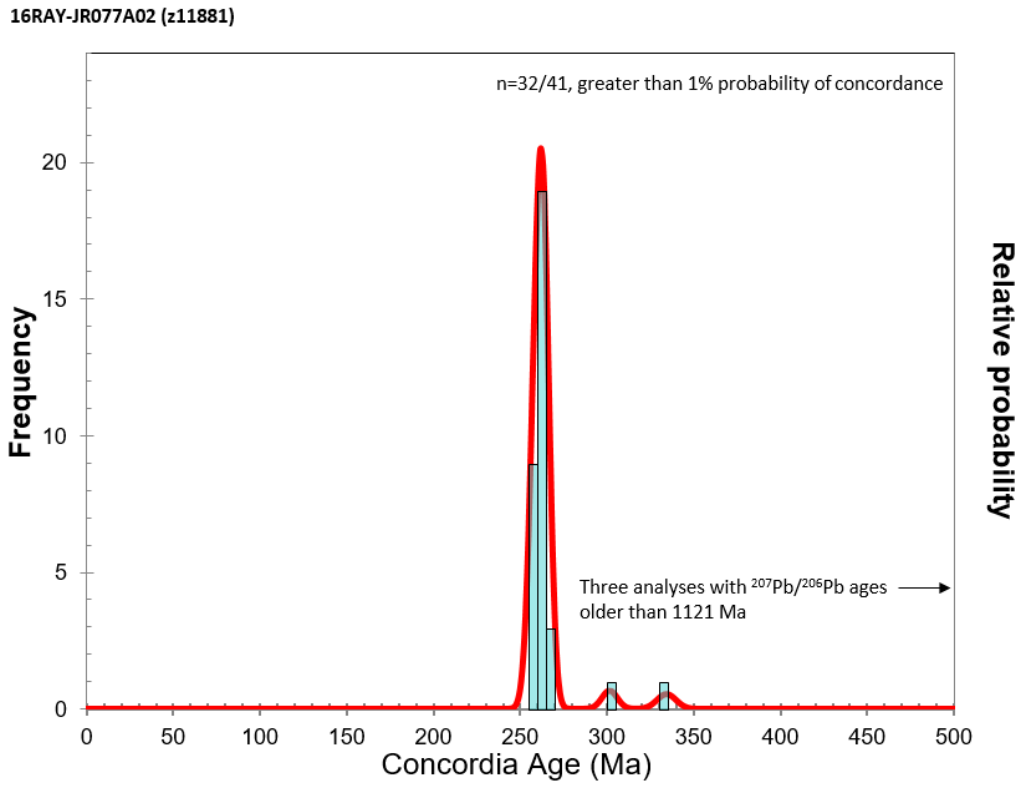

***Figure 14**: Probability plot for sample 16RAYJR-077A02 showing the dominant mode of the analyses at ca. 262 Ma (n=30 for the peak).*

Sample: 16RAY-JR178A01
Geological unit: Sulphur Creek suite
Sample description: Weakly foliated feldspar-quartz porphyry, probably a hypabyssal sill
GSC lab number: z11884
SHRIMP mount: 859

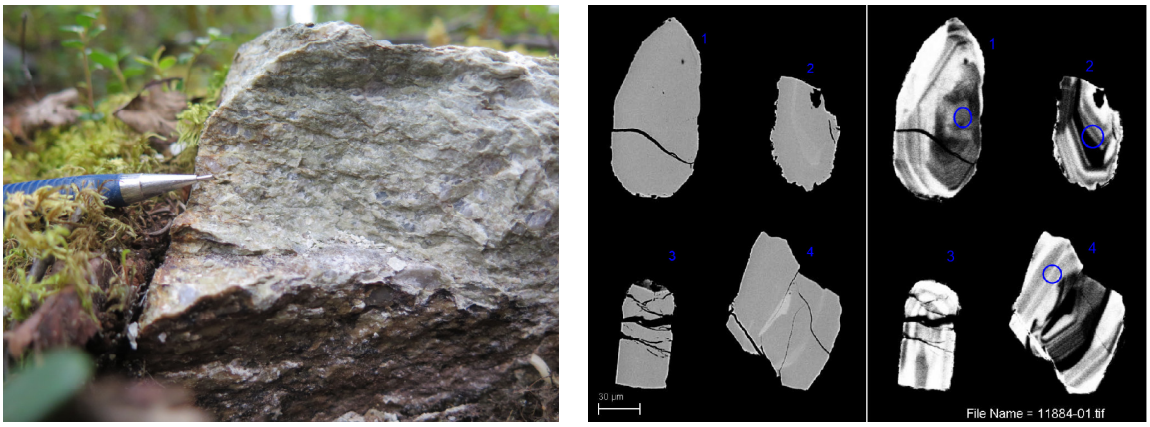

***Figure 15**: Left image shows an example in the field of sample 16RAY-JR178A01. Photograph by J.J. Ryan. NRCan photo 2021-534. Right image shows representative BS and CL images of zircon grains from the sample. No plain light photomicrograph of selected zircon grains was available.*

Zircon Description

Few zircon grains were recovered from this sample. These range between sub-equant to regular prisms/prism fragments with simple oscillatory zoning (Fig. 15; right image, grains 1-4). Ragged grain boundaries and fractures are common.

U-Pb Results and Interpretation

Twenty analyses were performed on 20 separate zircon grains, yielding a weighted mean $^{206}Pb/^{238}U$ age of 257.5±2.3 Ma (Fig. 16; MSWD=1.3). As this calculated error falls below the long term reproducibility threshold, this result is more appropriately reported as 257.5±2.6 Ma, interpreted as the igneous crystallization age of this porphyry.

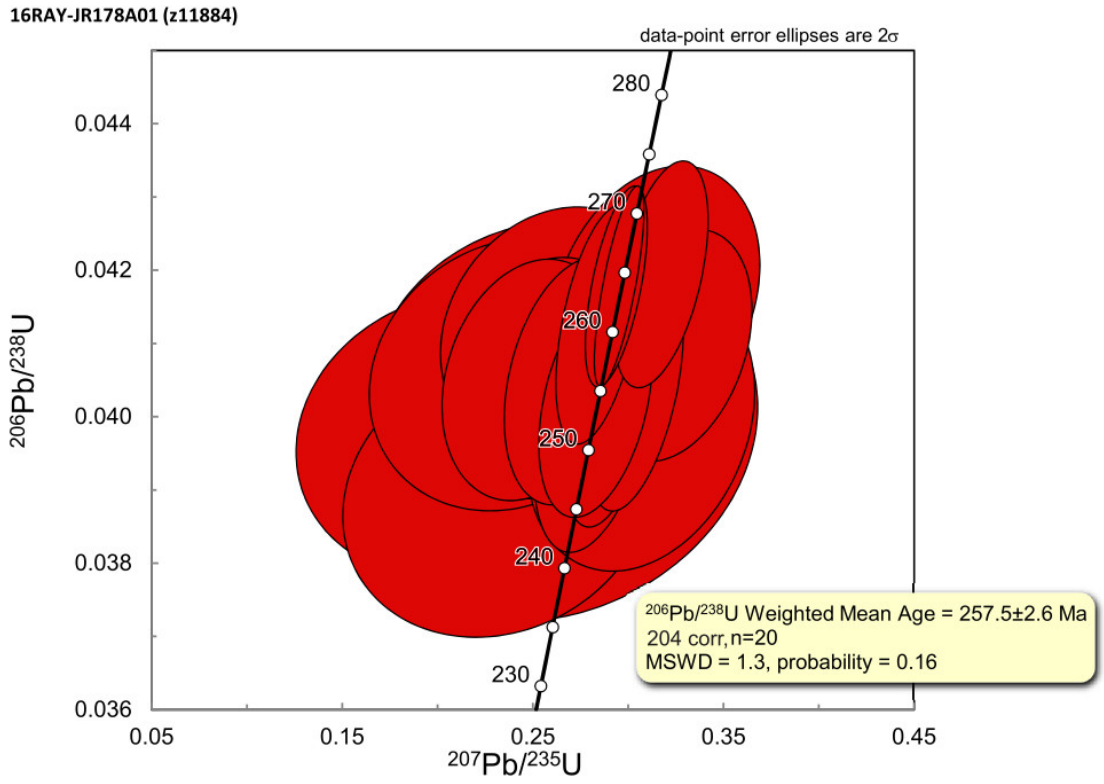

***Figure 16**: Concordia diagram for sample 16RAY-JR178A01. All analyses were included in the weighted mean age calculation.*

Sample: 16RAY-JR080A02
Geological unit: Metagabbro
Sample description: Metagabbro, sill, equigranular, fine to medium grained, more massive than typical amphibolite, and retains igneous texture
GSC lab number: z11885
SHRIMP mount: -

No zircon grains were recovered from this sample.

Sample: 16RAY-JR176A01
Geological unit: Simpson Range suite
Sample description: Well-foliated biotite- and muscovite-bearing, quartz porphyritic granodiorite
GSC lab number: z11886
SHRIMP mount: 844

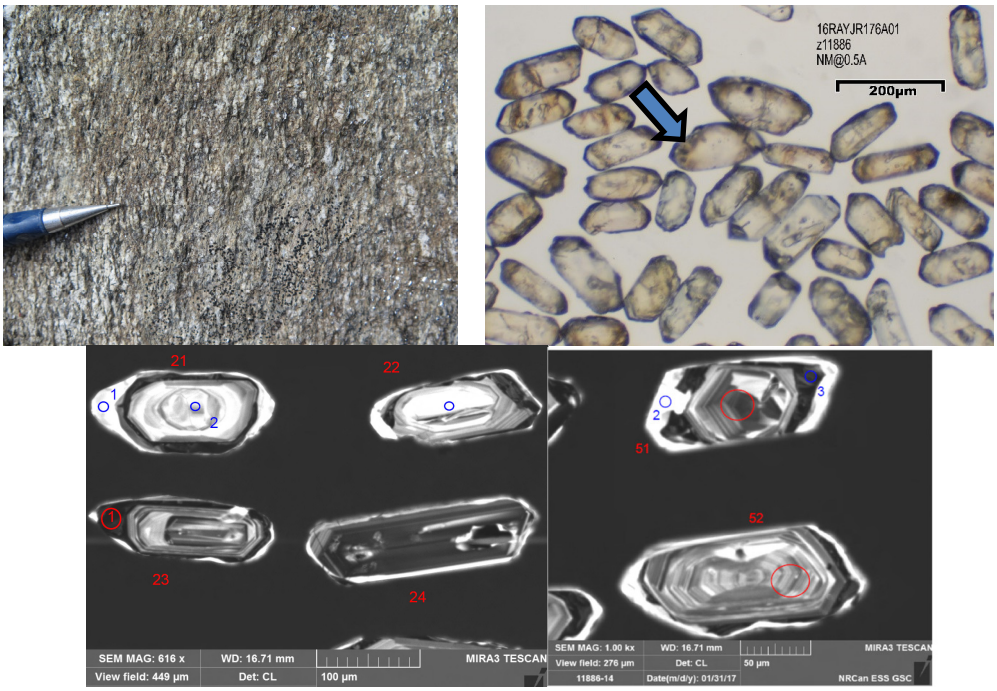

Figure 17*: Top left shows sample 16RAY-JR176A01 in outcrop. Photograph by J.J. Ryan. NRCan photo 2021-535. Top right is a plain light photomicrograph of zircons selected for analysis. Bottom two images show representative zircon grains in CL.*

Zircon Description

Zircon grains recovered from this sample are clear and colourless to pale brown with some fracturing; iron oxide staining is common around opaque/clear inclusions (Fig. 17, top right; blue arrow). Grains range between regular to elongate prisms. Under CL (Fig. 17, bottom images) grains display complex, sector or simple oscillatory zoning, surrounded by a dark rim with convoluted zoning, mantled by a bright unzoned/convolutedly zoned rim (grains 21-23). Some grains (~10%) also display an anhedral or rounded core (grains 21 and 22).

U-Pb Results and Interpretation

Sixty-seven analyses were carried out on 59 individual zircon grains over two separate sessions: *session 844_1* used a 19µm spot size to target cores and oscillatory zoned areas in grains, and *session 844_2* used an 11µm spot size to target dark and bright rims (under CL). Ellipses on the Concordia diagram are colour-coded to show analyses from different areas targeted on zircon grains (Fig. 18).

The three oldest analyses, targeting cores, yield $^{207}Pb/^{206}Pb$ older than 1.6 Ga (discordant) Analyses targeted on complex/sector/oscillatory areas of zircon grains yield a $^{206}Pb/^{238}U$ weighted mean age of 359.7±2.2 Ma (MSWD=2.2, n=33). As this calculated error falls below the long term reproducibility threshold, this result is more appropriately reported as 359.7±3.6 Ma.

Analyses targeting rims with dark convoluted zoning yield a $^{206}Pb/^{238}U$ weighted mean age of 262.1±3.7 Ma (MSWD=2.5, n=13), whereas analyses on bright rims yield a younger $^{206}Pb/^{238}U$ weighted

mean age of 242.1±5.1 Ma (MSWD=2.1, n=9). Analyses on either dark or bright rims yield low Th/U ratios <0.02.

The ca. 2149-1663 Ma discordant ages are interpreted as inherited and the 359.7±3.6 Ma age as the igneous crystallization age of the granodiorite. The low Th/U ratios observed in dark and bright rims may be an indication that the younger 262.1±3.7 Ma and 242.1±5.1 Ma ages are metamorphic in origin. Grain 51 in image above shows three different domains from which 3 distinct ages were obtained: spot 1 in the core (365 Ma), spot 3 in the dark convoluted-zoning mantle around the core (257 Ma) and spot 2 from the bright white outer rim of the grain (247 Ma). Four analyses were excluded from the ca. 359-241 Ma weighted mean calculations as the analysis spots straddled distinct domains (i.e. core/rim; grey ellipses) on the grains. Four analyses with elevated common lead content were also excluded from age calculations (pink ellipses).

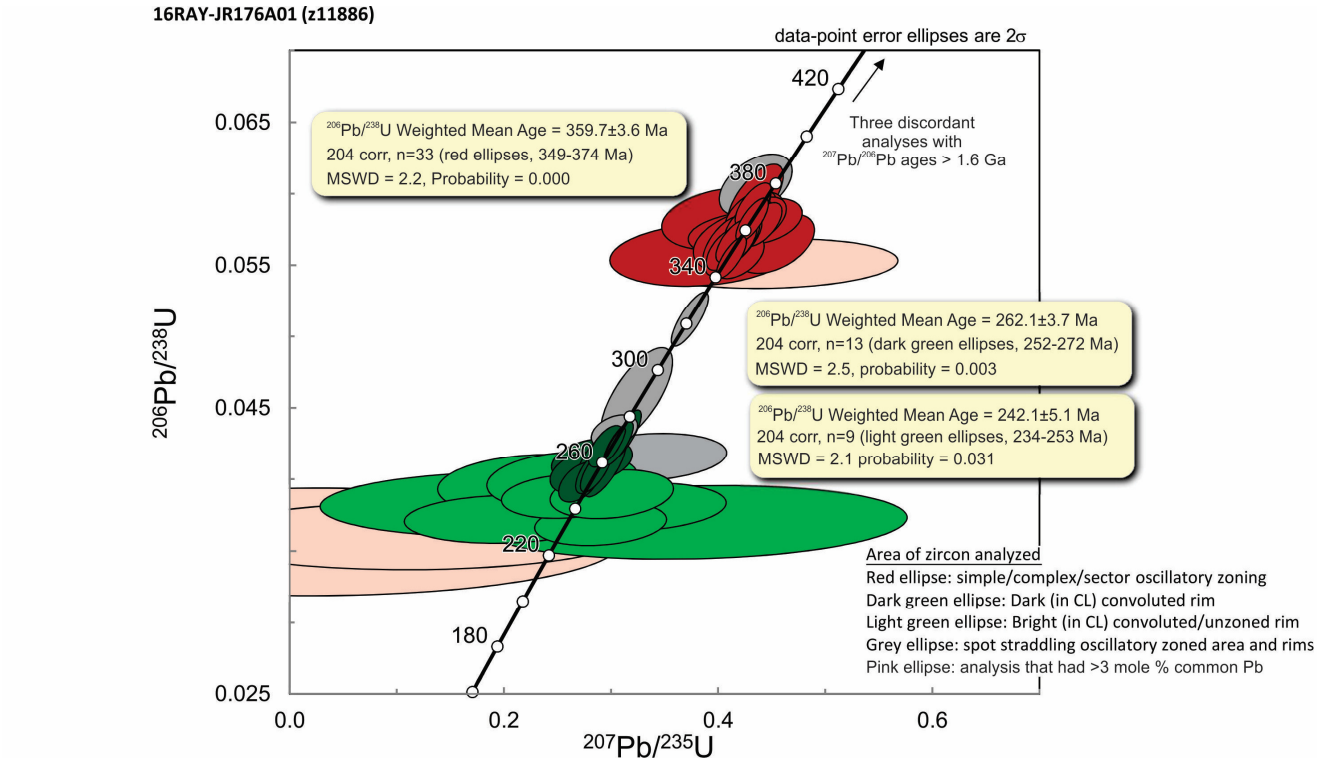

***Figure 18**: Concordia diagram for sample 16RAY-JR176A01.*

Sample: 16RAY-JR048A01
Geological unit: Ruby Range batholith
Sample description: Alkali feldspar rhyolite; either volcanic or hypabyssal; abundant quartz crystal-filled vugs
GSC lab number: z12302
SHRIMP mount: 906

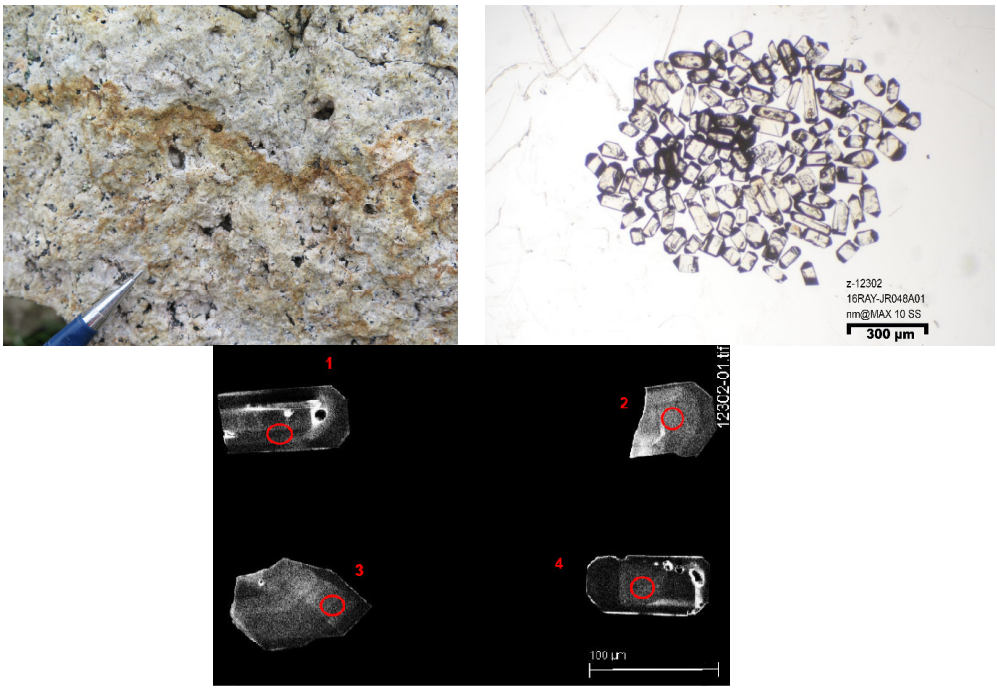

Figure 19*: Top left shows sample 16RAY-JR048A01 in outcrop. Photograph by J.J. Ryan. NRCan photo 2021-536. Top right is a plain light photomicrograph of zircons selected for analysis. Bottom image shows representative zircon grains in CL.*

Zircon Description

Zircon grains recovered from this sample are clear and colourless with some opaque inclusions, and range between well-faceted sub-equant to elongated prisms/prism fragments (Fig. 19; top right). Under CL most grains are unzoned, or display weak diffuse zoning (Fig. 19, bottom image).

U-Pb Results and Interpretation

Eleven analyses were performed on 11 separate zircon grains, yielding a weighted mean $^{206}Pb/^{238}U$ age of 56.9±0.6 Ma (MSWD=0.96; Fig. 20), interpreted as the igneous crystallization age of this rhyolite.

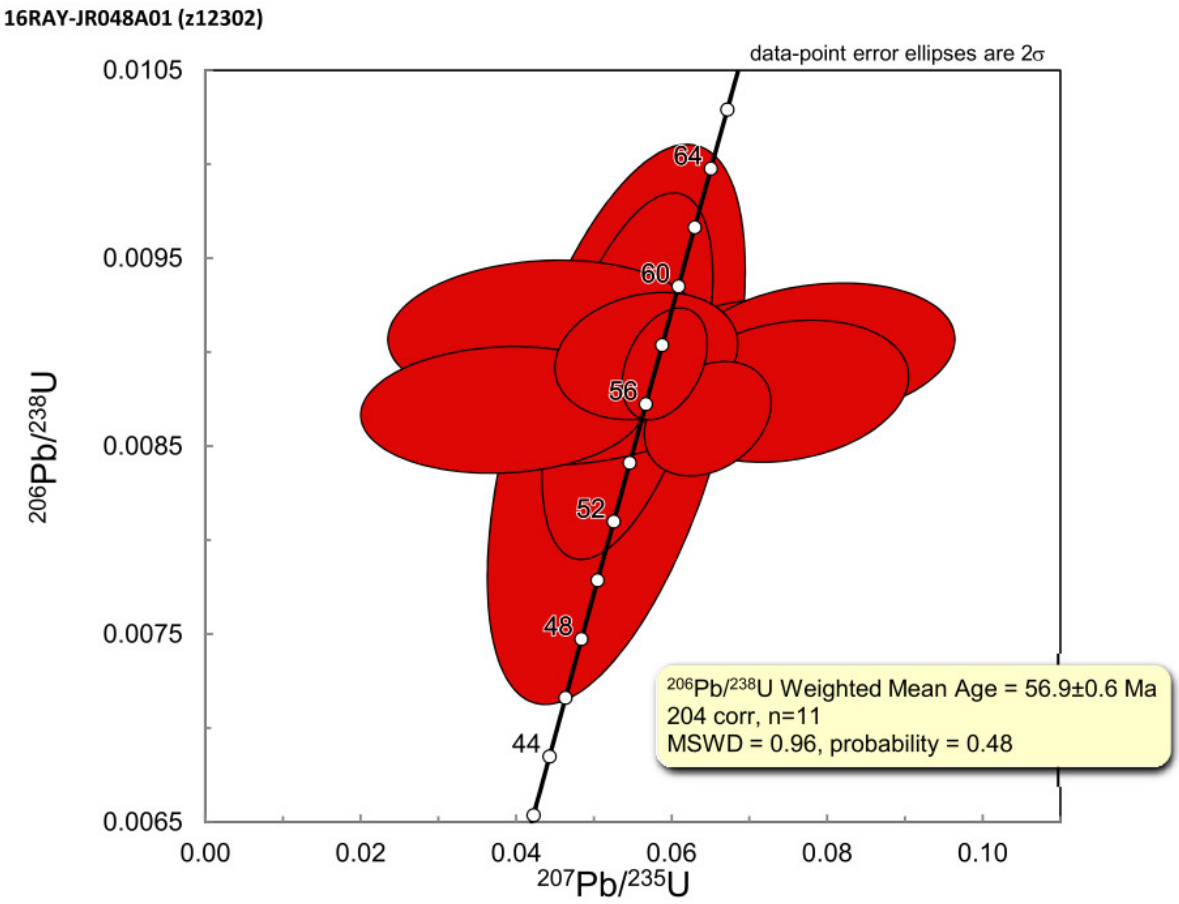

Figure 20: *Concordia diagram for sample 16RAY-JR048A01.*

Sample: 16RAY-JR077A01
Geological unit: Stevenson Ridge schist
Sample description: Metaquartzite, siliciclastic, granoblastic, sheared orthoquartzite beds in some quartz-feldspathic bed, cut by quartz veins, grey colour
GSC lab number: z12303
SHRIMP mount: -

No zircon grains were recovered from this sample.

Sample: 16RAY-AP046A01
Geological unit: Sulphur Creek suite
Sample description: Strongly foliated to gneissic granodiorite, stretched potassium feldspar augen; contains layers of amphibolite
GSC lab number: z12304
SHRIMP mount: 908

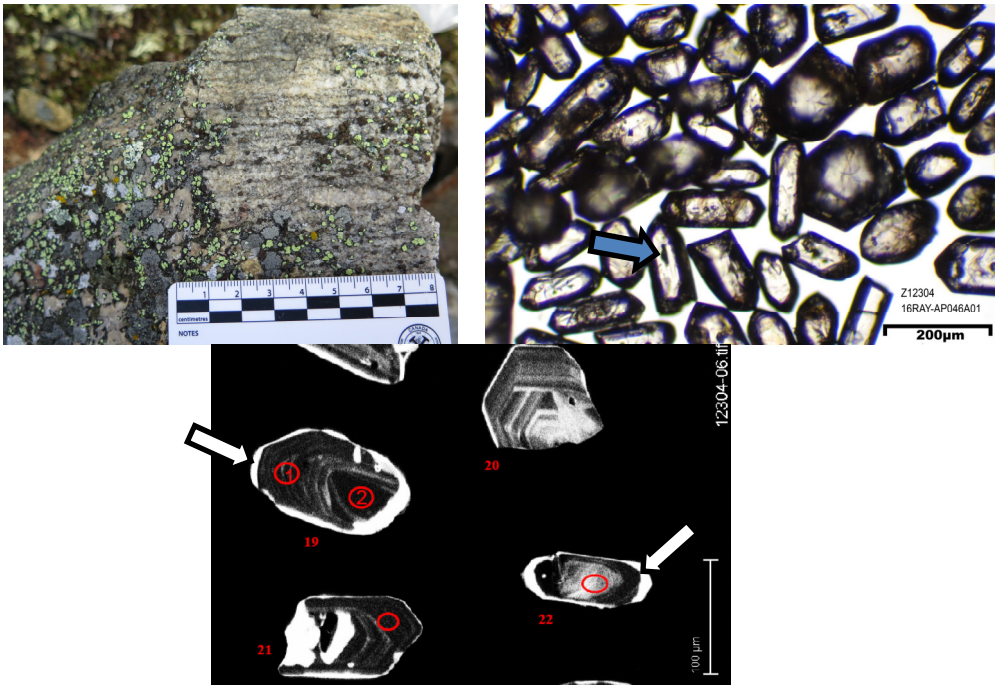

***Figure 21**: Top left shows sample 16RAY-AP046A01 in hand specimen. Photograph by A.J. Parsons. NRCan photo 2021-537. Top right is a plain light photomicrograph of zircons selected for analysis. Bottom image shows representative zircon grains in CL.*

Zircon Description

Zircon grains recovered from this sample range between clear-turbid and colourless-light brown; fractures and opaque inclusions are common (Fig. 21, blue arrow, top right image). Grains vary from sub-equant to regular prisms primarily displaying simple oscillatory zoning under CL (Fig. 21, bottom image, grains 19-21); few grains display broad or convoluted zoning. Rare grains (~3%) display small bright core (10-20µm) surrounded by an unzoned or oscillatory zoned rim (e.g. Fig. 21, bottom image, grain 22). Bright rims/patches are concentrated around the edges of grains and inclusions (Fig. 21; white arrows; bottom image); some of these bright areas may be due to fluorescence or charging from the inclusions as opposed to an inherent property of the zircon itself.

U-Pb Results and Interpretation

Forty-two analyses were conducted on 37 individual zircon grains. The oldest analyses, targeting small bright cores, yield $^{207}Pb/^{206}Pb$ discordant ages between 624 and 1824 Ma.

Twenty-two analyses, primarily targeting oscillatory or broadly zoned areas of zircon grains, yield a weighted mean $^{206}Pb/^{238}U$ age of 262.9±1.2 Ma (MSWD=1.2). As this calculated error falls

below the long term reproducibility threshold, this result is more appropriately reported as 262.9±2.6 Ma.

Analyses on bright rims yield the youngest ages in this sample, ranging from 227-182 Ma. The four youngest rims yield a weighted mean $^{206}Pb/^{238}U$ age of 184.1±3.0 Ma (MSWD=0.56), and contain low Th/U ratios of 0.003-0.019 ppm.

We interpret the ca.1824-272 Ma ages as inherited zircon and the 262.9±2.6 Ma age as the igneous crystallization age of this granodiorite. The low Th/U ratios observed in the youngest analyses may be an indication that the 184.1±3.0 Ma zircon growth is metamorphic in origin. Eleven analyses targeting either bright patches/rims or areas of convoluted zoning were excluded from the ca. 263-184 Ma weighted mean calculations as these may reflect Pb loss or potential mixing related to the ca. 184 Ma event (grey ellipses in plot).

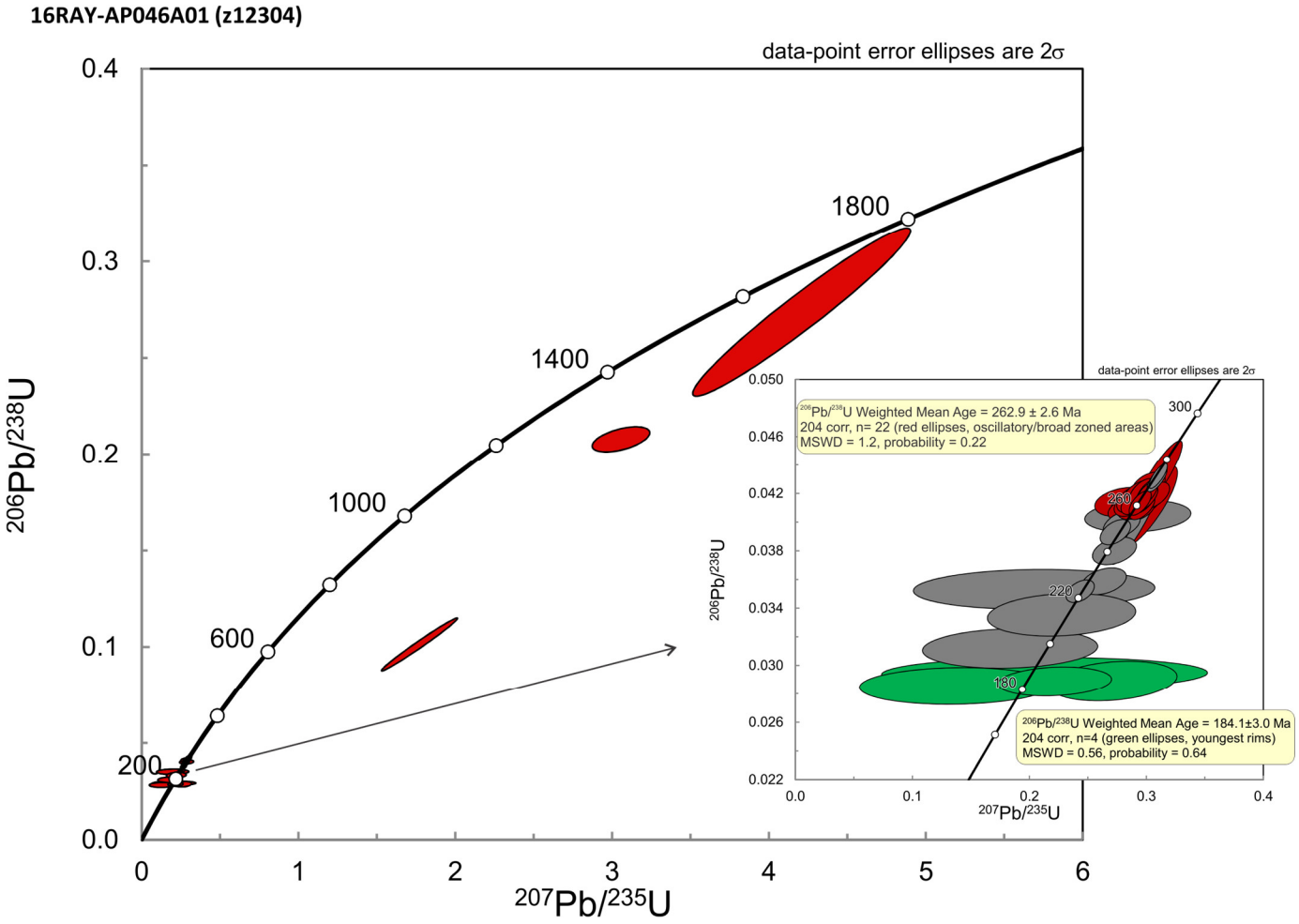

Figure 22: *Concordia diagram for sample 16RAY-AP046A01. Large plot shows the full data set, and the inset is a zoomed-in view of the younger data. Red ellipses are the analyses included in the weighted mean age of 262.9±2.6 Ma, which is interpreted as the crystallization age for the granodiorite. Green ellipses are the analyses interpreted to reflect 184.1±3.0 Ma metamorphic growth. Grey ellipses are those which were excluded from age calculations due to suspected lead loss, spot sampling multiple growth zones, or spot sampling inherited components and yielding mixed ages.*

Sample: 15RAY-EW011A01
Geological unit: Simpson Range suite
Sample description: Strongly lineated and foliated to gneissic, quartz and plagioclase augen granodiorite
GSC lab number: z12305
SHRIMP mount: 908

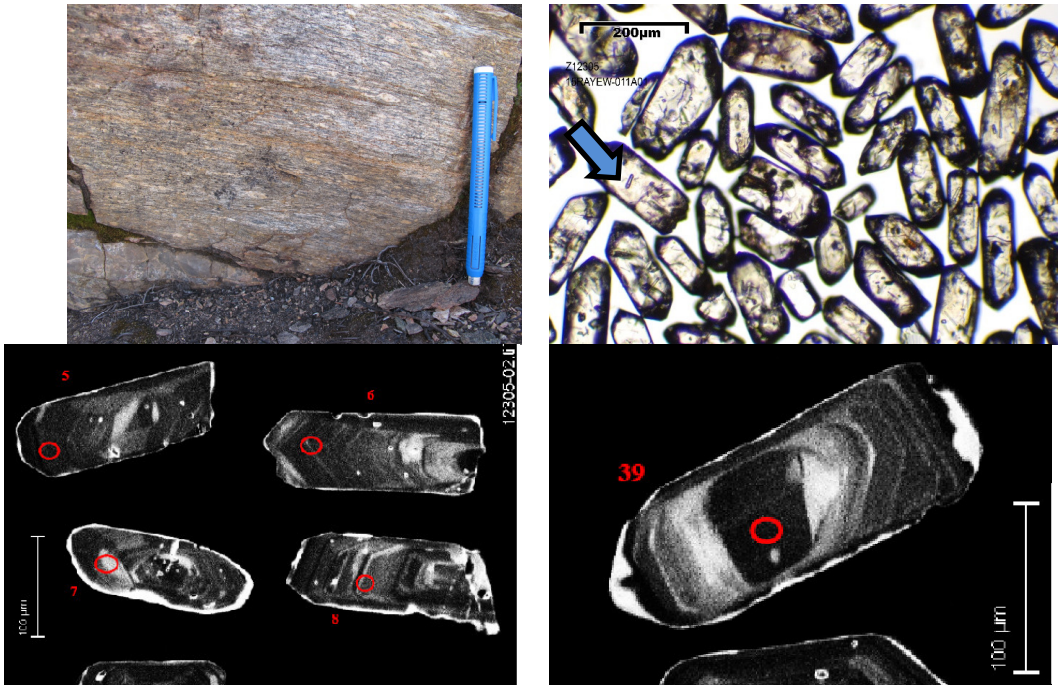

Figure 23*: Top left shows sample 15RAY-EW011A01 in outcrop. Photograph by E. E. Westberg. NRCan photo 2021-538. Top right is a plain light photomicrograph of zircons selected for analysis. Bottom images show representative zircon grains in CL.*

Zircon Description

Zircon grains recovered from this granodiorite are clear prisms ranging from colourless to pale brown, displaying fracturing and abundant clear/opaque inclusions (Fig. 23, blue arrow, top right image). Under CL, (Fig. 23, bottom images) grains display simple oscillatory zoning (grains 5-8). Rare grains display an unzoned core surrounded by an oscillatory zoned rim (grain 39). Most grains display irregular bright patches concentrated along rims or around inclusions.

U-Pb Results and Interpretation

Thirty-five analyses were conducted on 34 individual zircon grains. One of these analyses, targeting an unzoned core, yields a $^{207}Pb/^{206}Pb$ age of 1854±16 Ma (grain 39).

Thirty-three analyses targeting oscillatory-zoned areas of grains and unzoned cores, yield a weighted mean $^{206}Pb/^{238}U$ age of 360.8±1.7 Ma (Fig. 24, MSWD=2.0). As this calculated error falls below the long term reproducibility threshold, this result is more appropriately reported as 360.8±3.6 Ma. One younger analysis at 328.8±4.1 Ma was excluded; the spot is located on the bright rim of grain 93, and may reflect later stage of growth. However, due to the fact that the bright rims on the rest of the

grains were not broad enough to fit an analysis spot on, the significance of the single 328.8±4.1 Ma age result remains uncertain.

There appear to be two chemical groups of zircon growth (see Appendix A); twenty-five analyses contain relatively lower U (<710ppm) and Yb (<500ppm), and eight analyses contain relatively higher U (>710ppm) and Yb (>700ppm). The weighted mean age for the 25 lower U grains is 360.4±3.6 (MSWD = 1.4); this age is indistinguishable from the 360.8±3.6 Ma age incorporating all 33 analyses. The reason for the chemical inhomogeneity of the grains is unclear. In addition, the origin of one analysis with distinctly lower Th/U than the other 32 analyses is uncertain (grain 28, Th/U = 0.04, see Appendix A). We interpret the 1854±8 Ma age as inherited and the 360.8±3.6 Ma age as the igneous crystallization age of this granodiorite.

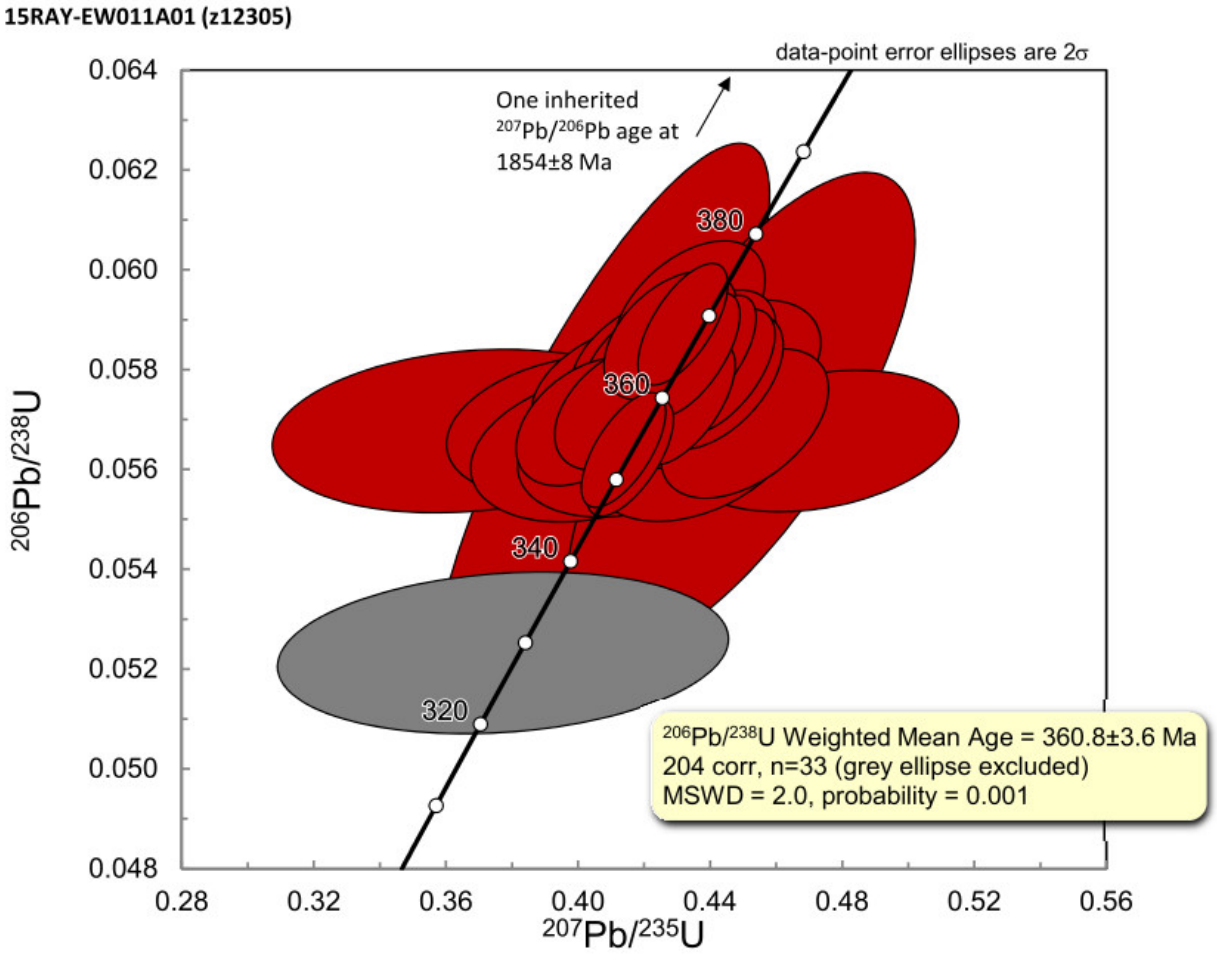

Figure 24: *Concordia diagram for sample 15RAY-EW011A01.*

$^{40}Ar/^{39}Ar$ RESULTS (listed by GSC lab number)

Sample: 16RAY-JR080A02
Geological unit: Metagabbro
Sample description: Metagabbro, sill, equigranular, fine to medium grained, more massive than typical amphibolite, and retains igneous texture
Mineral: Hornblende

GSC lab number: z11885
Ar#: 3628
Age: 157 ± 5 Ma
Age interpretation: Cooling age
Confidence: Intermediate

***Figure 25**: field photo of metagabbro sample 16RAY-JR080A02, pencil tip for scale Photograph by J.J. Ryan. NRCan photo 2021-539.*

Summary of single crystal step heating results:

Three aliquots of hornblende were analyzed for this sample. Step heat spectra show a similar pattern for each crystal; old age steps comprise the first ~20% of gas released, followed by a relatively flat pattern for the remaining gas steps (Fig. 26). However, individual crystals gave a range of plateau and integrated, or total gas ages. The inverse isochron indicates a significant component of non-radiogenic Ar that is slightly enriched in excess Ar ($^{40}Ar/^{36}Ar = 322 \pm 3$, free intercept).

$^{40}Ar/^{39}Ar$ Interpretation

The inverse isochron age of 157 ± 5 Ma (MSWD = 0.8, n = 19), determined by combining data from all three aliquots, is considered the best estimate for the cooling age of this hornblende.

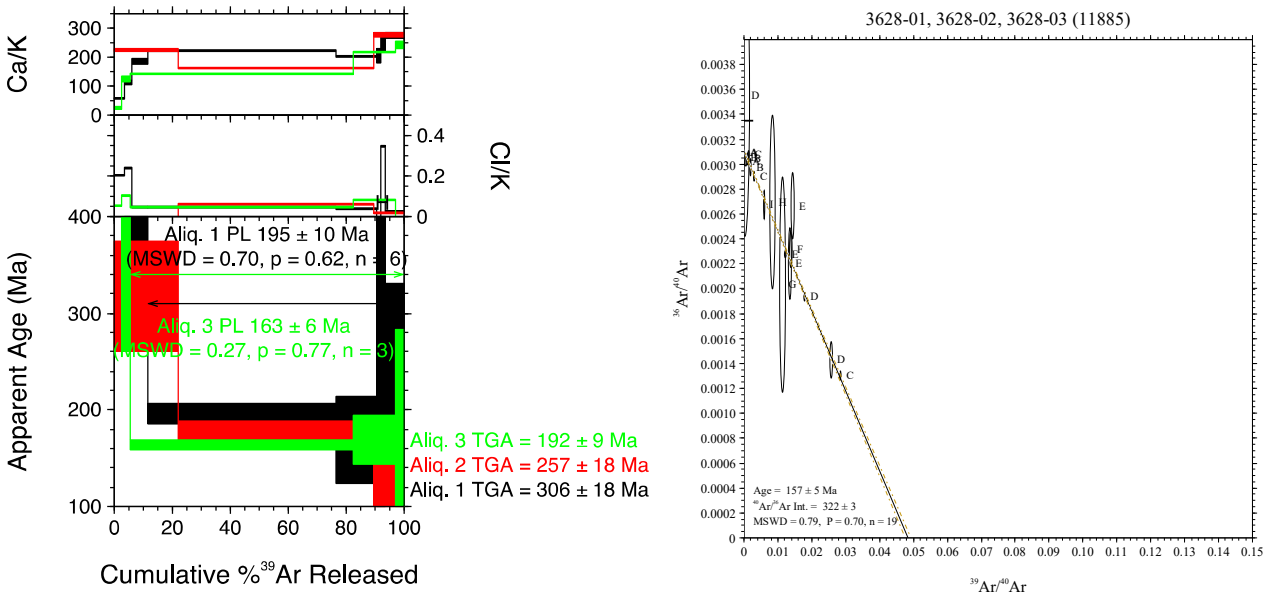

***Figure 26**: Gas release spectra (left) and inverse isochron plot (right) for 3 aliquots of hornblende from sample 16RAY-JR080A02.*

Sample: 16RAY-JR176A01
Geological unit: Simpson Range suite
Sample description: Well foliated biotite and muscovite bearing, quartz porphyritic granodiorite
Mineral: Muscovite

GSC lab number: z11886
Ar#: 3634
Age: 152 ± 1 Ma
Age interpretation: Cooling age
Confidence: Intermediate

Figure 27*: Field shot of granodiorite sample 16RAY-JR176A01 (pencil tip for scale). Photograph by J.J. Ryan. NRCan photo 2021-535.*

Summary of single crystal step heating results:

Aliquots 1 and 3 of muscovite from this sample yielded similar step heat patterns with heterogeneous, but relatively flat step heat age patterns. In contrast, aliquot 2 yielded a much older, and more heterogeneous step heat age pattern (Fig. 28).

No aliquot yielded a plateau age, and the data do not permit an accurate regression in inverse isochron space. The flattest portions of aliquots 1 and 3 yield similar integrated ages of ca. 152 Ma.

^{40}Ar/^{39}Ar Interpretation

The reasons for Aliquot 2 having produced such a different result are not clear; older ages could reflect the presence of either excess argon and/or older inherited components that were not visible during grain selection.

The integrated age for aliquot 3, comprising 99% of ^{39}Ar released, is considered to be the best estimate of muscovite cooling age for this sample at 152 ± 1 Ma (MSWD=16.3, n=18).

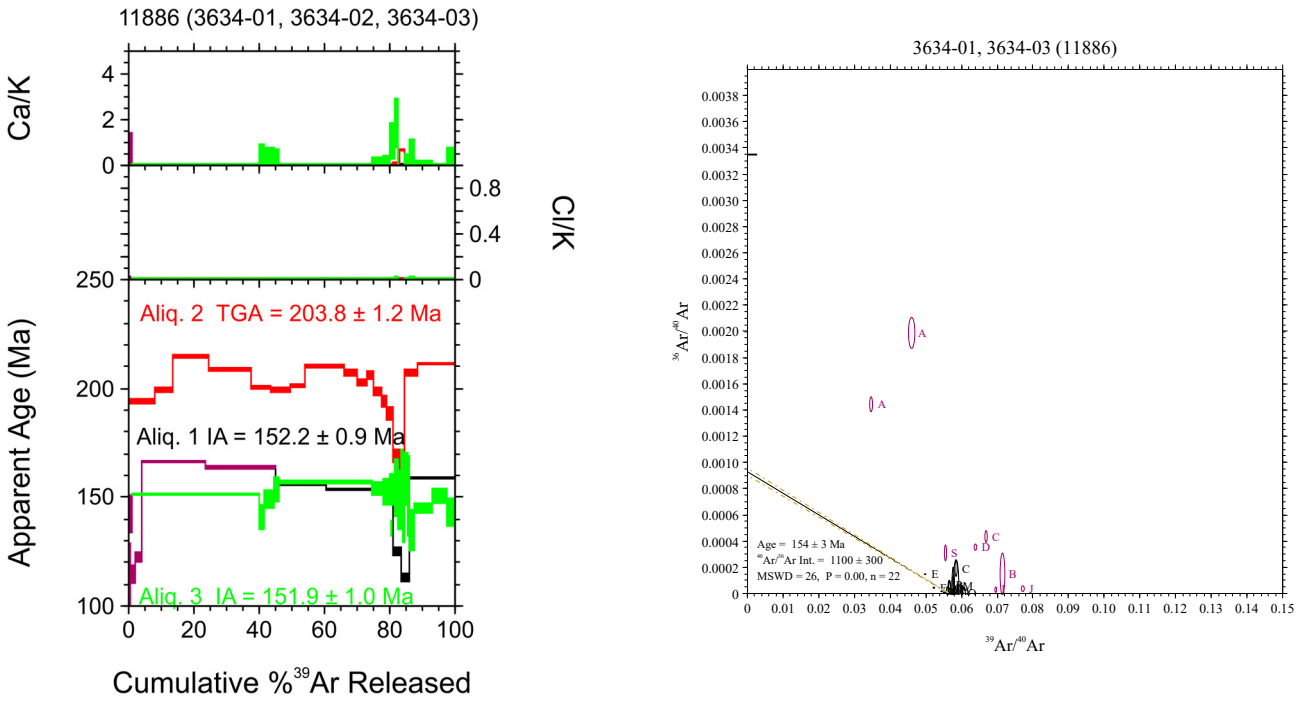

Figure 28: *(Left) Gas release spectra for 3 aliquots of muscovite from sample 16RAYJR-176A01. (Right) Inverse isochron plot for aliquots 1 and 3 of the same sample.*

Sample: 16RAY-JR176A01
Geological unit: Simpson Range suite
Sample description: Well foliated biotite and muscovite bearing, quartz porphyritic granodiorite
Mineral: Biotite

GSC lab number: z11886
Ar#: 3659
Age: 70.7 ± 0.8 Ma
Age interpretation: Cooling age
Confidence: High

Figure 29: *Field shot of granodiorite sample 16RAY-JR176A01 (pencil tip for scale). Photograph by J.J. Ryan. NRCan photo 2021-535.*

Summary of single crystal step heating results:

Aliquots 1 and 3 of biotite from this sample yielded similar, and fairly homogeneous step heat patterns (Fig. 30) with a staircase in the initial 25-30% of ^{39}Ar released. Aliquot gave a robust plateau age of 70.7 ± 0.8 Ma (MSWD = 1.54, n = 15, 74.8% of total ^{39}Ar) Aliquot 2 yielded a more heterogeneous step heat age pattern. In inverse isochron space, aliquots 1 and 3 yield a fairly good regression, yielding an age of 73± 3 Ma (MSWD = 3.3, n=24) with a ^{40}Ar/^{36}Ar intercept of 287 ± 20 (indistinguishable from atmospheric composition).

^{40}Ar/^{39}Ar Interpretation

The plateau age for aliquot 1, which includes 74.8% of ^{39}Ar released, is considered the biotite cooling age for this sample at 70.7 ± 0.8 Ma (MSWD = 1.54, n = 15).

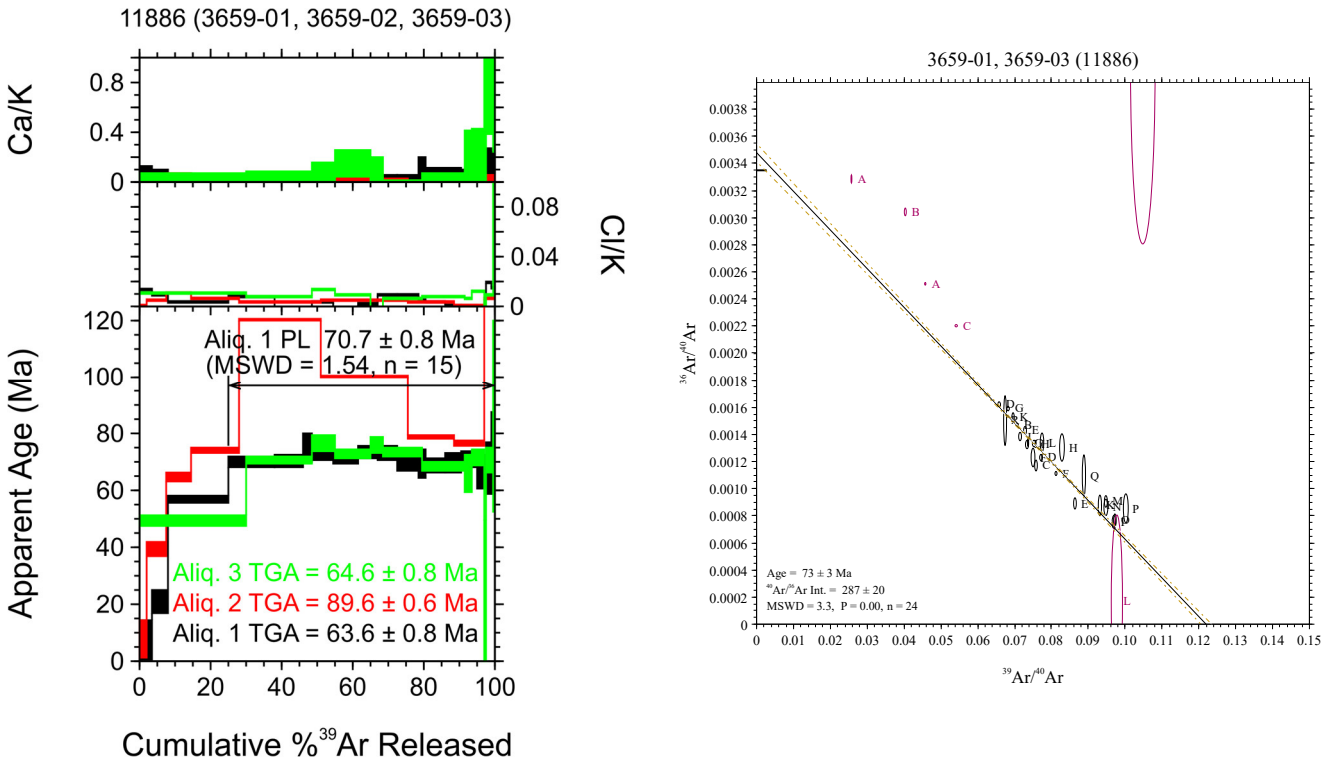

***Figure 30**: (Left) Gas release spectra for 3 aliquots of biotite from sample 16RAYJR-176A01. (Right) Inverse isochron plot for aliquots 1 and 3 of the same sample.*

Sample: 11RAYTK073A01
Geological unit: Simpson Range suite
Sample description: Felsic orthogneiss, foliated, muscovite and biotite bearing, light and dark layers
Mineral: Biotite

GSC lab number: z11904
Ar#: 3608
Age: 168.9 ± 1.4 Ma
Age interpretation: Cooling age
Confidence: High

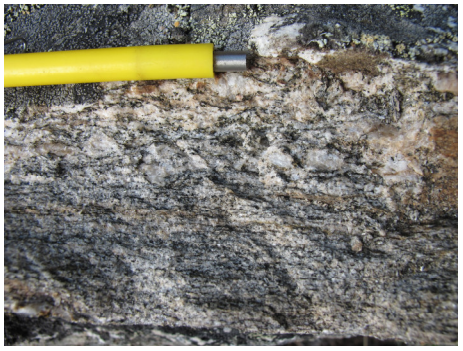

***Figure 31**: Field shot of orthogneiss sample 11RAYTK073A01. Photograph by T. Kelly. NRCan photo 2021-540.*

Summary of single crystal step heating results:

Both aliquots of biotite from this sample yielded plateau ages (Fig. 32, left). The plateau age for aliquot 1 of 169.0 ± 1.4 Ma (MSWD = 0.67, n=14), comprising 90% of ^{39}Ar released. The plateau age for aliquot 2 is 168.8 ± 1.4 Ma (MSWD=1.57, n=10). The data are highly radiogenic, and thus do not allow an accurate regression in inverse isochron space (Fig. 32, right).

^{40}Ar/^{39}Ar Interpretation

The weighted mean of the plateau ages for both aliquots is 168.9 ± 1.0 Ma. As this calculated error falls below the precision of the individual plateau age results, this result is more appropriately reported as 168.9 ± 1.4 Ma, and is interpreted as the biotite cooling age for this sample.

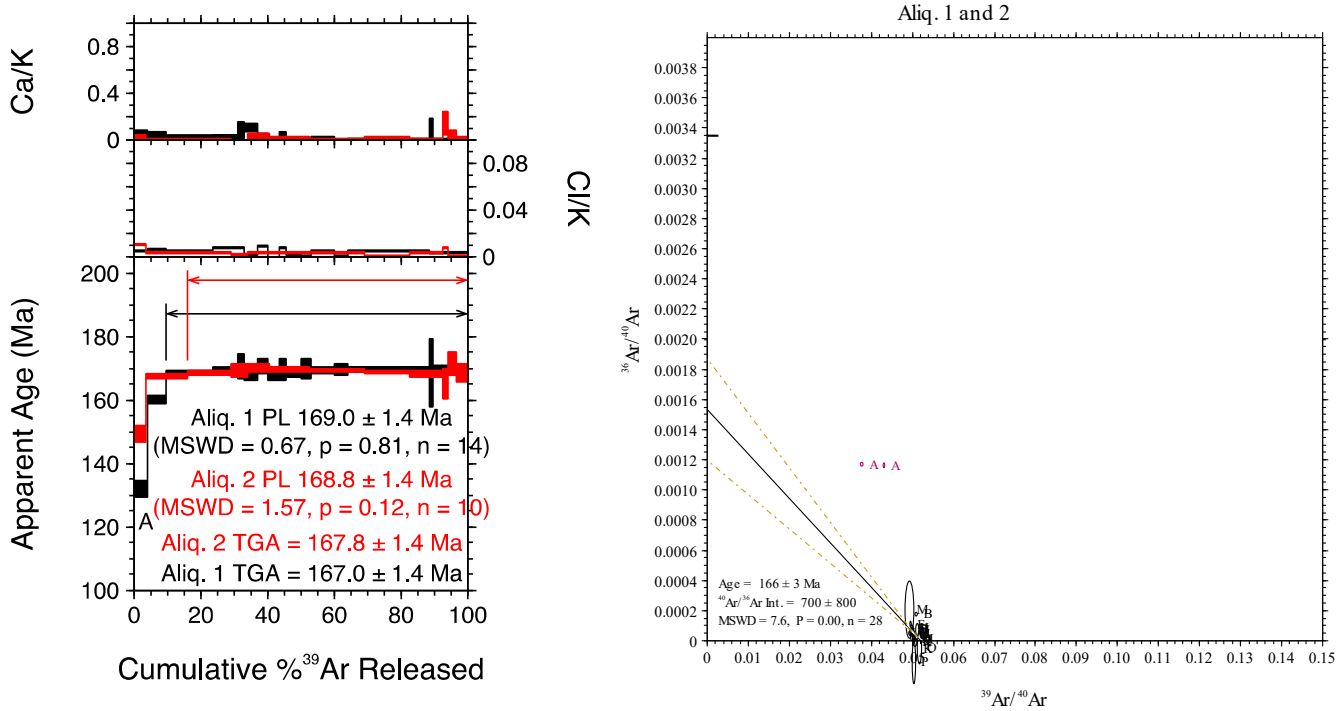

***Figure 32**: (Left) Gas release spectra for 2 aliquots of biotite from sample 11RAYTK073A01. (Right) Inverse isochron plot for aliquots 1 and 2 of the same sample.*

Sample: 16RAY-AP030A02
Geological unit: Snowcap Assemblage
Sample description: Quartz mica schist, interbedded with quartzite layers and possible igneous injections
Mineral: Muscovite

GSC lab number: z11905
Ar#: 3612
Age: 118.1 ± 0.8 Ma
Age interpretation: Cooling age
Confidence: High

***Figure 33**: Field photo of schist sample 16RAY-AP030A02. Photograph by A.J. Parsons. NRCan photo 2021-541.*

Summary of single crystal step heating results:

Three aliquots have yielded similar step heat spectra with old initial steps that decrease in age over the first 50% of ^{39}Ar released, and a relatively flat age pattern for the final 50% (Fig. 34, left). In the case of aliquot 3, these final steps form a plateau at 118.1 ± 0.8 Ma. Regression of the data in inverse isochron space for aliquot 3 yielded an age of 117.7 ± 1.0 Ma, and a ^{40}Ar/^{36}Ar intercept of 380 ± 70 (Fig. 34, right).

^{40}Ar/^{39}Ar Interpretation:

The plateau age for aliquot 3 of 118.1 ± 0.8 Ma (MSWD = 1.38, n = 7), comprising 58% of ^{39}Ar released, is considered the muscovite cooling age for this sample.

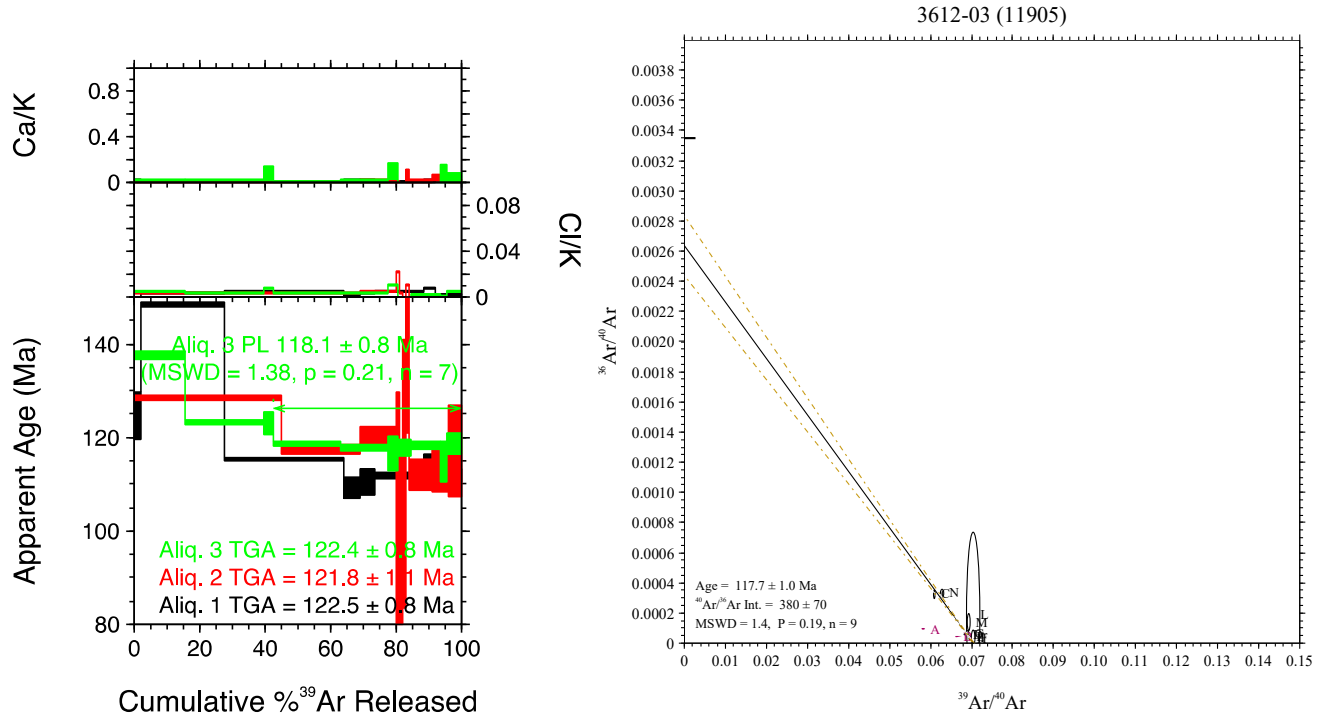

***Figure 34:** (Left) Gas release spectra for 3 aliquots of muscovite from sample 16RAY-AP030A02. (Right) Inverse isochron plot for aliquot 3 of the same sample.*

Sample: 16RAY-AP030A02
Geological unit: Snowcap Assemblage
Sample description: Quartz mica schist, interbedded with quartzite layers and possible igneous injections
Mineral: Biotite

GSC lab number: z11905
Ar#: 3611
Age: 102.5 ± 0.6 Ma
Age interpretation: Cooling age
Confidence: High

Figure 35: *Field photo of schist sample 16RAY-AP030A02. Photograph by A.J. Parsons. NRCan photo 2021-541*

Summary of single crystal step heating results:

Four biotite aliquots from this sample yielded similar spectra with argon loss profiles in younger initial heating steps, rising to older, relatively flat patterns for the mid- to high-temperature steps, including plateaus for aliquots 2, 3 and 4 (Fig. 36, below).

$^{40}Ar/^{39}Ar$ Interpretation

Since aliquots 1 and 3 gave slightly hump-shaped spectra, and aliquot 2 has poorer statistics (MSWD = 2.83), the plateau age for aliquot 4 is considered the cooling age of biotite for this sample, at 102.5 ± 0.6 Ma (MSWD = 0.96, n = 8, 60% of ^{39}Ar released).

Figure 36: *(Below) Gas release spectra for 4 aliquots of biotite from sample 16RAY-AP030A02. (Right) Inverse isochron plot for the same 4 aliquots.*

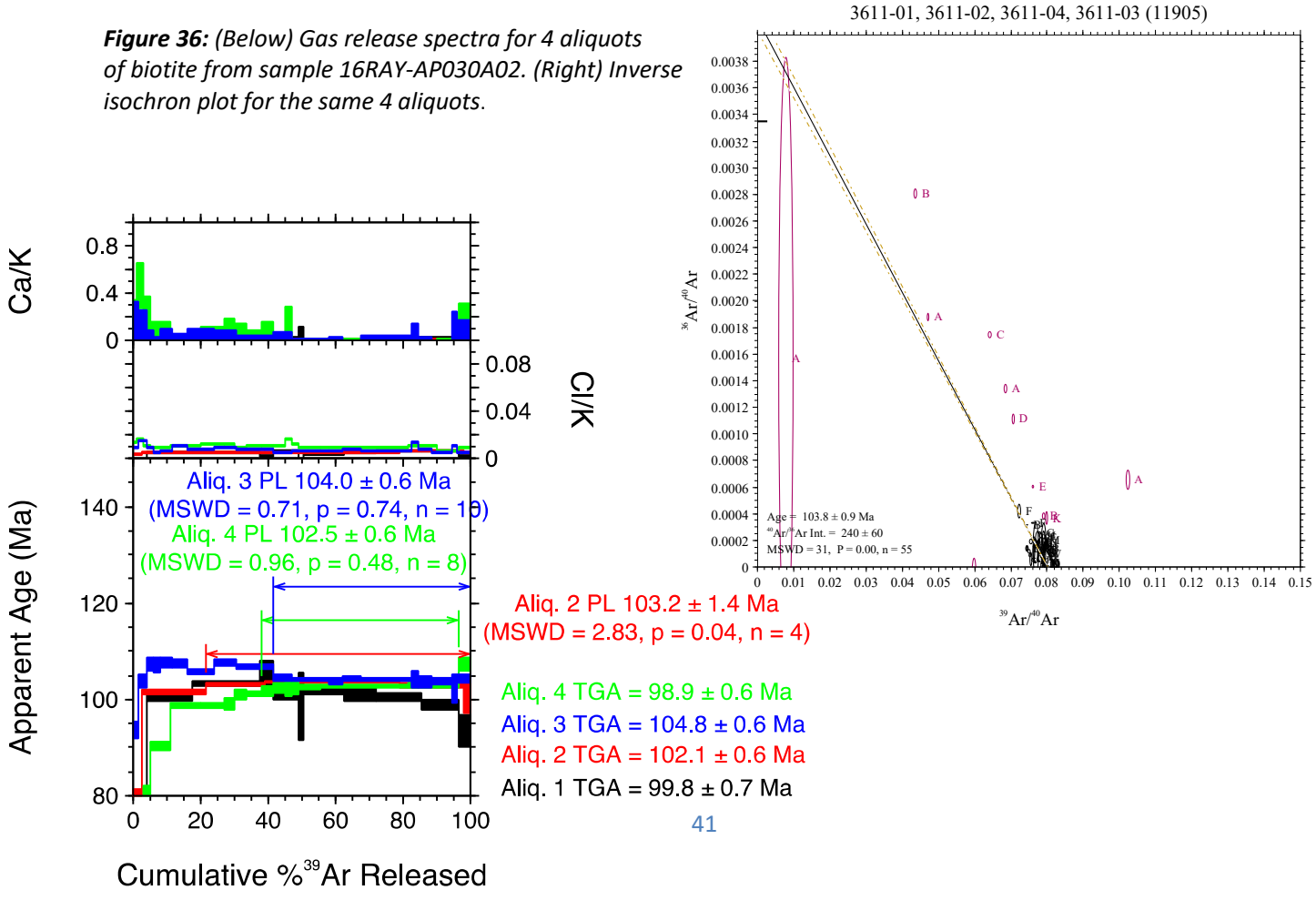

Sample: 16RAY-JR042A02
Geological unit: Rhyolite Creek suite
Sample description: Smoky quartz-biotite porphyritic rhyolite, with minor acicular hornblende
Mineral: Biotite

GSC lab number: z11913
Ar#: 3625
Age: 57.8 ± 0.7 Ma
Age interpretation: Cooling age
Confidence: High

Figure 37: *field shot of rhyolite sample 16RAY-JR042A02, pencil tip for scale. Photograph by J.J. Ryan. NRCan photo 2021-542*

Summary of single crystal step heating results:

Two aliquots of biotite in this sample yielded disparate step heat spectra, and both showed elevated Ca/K in the final heating steps, with aliquot 1 also releasing elevated Ca/K in initial heating steps (Fig. 38, left). Aliquot 1 yielded a plateau at 57.8 ± 0.7 Ma, and a correspondingly well-defined regression in inverse isochron space at 58.3 ± 0.9 Ma (MSWD = 1.9, n = 14) indicating a significant component of atmospheric Ar (Fig. 38, right).

^{40}Ar/^{39}Ar Interpretation:

The plateau age of 57.8 ± 0.7 Ma (MSWD = 1.3, n = 12) for aliquot 1, comprising 83% of ^{39}Ar released, is considered the biotite cooling age for this sample.

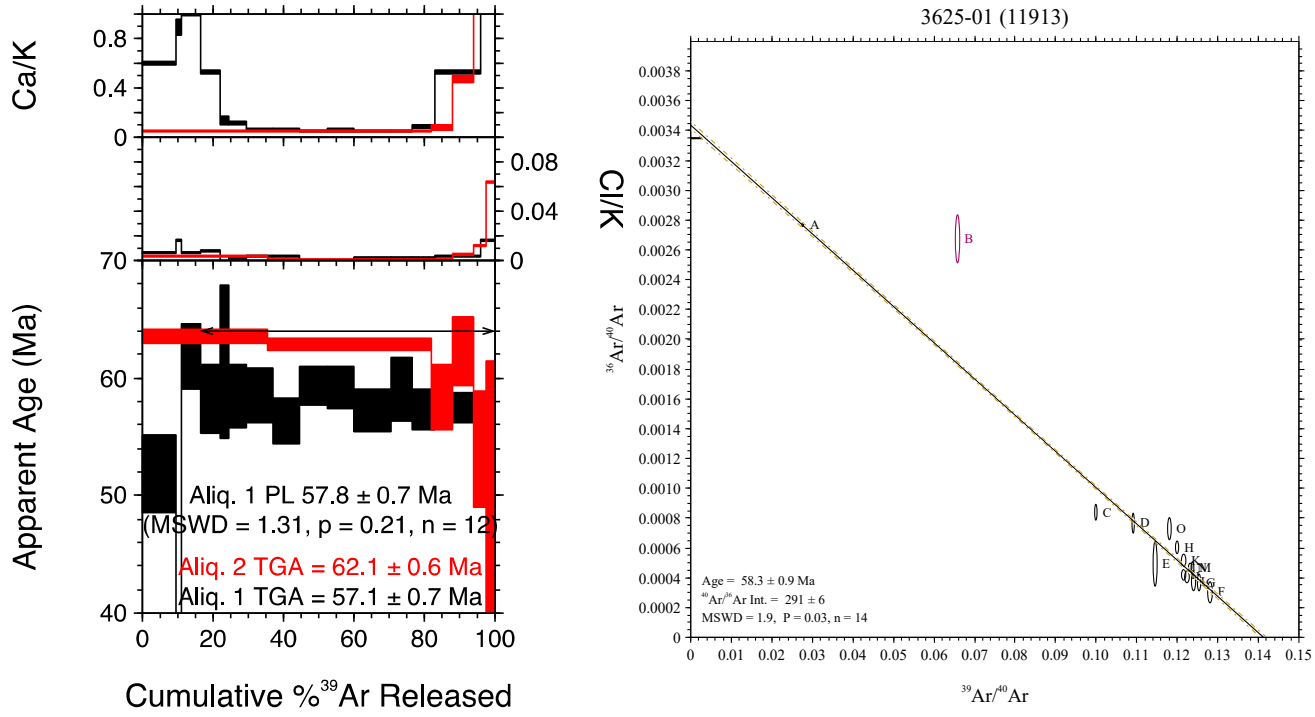

Figure 38*: (Left) Gas release spectra for 2 aliquots of biotite from sample 16RAY-JR042A02. (Right) Inverse isochron plot for aliquot 1 of the same sample.*

Sample: 16RAY-JR067A01
Geological unit: Snowcap Assemblage amphibolite
Sample description: Gneissic, high-strain amphibolite; compositional layering, looks metaplutonic
Mineral: Hornblende

GSC lab number: z11914
Ar#: 3626
Age: 124.0 ± 1.3 Ma
Age interpretation: Cooling age
Confidence: High

Figure 39: *field shot of amphibolite sample 16RAY-JR067A01. Photograph by J.J. Ryan. NRCan photo 2021-543*

Summary of single crystal step heating results:

Four aliquots of hornblende from this sample yielded quite heterogeneous, generally hump-shaped step heat spectra (Fig. 40, left). There is an apparent correlation between age and Ca/K. Aliquot 1 is the most homogeneous of the grains analyzed, in terms of Ca/K. It yielded a plateau age of 124.0 ± 1.3 Ma, and the inverse isochron for the same aliquot confirms this result at 122 ± 3 Ma (MSWD = 0.98, n = 8, $^{40}Ar/^{36}Ar$ intercept of 430 ± 170)(Fig. 40, right).

$^{40}Ar/^{39}Ar$ Interpretation

The plateau age of aliquot 1, 124.0 ± 1.3 Ma (MSWD = 1.5, n = 7) is considered the hornblende cooling age for this sample.

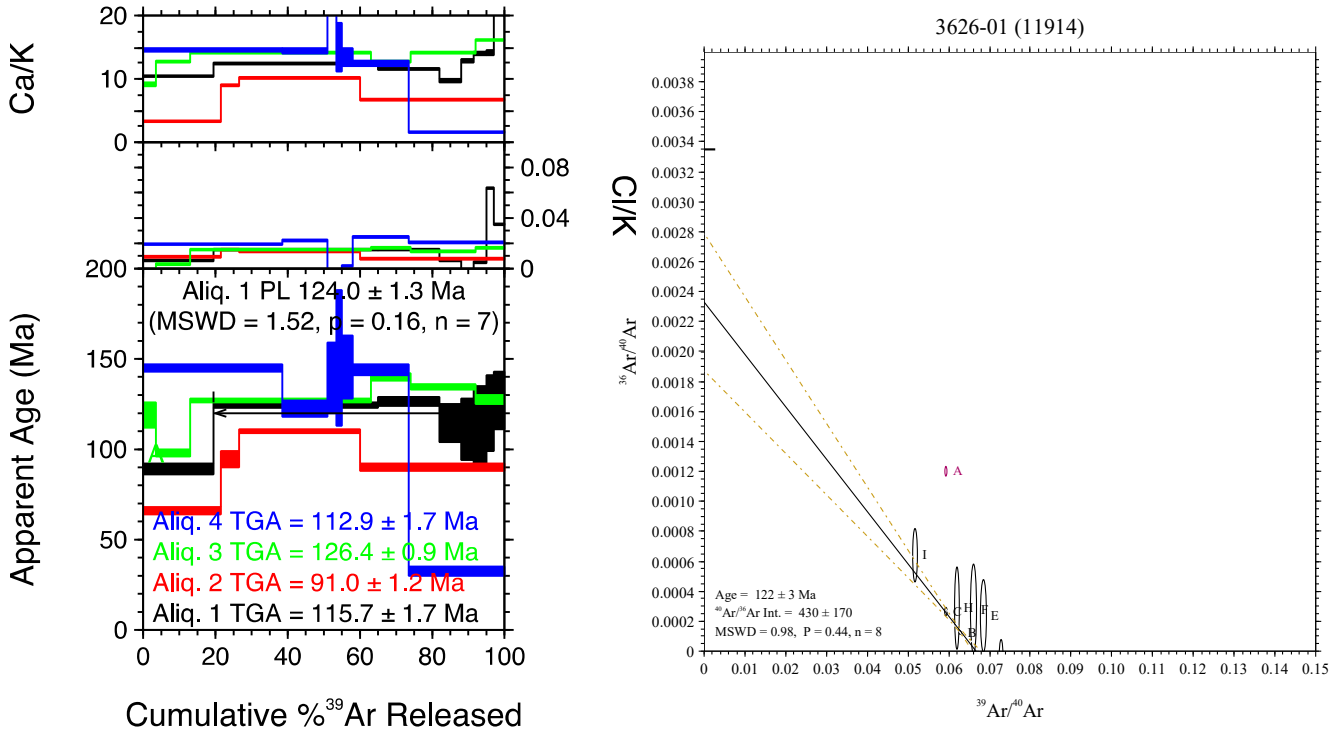

Figure 40*: (Left) Gas release spectra for 4 aliquots of hornblende from sample 16RAY-JR067A01. (Right) Inverse isochron plot for aliquot 1 of the same sample.*

Sample: 16RAY-JR075A02
Geological unit: Stevenson Ridge Schist
Sample description: Felsic schist, garnet porphyroblastic, unclear if metapelitic or metavolcanic protolith; garnet may predate crenulation
Mineral: Muscovite

GSC lab number: z11915
Ar#: 3627
Age: ca. 155 Ma
Age interpretation: Cooling age
Confidence: Low

Figure 41*: Field shot of schist sample 16RAY-JR075A02, pencil tip for scale. Photograph by J.J. Ryan. NRCan photo 2021-544*

Age: ca. 130 Ma
Age interpretation: Partial resetting
Confidence: Low

Summary of single crystal step heating results:

This sample yielded complex increasing staircase spectra for three aliquots (Fig. 42). Integrated ages for the high temperature steps for all aliquots are ca. 155 Ma (Fig. 42, left), and all three aliquots yielded a relatively flat patterns in the central portions of the spectra with integrated ages of ca. 130 Ma (Fig. 42, right).

^{40}Ar/^{39}Ar Interpretation

The step heat spectra suggest that muscovite, with an initial cooling age of ca. 155 Ma, was partially reset with respect to Ar by heating during ca. 130 Ma. Although no robust plateaus were achieved, the reproducibility of the spectra suggest that the integrated ages of ca. 155 Ma and ca. 130 Ma are geologically significant.

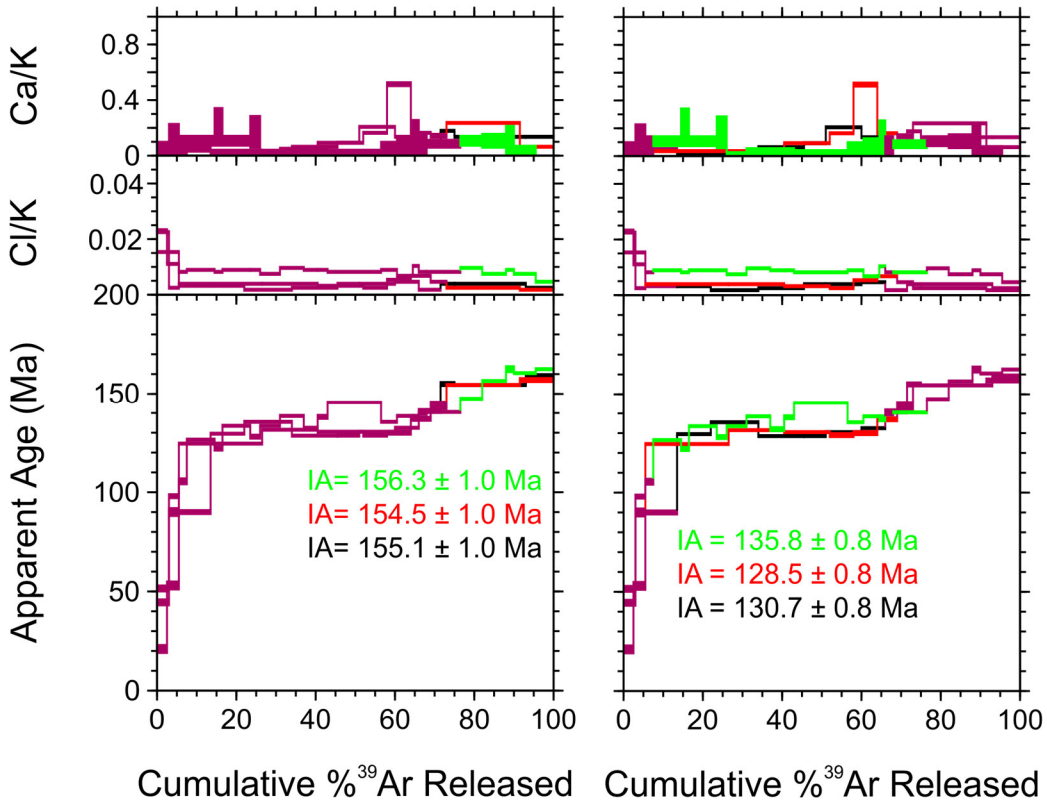

***Figure 42**: Gas release spectra for 3 aliquots of muscovite from sample 16RAY-JR075A02. (Left) Highest temperature heating steps for all three aliquots gave integrated ages of ca. 155 Ma. (Right) The low to mid-temperature steps for all three aliquots gave integrated ages of ca. 130 Ma.*

Sample: 16RAY-JR087C01
Geological unit: Snowcap Assemblage amphibolite
Sample description: Amphibolite layer, interlayered with marble and schist, strongly layered
Mineral: Hornblende

GSC lab number: z11916
Ar#: 3609
Age: 175.2 ± 1.9 Ma
Age interpretation: Cooling age
Confidence: High

Figure 43*: Photograph of layered amphibolite in outcrop. Photograph by J.J. Ryan. NRCan photo 2021-545.*

Summary of single crystal step heating results:

Three aliquots of hornblende from this sample yielded two plateau ages within error at 168 ± 7 Ma and 175.2 ± 1.9 Ma (Fig. 44, left). The inverse isochron for all three aliquots indicates a significant component of atmospheric Ar (Fig. 44, right; $^{40}Ar/^{39}Ar = 300 \pm 8$).

$^{40}Ar/^{39}Ar$ Interpretation:

Age dispersion and spectra heterogeneity for the three aliquots may be a result of the presence of variable argon loss due to crystal defects, or to the degassing of other mineral species that were not visible during grain selection. The Ca/K and Cl/K profiles show significant compositional heterogeneity. Aliquot 1 has the flattest Ca/K profile and produced a robust plateau age; therefore, we favour the aliquot 1 plateau age of 175.2 ± 1.9 Ma (MSWD = 0.96, n = 7) as the hornblende cooling age for this sample.

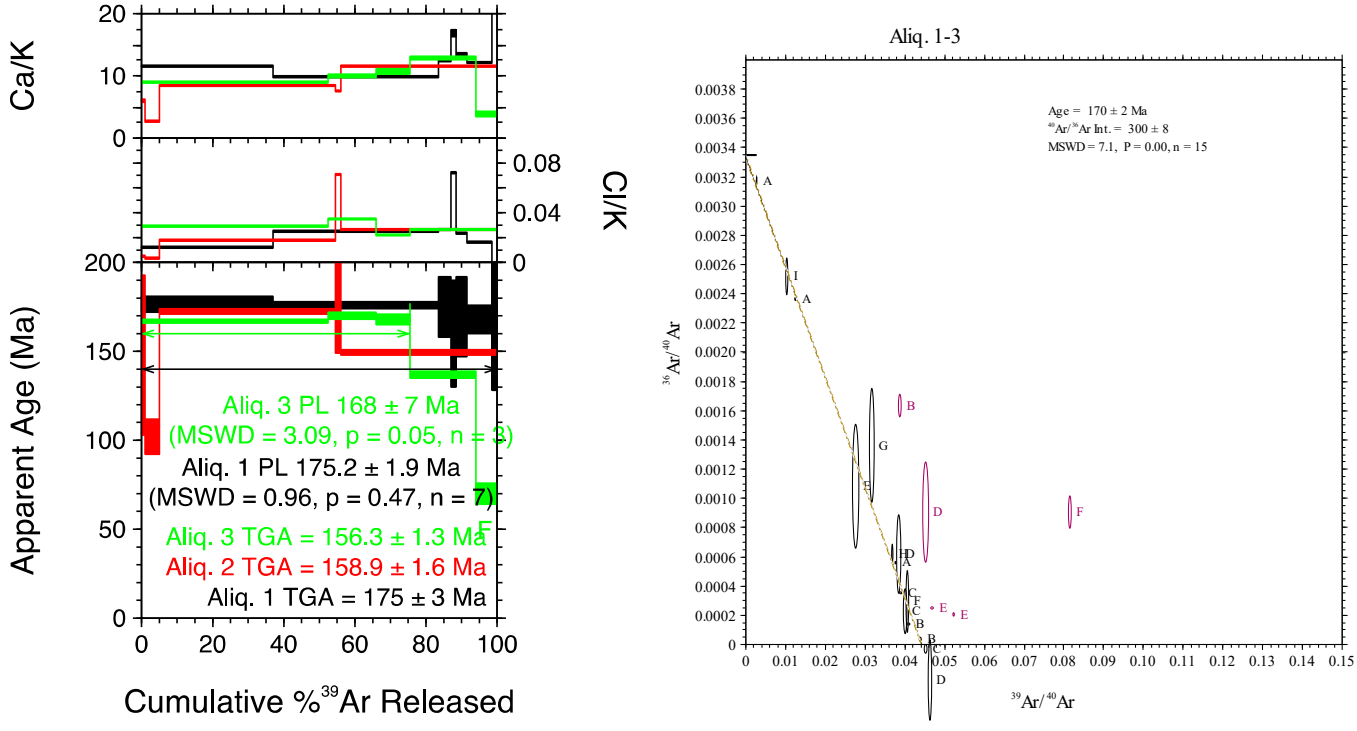

Figure 44: *(Left) Gas release spectra for 3 aliquots of hornblende from sample 16RAY-JR087C01. (Right) Inverse isochron plot for the same 3 hornblende aliquots.*

Sample: 16RAY-JR087C01
Geological unit: Snowcap Assemblage amphibolite
Sample description: Amphibolite layer, interlayered with marble and schist, strongly layered
Mineral: Impure muscovite

GSC lab number: z11916
Ar#: 3610
Age: 96.5 ± 1.5 Ma
Age interpretation: Cooling age
Confidence: Intermediate

Figure 45*: Photograph of layered amphibolite in outcrop. Photograph by J.J. Ryan. NRCan photo 2021-545.*

Summary of single crystal step heating results:

Muscovite from this sample is impure, discoloured, and appears to be intergrown with other material. Muscovite may be a retrograde phase after hornblende in this unit. Grains that were selected for analysis were the cleanest ones available.

Four aliquots from this sample yielded similar step heat age spectra (aliquot 2 failed) with variable amounts of Ar loss from the initial heating steps, and heterogeneous Cl/K and Ca/K during step heating. Aliquot 3 provided a plateau of 89 ± 5 Ma, which is younger than the inverse isochron age for all aliquots of 99.2 ± 1.4 Ma. Aliquots 4 and 5 gave slightly older and more precise step-heat ages, which fall along an excess argon regression line in inverse isochron space. The inverse isochron age for aliquots 4 and 5 is 96.5 ± 1.5 Ma (MSWD=1.1, $^{40}Ar/^{39}Ar = 690 \pm 130$)

$^{40}Ar/^{39}Ar$ Interpretation:

The inverse isochron age for aliquots 4 and 5 of 96.5 ± 1.5 Ma (MSWD=1.1, $^{40}Ar/^{39}Ar = 690 \pm 130$) is interpreted as the cooling age for this sample. This age is preferred over the less precise aliquot 3 plateau age, and because it is calculated using 2 aliquots from this sample for which age dispersion and grain quality were problematic.

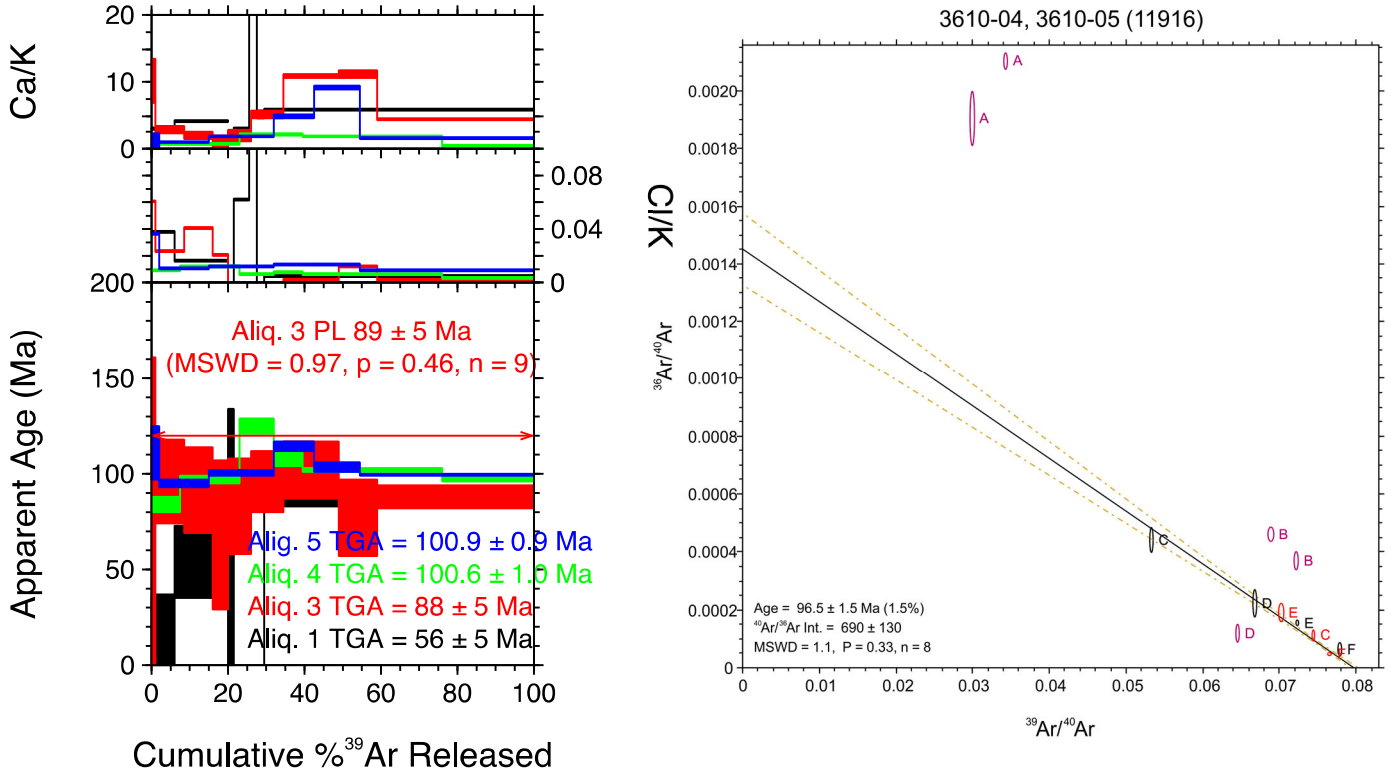

***Figure 46**: (Left) Gas release spectra for 4 aliquots of muscovite from sample 16RAY-JR087C01. (Right) Inverse isochron plot for aliquots 4 and 5 for the same sample.*

Sample: 16RAY-JR092B01
Geological unit: Snowcap Assemblage amphibolite
Sample description: Amphibolite layer, interlayered foliated amphibolite that is quite homogeneous
Mineral: Hornblende

GSC lab number: z11917
Ar#: 3629
Age: 172.1 ± 1.5 Ma
Age interpretation: Cooling age
Confidence: High

***Figure 47**: Field shot of amphibolite sample 16RAY-JR092B01, pencil tip for scale. Photograph by J.J. Ryan. NRCan photo 2021-546.*

Summary of single crystal step heating results:

Step heat spectra, Ca/K, and Cl/K profiles for 4 aliquots of hornblende from this sample were heterogeneous (Fig. 48, left). Mineral inclusions, fluid inclusions, crystal defects, or trapped argon in the grains, all of which were not visible during grain selection, could explain the age dispersion and compositional variability between aliquots. Aliquot 4 yielded a robust plateau with an age of 172.1 ± 1.5 Ma. The inverse isochron regression including all four aliquots is within error of this result at 174 ± 2 Ma and indicates an atmospheric component at $^{40}Ar/^{36}Ar = 312 \pm 8$ (MSWD = 9.2, n = 21).

$^{40}Ar/^{39}Ar$ Interpretation:

The plateau age for aliquot 4 of 172.1 ± 1.5 Ma (MSWD = 1.7, n = 5), comprising 100% of ^{39}Ar released is the interpreted hornblende cooling age for this sample.

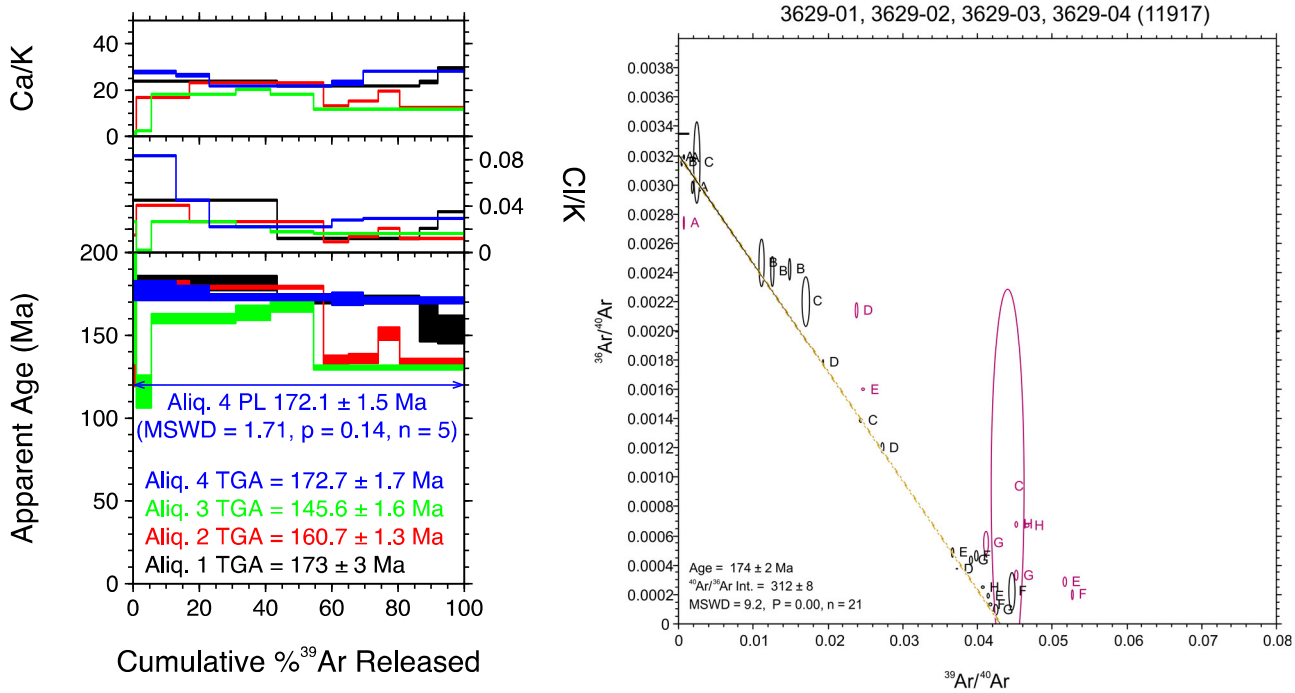

***Figure 48**: (Left) Gas release spectra for 4 aliquots of hornblende from sample 16RAY-JR092B01. (Right) Inverse isochron plot for the same 4 aliquots.*

Sample: 16RAYJR140A01
Geological unit: Sulphur Creek suite
Sample description: High strain potassium feldspar augen porphyroclastic granodiorite; above mylonitized quartzite below
Mineral: Biotite

GSC lab number: z11918
Ar#: 3630
Age: 167.3 ± 1.2 Ma
Age interpretation: Cooling age
Confidence: Intermediate

***Figure 49**: Sample 16RAYJR140A01 in outcrop. Photograph by J.J. Ryan. NRCan photo 2021-547.*

Summary of single crystal step heating results:

Three aliquots of biotite from this sample yielded relatively flat step heat age spectra, despite some variability in Ca/K for aliquot 2. Aliquots 1 and 2 both yielded plateaus, but with discordant ages: 167.3 ± 1.0 Ma and 159.7 ± 1.0 Ma, respectively (Fig. 50, left). Aliquot 3 gave a hump-shaped spectrum. The majority of data in inverse isochron space for all aliquots are concentrated at the radiogenic ($^{39}Ar/^{40}Ar$) axis, which precludes any meaningful regression or intercept calculation (Fig. 50, right).

$^{40}Ar/^{39}Ar$ Interpretation

Both aliquots 1 and 2 yielded robust plateau ages. The plateau age for aliquot 1 of 167.3 ± 1.2 Ma (MSWD = 1.19, n = 8, 93% of ^{39}Ar released) is interpreted as the biotite cooling age for this sample, based on the fact that it is compositionally more homogeneous than aliquot 2, and the plateau comprises more steps and a larger proportion of the total released gas than the plateau from aliquot 2.

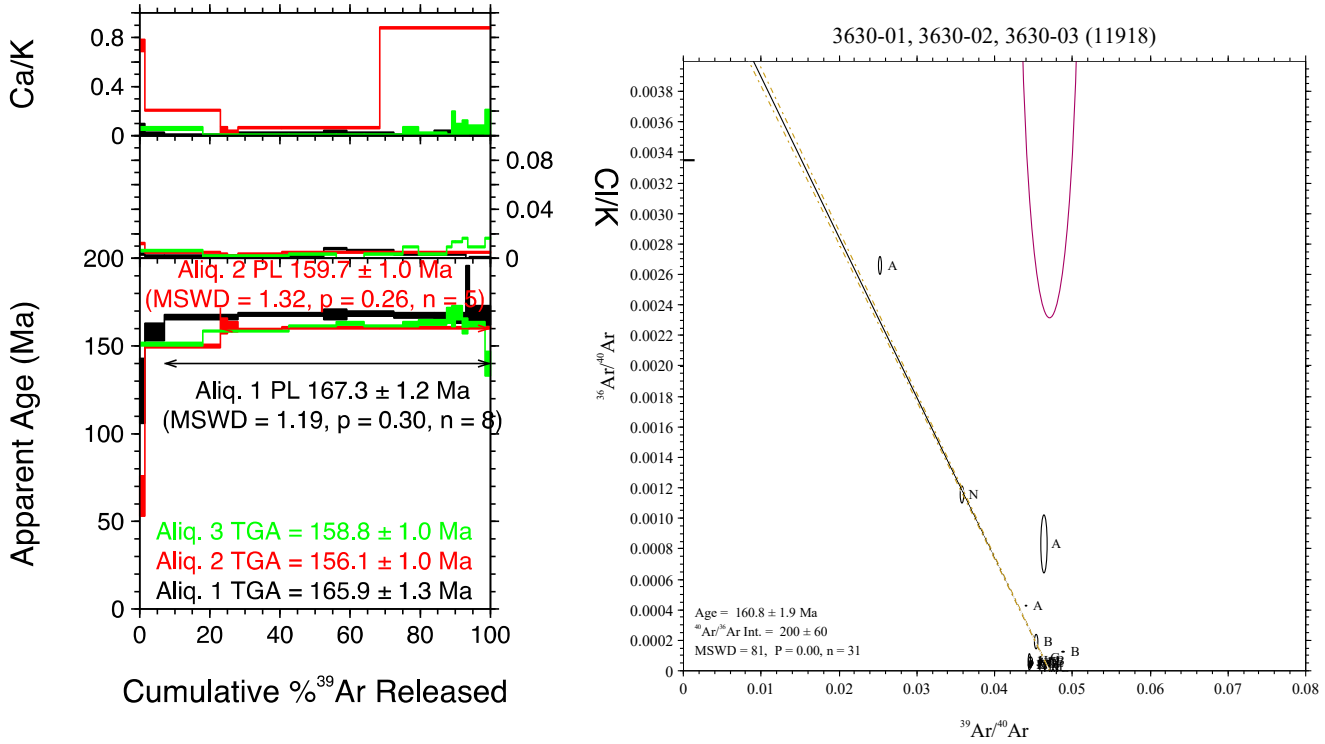

***Figure 50**: (Left) Gas release spectra for 3 aliquots of biotite from sample 16RAYJR140A01. (Right) Inverse isochron plot for the same 3 aliquots.*

Sample: 16RAY-JR140D01
Geological unit: Snowcap Assemblage
Sample description: Quartz mica schist with coarse muscovite
Mineral: Biotite

GSC lab number: z11919
Ar#: 3637
Age: 198.8 ± 1.5 Ma
Age interpretation: Cooling age
Confidence: Low

Figure 51*: Field photo of schist sample 16RAY-JR140D01. Photograph by J.J. Ryan. NRCan photo 2021-548.*

Summary of single crystal step heating results:

Two biotite aliquots provided similar staircase step heat spectra, with aliquot 2 producing a plateau age of 198.8 ± 1.5 Ma for the majority of the high-temperature heating steps. The data do not allow for a regression in inverse isochron space.

^{40}Ar/^{39}Ar Interpretation:

The plateau age for aliquot 2 of 198.8 ± 1.5 Ma (MSWD = 1.13, n = 7) comprising 76% of ^{39}Ar released is interpreted as the best estimate for the biotite cooling age for this sample. However, note that it is >10% older than muscovite from the same sample (Ar# 3631), which may be an indication of excess Ar. Consequently, this interpretation has been assigned a low confidence.

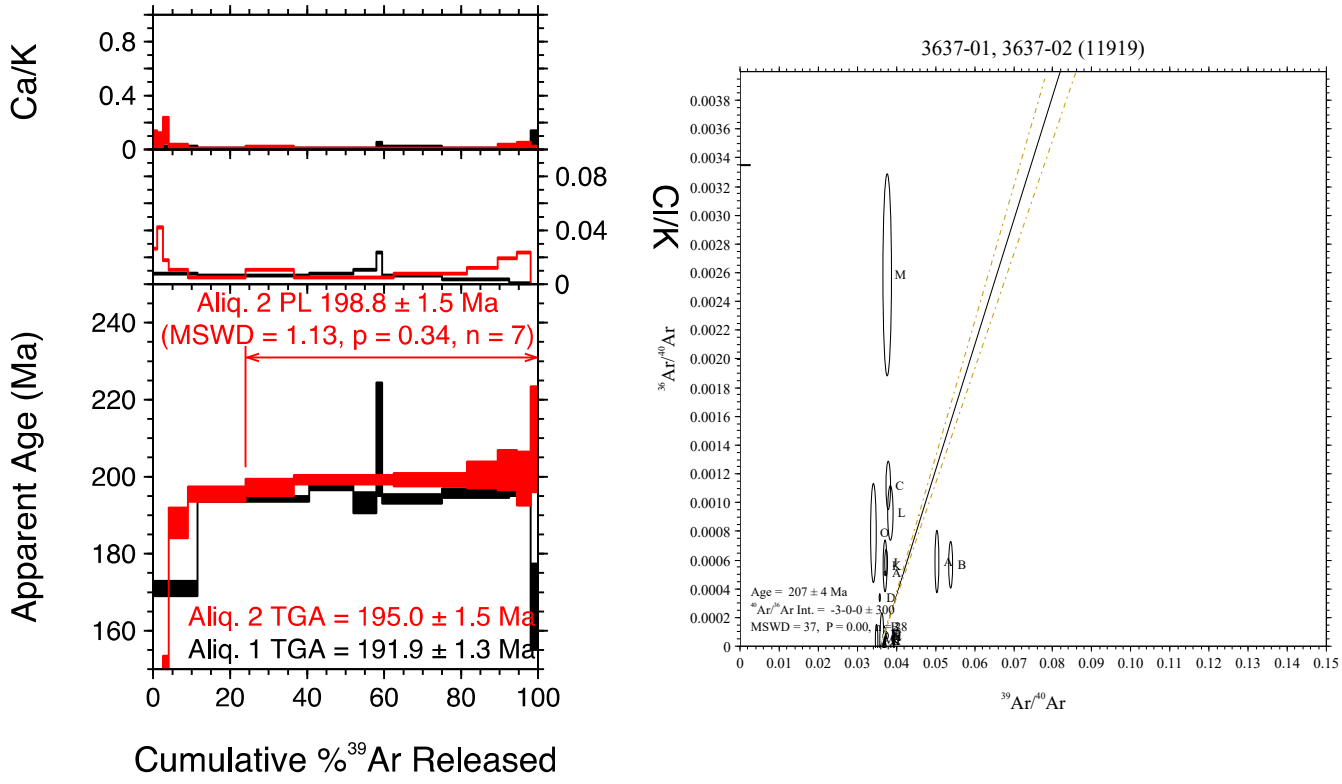

***Figure 52**: (Left) Gas release spectra for 2 aliquots of biotite from sample 16RAY-JR140D01. (Right) Inverse isochron plot for the same 2 aliquots. Data for the mid- to high-temperature steps cluster near the x-axis, precluding a linear regression and any evaluation of possible excess argon presence.*

Sample: 16RAY-JR140D01
Geological unit: Snowcap Assemblage
Sample description: Quartz mica schist with coarse muscovite
Mineral: Muscovite

GSC lab number: z11919
Ar#: 3631
Age: 172.4 ± 1.0 Ma
Age interpretation: Cooling age
Confidence: High

Figure 53*: Field photo of schist sample 16RAY-JR140D01. Photograph by J.J. Ryan. NRCan photo 2021-548.*

Summary of single crystal step heating results:

Two aliquots of muscovite provide similar, homogeneous step heat spectra (Fig. 54) Aliquot 1 yielded a plateau age of 171.6 ± 1.1 Ma (MSWD = 1.02, n = 10, 98.8% of ^{39}Ar released) and aliquot 2 gave a plateau age of 173.6 ± 1.3 Ma (MSWD = 1.02, n = 8, 97% of ^{39}Ar released). The inverse isochron plot including both aliquots yields a similar result of 173.2± 1.4 Ma (MSWD = 2.8, n = 19).

^{40}Ar/^{39}Ar Interpretation:

The ages differ by 2 Ma, which could reflect contracted crystal growth history. Because both plateau ages are robust, we calculated the weighted mean plateau age for aliquots 1 and 2, to give 172.4 ± 0.8 Ma (2σ internal errors). As this calculated error falls below the precision of the 0.6% (2σ) long term reproducibility of the FCT-Sanidine flux monitor age, this result is more appropriately reported as 172.4 ± 1.0 Ma, and is interpreted as the muscovite cooling age for this sample.

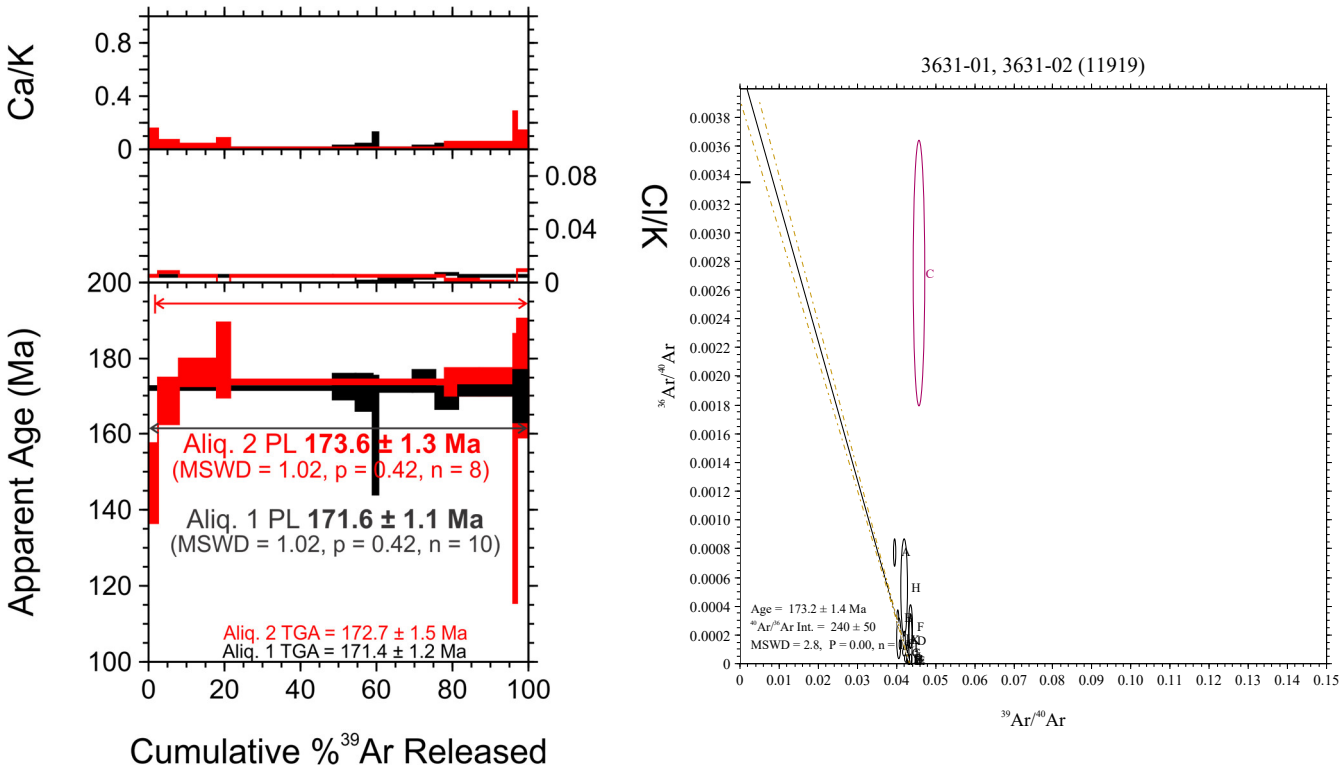

***Figure 54**: (Left) Gas release spectra for 2 aliquots of muscovite from sample 16RAY-JR140D01. (Right) Inverse isochron plot for the same 2 aliquots.*

Sample: 16RAY-JR143A01
Geological unit: Snowcap Assemblage
Sample description: Metaquartzite; grey to white impure quartzite; abundant isoclinal folds showing relatively high strain
Mineral: Biotite

GSC lab number: z11920
Ar#: 3632

Age: ~130 Ma
Age interpretation: Cooling age estimate
Confidence: Low

Figure 55*: Field photo of metaquartzite sample 16RAY-JR143A01. Photograph by J.J. Ryan. NRCan photo 2021-549.*

Age: ~100 Ma
Age interpretation: Minimum cooling age
Confidence: Low

Summary of single crystal step heating results:

Aliquot 1 from this sample yielded a generally older step heat pattern than aliquots 2 and 3, but with the same staircase pattern (Fig. 56). Aliquots 2 and 3 are similar, with high temperature age steps of ca. 100 Ma.

^{40}Ar/^{39}Ar Interpretation:

Aliquot 2 and 3 step heat patterns suggest incomplete resetting of biotite with an initial cooling age of ca. 100 Ma. However, the discordance of aliquot 1, and the general heterogeneity of both 2 and 3 prevent an accurate age interpretation. For context, the grain sizes of aliquots 1, 2, and 3 were 400µm, 350µm, and 750µm, respectively. If grain size difference was a driving factor in yielding discordant ages, then the aliquot with the largest grain size would be expected to yield the least-reset and, hence, oldest age. This is not the case, given that aliquots 2 and 3 gave the same age despite being very different in size.

The ca. 130 Ma age for the high temperature steps in aliquot 1 may reflect an earlier cooling event not preserved in aliquots 2 and 3, but the confidence in this age is low.

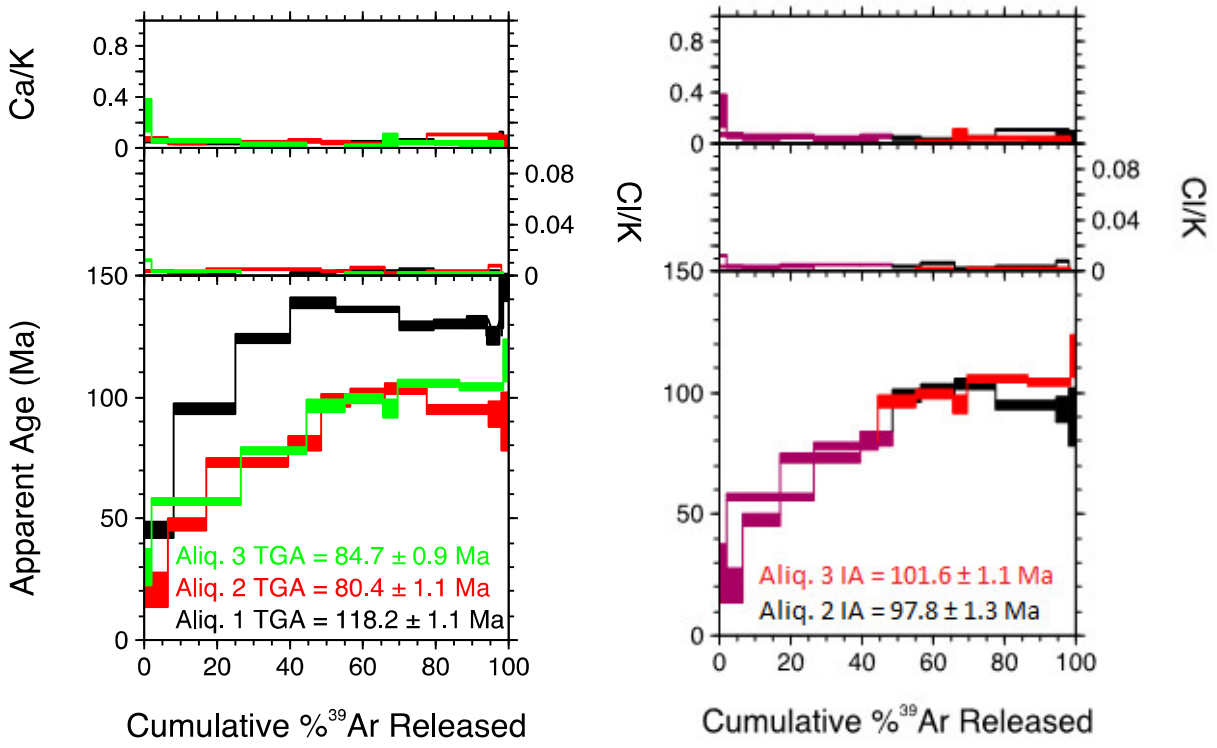

***Figure 56**: (Left) Gas release spectra for 3 aliquots of biotite from sample 16RAY-JR143A01, showing total gas ages. (Right) Same spectra with ca. 100 Ma high-temperature steps of aliquots 2 and 3 highlighted. Integrated ages for the high temperature steps are shown.*

Sample: 16RAY-JR174A02
Geological unit: Klondike Schist
Sample description: Sheared greenschist with relict hornblende
Mineral: Hornblende

GSC lab number: z11921
Ar#: 3633
Age: 131 ± 4 Ma
Age interpretation: Cooling age
Confidence: Low

***Figure 57**: Field photo of greenschist sample 16RAY-JR174A02. Photograph by J.J. Ryan. NRCan photo 2021-550.*

Summary of single crystal step heating results:

Three aliquots of hornblende yielded generally hump-shaped and heterogeneous step heat spectra (Fig. 58, left). The inverse isochron age for these combined data is 131 ± 4 Ma, with an atmospheric $^{40}Ar/^{36}Ar$ intercept of 300 ± 20 (Fig. 58, right).

$^{40}Ar/^{39}Ar$ Interpretation:

The inverse isochron age of 131 ± 4 Ma (MSWD = 28, n = 11) is the best estimate for the hornblende cooling age of this sample.

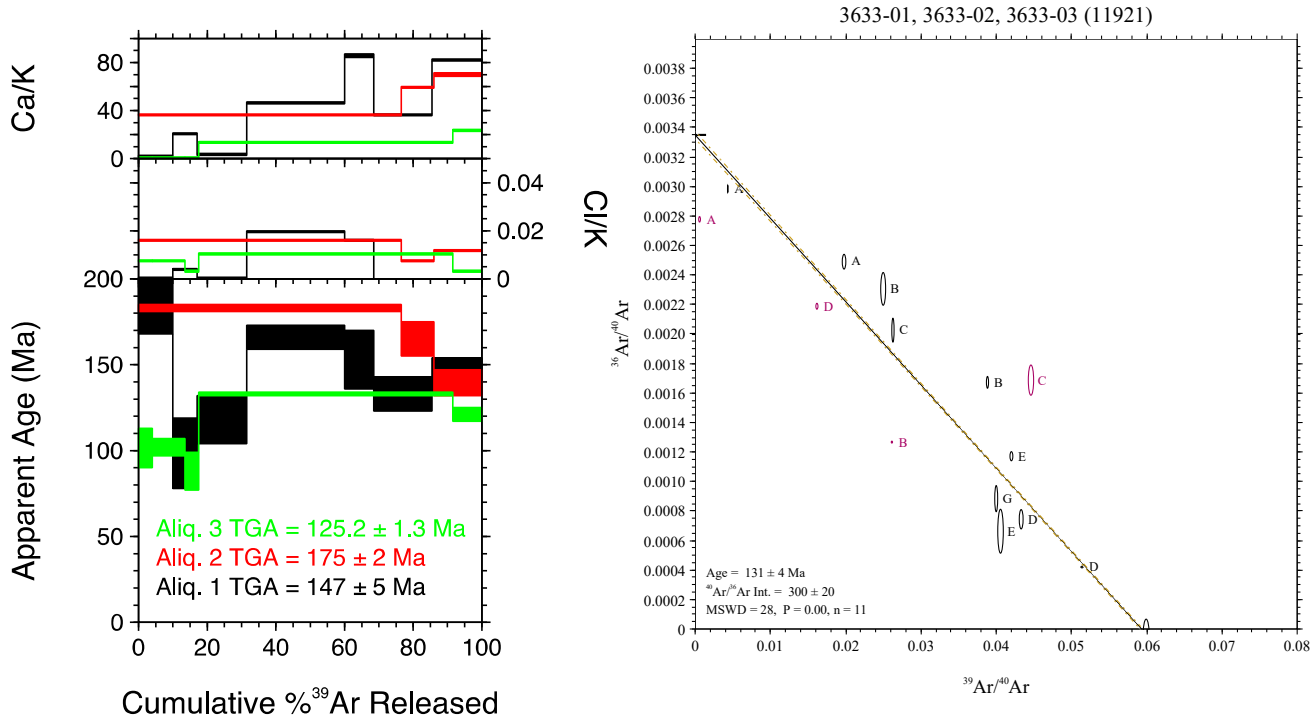

***Figure 58**: (Left) Gas release spectra for 3 aliquots of hornblende from sample 16RAY-JR174A02. (Right) Inverse isochron plot for the same 3 aliquots.*

Sample: 16RAY-JR182A01
Geological unit: Sulphur Creek suite
Sample description: Felsic orthogneiss, muscovite rich. Very high strain, highly fissile, almost a schist, unclear if it is derived from a porphyry or granitoid
Mineral: Biotite

GSC lab number: z11922
Ar#: 3662
Age: 100.6 ± 0.7 Ma
Age interpretation: Cooling age
Confidence: High

***Figure 59**: Hand sample of felsic orthogneiss sample 16RAY-JR182A01. Photograph by J.J. Ryan. NRCan photo 2021-551.*

Summary of single crystal step heating results:

Two aliquots of biotite produced concordant plateau ages of 100.4 ± 0.7 Ma (Aliq. 1; MSWD = 1.35, n = 9, 88.4% of ^{39}Ar released) and 100.8 ± 0.7 Ma (Aliq. 2; MSWD = 0.35, n = 6, 91% of ^{39}Ar released)(Fig. 60, left).

^{40}Ar/^{39}Ar Interpretation:

The weighted mean of the plateau ages for both aliquots is 100.6 ± 0.5 Ma. As this calculated error falls below the precision of the individual plateau age results, this result is more appropriately reported as 100.6 ± 0.7 Ma, and is interpreted as the biotite cooling age for this sample.

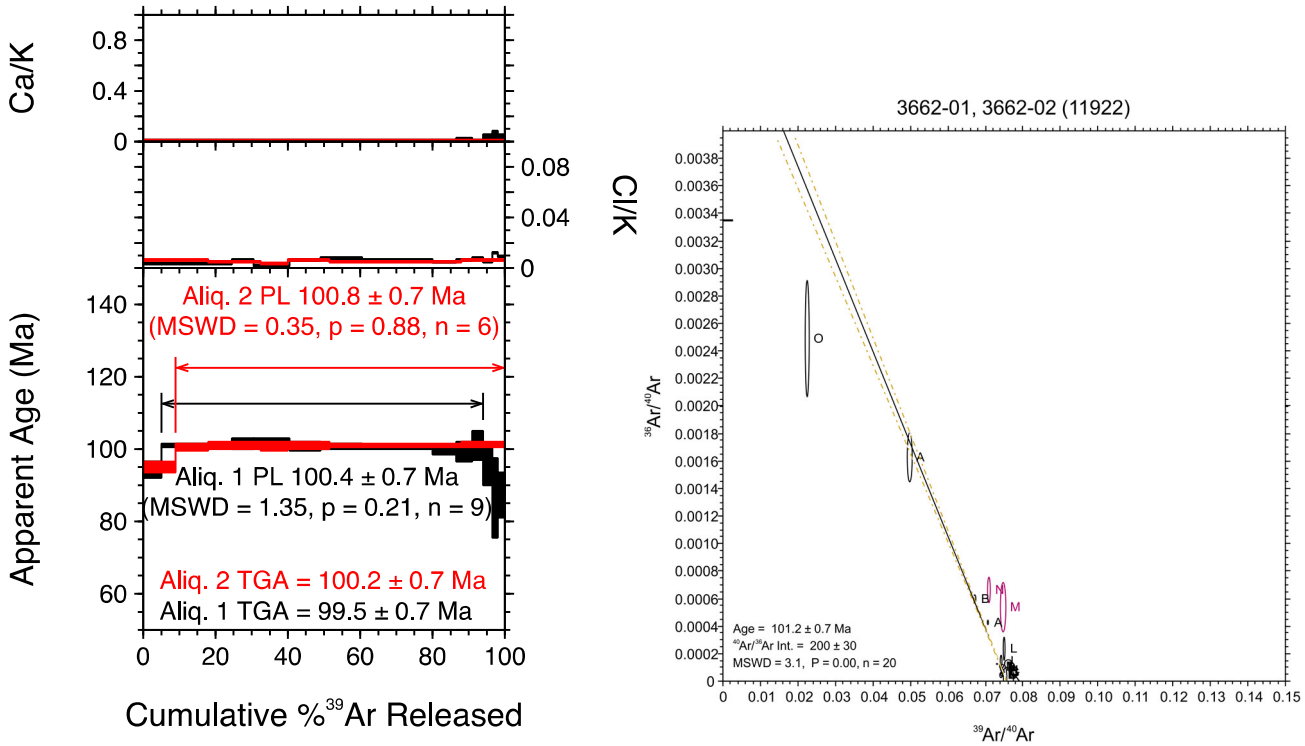

***Figure 60**: (Left) Gas release spectra for 2 aliquots of biotite from sample 16RAY-JR182A01. (Right) Inverse isochron plot for the same 2 aliquots.*

Sample: 16RAY-JR182A01
Geological unit: Sulphur Creek suite
Sample description: Felsic orthogneiss, muscovite rich. Very high strain, highly fissile, almost a schist, unclear if it is derived from a porphyry or granitoid
Mineral: Muscovite

Figure 61*: Hand sample of felsic orthogneiss sample 16RAY-JR182A01. Photograph by J.J. Ryan. NRCan photo 2021-551.*

GSC lab number: z11922
Ar#: 3635
Age: ca. 170 Ma
Age interpretation: Minimum cooling age
Confidence: Low

Age: 159.0 ± 1.0 Ma
Age interpretation: Partially reset
Confidence: Low

Summary of single crystal step heating results:

Three aliquots produced similar staircase pattern step heat spectra, with aliquot 1 producing a plateau of 159 ± 1 Ma (MSWD = 1.2, n = 5), comprising 72% of ^{39}Ar released, but having overall a younger total gas age, and general younger heating steps at all stages of the step heat spectra compared to aliquots 2 and 3 (Fig. 62, left).

^{40}Ar/^{39}Ar Interpretation:

The plateau age for aliquot 1 of 159.0 ± 1.0 Ma (MSWD = 1.18, n = 5), comprising 72% of ^{39}Ar released, provides an estimate of the cooling age for this sample. However, aliquots 2 and 3 are discordant with this interpretation. Their high temperature heating steps suggest the muscovite may have been reset from an initial cooling age of ca. 170 Ma. A low confidence level has been assigned to this age interpretation due to the discordance between aliquots and lack of plateau to confirm an earlier cooling event that appears to be recorded in aliquots 2 and 3.

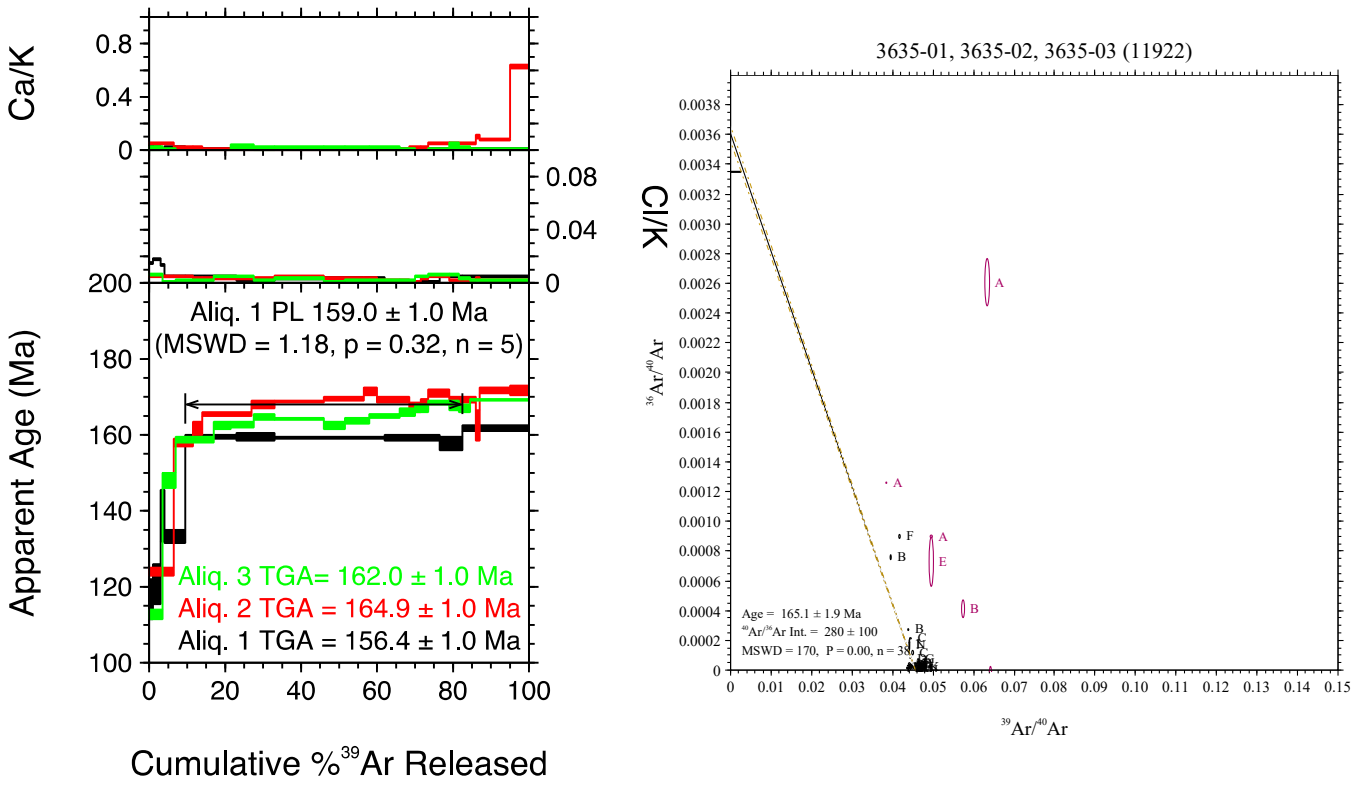

***Figure 62**: (Left) Gas release spectra for 3 aliquots of muscovite from sample 16RAY-JR182A01. (Right) Inverse isochron plot for the same 3 aliquots.*

Sample: 16RAY-SI015A01
Geological unit: Mount Nansen Group
Sample description: Hornblende-plagioclase porphyritic volcanic breccia, weathers bleached blue-grey
Mineral: Hornblende

GSC lab number: z11923
Ar#: 3636
Age: 100 ± 2 Ma
Age interpretation: Cooling age
Confidence: High

***Figure 63**: Hand specimen of volcanic breccia sample 16RAY-SI015A01. Photo courtesy of S.A. Israel*

Summary of single crystal step heating results:

All four aliquots analyzed for this sample produced plateaus ranging from 96-101 Ma (Fig. 64, left). Most data points for all four aliquots plot along the atmospheric line on the inverse isochron plot (Fig. 64, right), giving an inverse isochron age of 100 ± 2 Ma (MSWD = 2.5, n = 23, $^{40}Ar/^{36}Ar$ = 292 ± 5).

$^{40}Ar/^{39}Ar$ Interpretation:

The inverse isochron age of 100 ± 2 Ma (MSWD = 2.5, n = 23, $^{40}Ar/^{36}Ar$ = 292 ± 5), provides the cooling age for this sample.

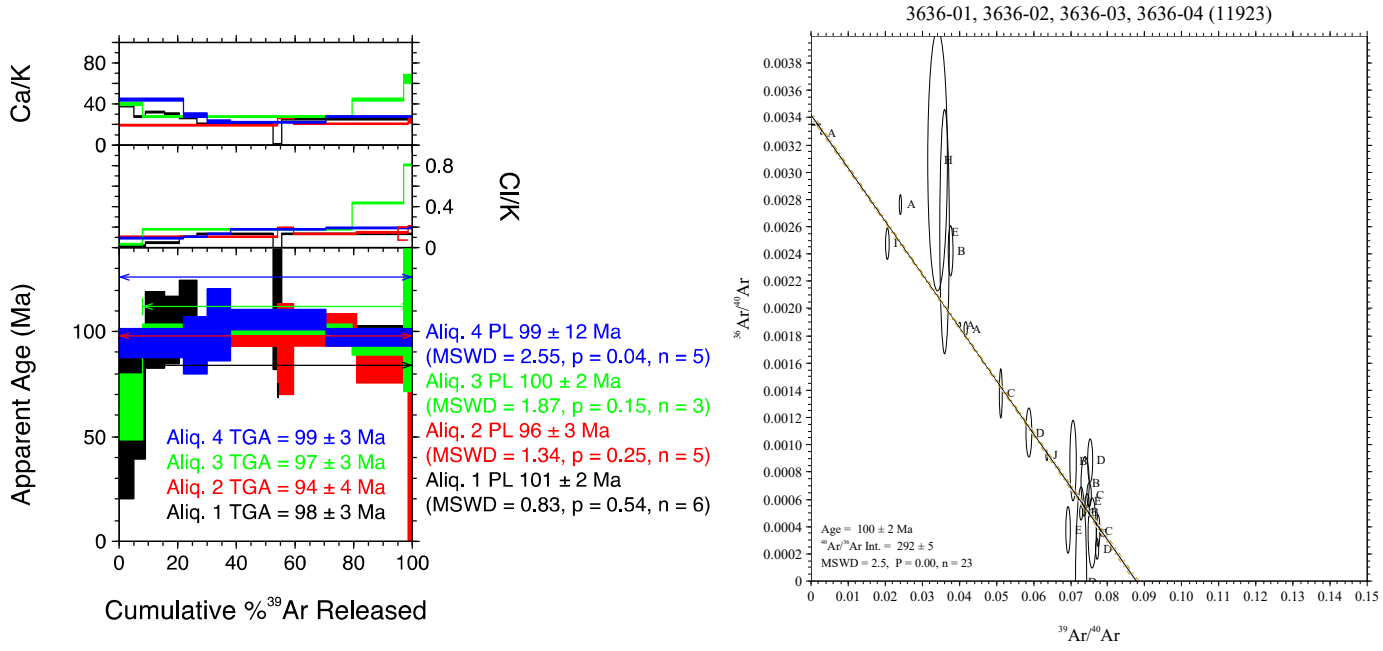

***Figure 64**: (Left) Gas release spectra for 4 aliquots of hornblende from sample 16RAY-SI015A01. (Right) Inverse isochron plot for the same 4 aliquots.*

Sample: 16RAY-JR038A02
Geological unit: Snowcap Assemblage
Sample description: Siliciclastic paragneiss Laminated to gneissic; leucosome or injections present
Mineral: Muscovite

GSC lab number: z11924
Ar#: 3624
Age: 177.5 ± 1.1 Ma
Age interpretation: Cooling age
Confidence: High

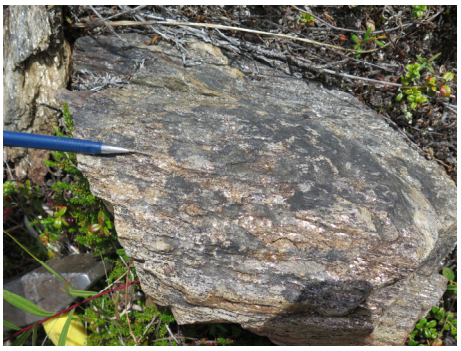

***Figure 65**: Field photo of paragneiss sample 16RAY-JR038A02. Photograph by J.J. Ryan. NRCan photo 2021-552.*

Summary of single crystal step heating results:

Two muscovite aliquots produced identical plateau age results of 177.8 ± 1.6 Ma (Aliq. 1) and 177.4 ± 1.0 Ma (Aliq. 2)(Fig. 66, left). These results are also concordant with the inverse isochron age (combining both aliquots) of 177.7 ± 1.1 Ma (Fig. 66, right; MSWD = 2, n = 23).

^{40}Ar/^{39}Ar Interpretation:

The weighted mean of both plateau ages for aliquots 1 and 2 is 177.5 ± 0.9 Ma. As this calculated error falls below the precision of the 0.6% (2σ) long term reproducibility of the FCT-Sanidine flux monitor age, this result is more appropriately reported as 177.5 ± 1.1 Ma, and is interpreted as the muscovite cooling age for this sample.

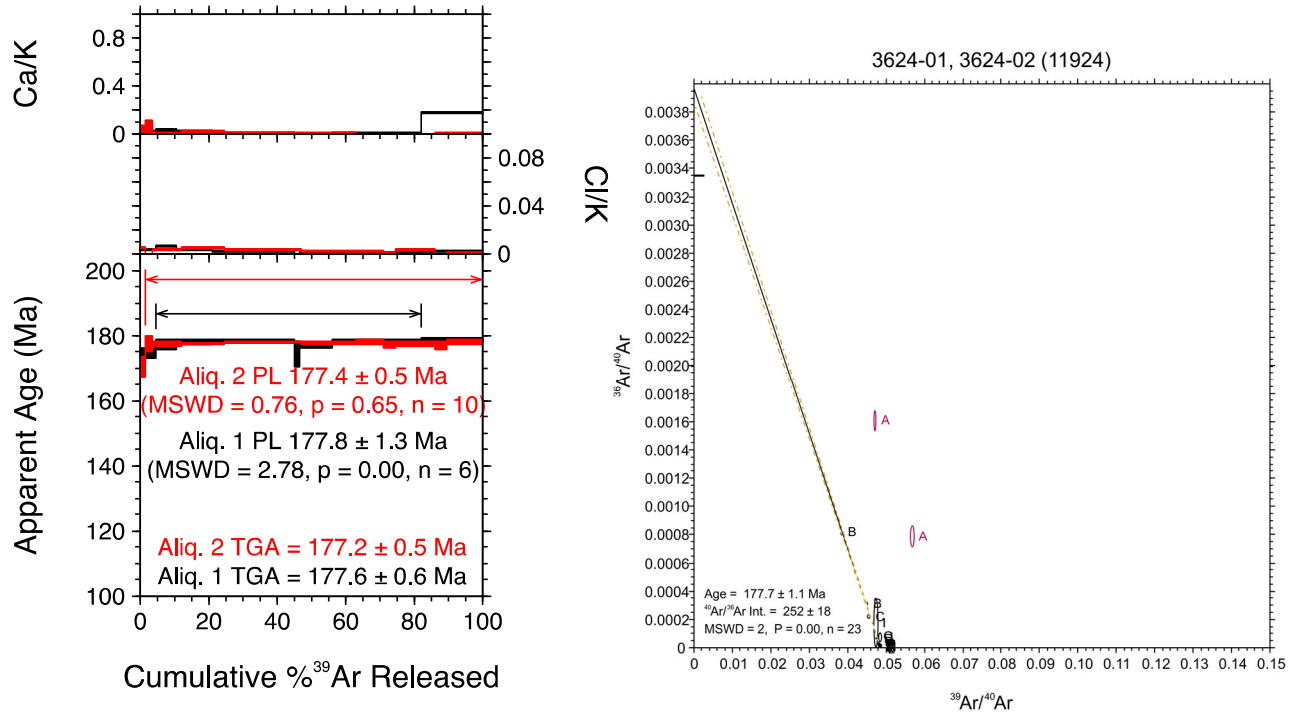

***Figure 66**: (Left) Gas release spectra for 2 aliquots of muscovite from sample 16RAY-JR038A02. (Right) Inverse isochron plot for the same 2 aliquots.*

Sample: 16RAY-JR038A02
Geological unit: Snowcap Assemblage
Sample description: Siliciclastic paragneiss
Laminated to gneissic; leucosome or injections present
Mineral: Biotite

GSC lab number: z11924
Ar#: 3623
Age: No age
Age interpretation: N/A

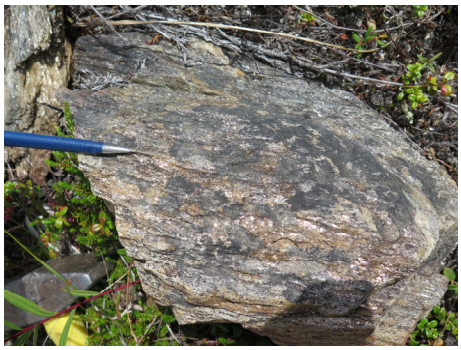

***Figure 67**: Field photo of paragneiss sample16RAY-JR038A02. Photograph by J.J. Ryan. NRCan photo 2021-552.*

Summary of single crystal step heating results:
Three biotite aliquots yielded disparate step heat spectra with similar hump-shaped patterns (Fig. 68, left). Data on the inverse isochron plot were scattered and inconclusive (Fig. 68, right).

$^{40}Ar/^{39}Ar$ Interpretation:
No possible age interpretation can be formulated.

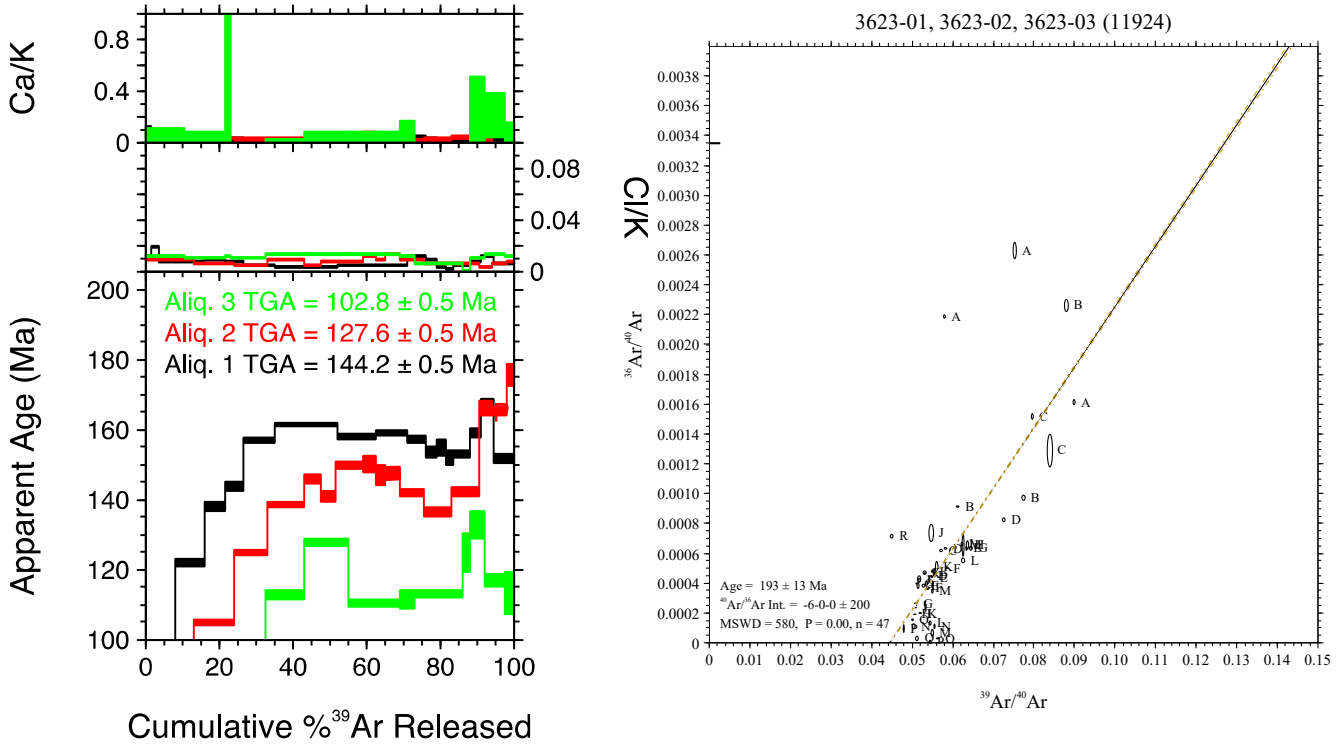

***Figure 68**: (Left) Gas release spectra for 2 aliquots of biotite from sample 16RAY-JR038A02. (Right) Inverse isochron plot for the same 2 aliquots.*

ACKNOWLEDGMENTS

The authors wish to thank Tom Pestaj, Pat Hunt and Linda Cataldo for analytical assistance, and Steve Israel, Andy Parsons, Mark Coleman, Yannick Morneau and Melissa Friend for field mapping and sample collection. This work benefitted from a thorough critical review by Bill Davis, and fruitful discussions with Jeremy Powell.

REFERENCES

Berman, R.G., Ryan, J.J., Gordey, S.P., and Villeneuve, M., 2007. Permian to Cretaceous polymetamorphic evolution of the Stewart River region, Yukon-Tanana terrane, Yukon, Canada: P-T evolution linked with in-situ SHRIMP monazite geochronology: Journal of Metamorphic Geology, v. 25, p. 803–827.

Black, L.P., Kamo, S.L., Allen, C.M., Davis, D.W., Aleinikoff, J.N., Valley, J.W., Mundil, R., Campbell, I.H., Korsh, R.J., Williams, I.S., Foudoulis, C., 2004. Improved $^{206}Pb/^{238}U$ microprobe geochronology by monitoring of a trace-element-related matrix effect; SHRIMP, ID-TIMS, ELA-ICP-MS and oxygen isotope documentation for a series of zircon standards: Chemical Geology, 205, 115-140.

Colpron, M. and Nelson, J. L., 2011. A digital atlas of Terranes for the Northern Cordillera; BC GeoFile 2011-11.

Deino, A.L., 2001. User's manual for Mass Spec v. 5.02. Berkeley Geochronology Center Special Publication 1a, Berkeley Geochronology Center, Berkeley California, 119 p.

Dickinson, W. R., and Gehrels, G. E., 2009. Use of U-Pb ages of detrital zircons to infer maximum depositional ages of strata: A test against a Colorado Plateau Mesozoic database. Earth and Planetary Science Letters, 288 (1-2), 115-125.

Dubman, M., 2016. Petrogenesis and significance of the Schist Creek mafic-ultramafic complex, southwest Yukon; B.Sc. Dissertation, Simon Fraser University, Burnaby, BC. p. 73.

Grond, H.C., Churchill, S.J., Armstrong, R.L., Harakal, J.E., and Nixon, G.T., 1984. Late Cretaceous age of the Hutshi, Mount Nansen, and Carmacks groups, southwestern Yukon Territory and northwestern British Columbia. Canadian Journal of Earth Sciences, 21, 554-558. doi:10.1139/e84-060.

Israel, S., Murphy, D.C., Bennett, V., Mortensen, J.K. and Crowley, J., 2011. New insights into the geology and mineral potential of the Coast Belt in southwestern Yukon. In: Yukon Exploration and Geology 2010, K.E. MacFarlane, L.H. Weston and C. Relf (eds.), Yukon Geological Survey, p. 101-123.

Joyce, N. L., Iraheta Muniz, P., Rayner, N. M., Ryan, J. J., 2020. Geochronology of the Mount Nansen-Nisling River area, Yukon; Geological Survey of Canada, Open File 8614, 28 p. https://doi.org/10.4095/321802

Kellett, D.A., and Joyce, N., 2014. Analytical details of single- and multicollection $^{40}Ar/^{39}Ar$ measurements for conventional step-heating and total-fusion age calculation using the Nu Noblesse at the Geological Survey of Canada. Geological Survey of Canada, Technical Note 8, 27 p.

Klocking, M., Mills, L. Mortensen, J., and Roots, C., 2016. Geology of mid-Cretaceous volcanic rocks at Mount Nansen, central Yukon, and their relationship to the Dawson Range batholith; Yukon Geological Survey, Open File 2016-25, 37 p.

Lee, J.-Y., Marti, K., Severinghaus, J.P., Kawamura, K., Yoo, H.-S., Lee, J.B., Kim, J.S., 2006. A redetermination of the isotopic abundances of atmospheric Ar. Geochimica et Cosmochimica Acta 70, 4507–4512.

Ludwig, K.R., 2003. User's manual for Isoplot/Ex rev. 3.00: a Geochronological Toolkit for Microsoft Excel. Special Publication, 4, Berkeley Geochronology Center, Berkeley, 70 p.

Min, K., Mundil, R., Renne, P.R. and Ludwig, K.R., 2000. A test for systematic errors in 40Ar/39Ar geochronology through comparison with U/Pb analysis of a 1.1-Ga rhyolite. Geochimica et Cosmochimica Acta, 64(1), 73-98.

Mortensen, J.K., 1992. Pre-mid-Mesozoic tectonic evolution of the Yukon-Tanana terrane, Yukon and Alaska; Tectonics, v. 11, p. 836–853.

Mortensen, J.K., Appel, V.L., and Hart, C.J.R., 2003. Geological and U-Pb age constraints on base and precious metal vein systems in the Mount Nansen area, eastern Dawson Range, Yukon; in Yukon Exploration and Geology 2002, (ed.) D.S. Emond and L.L. Lewis; Exploration and Geological Services Division, Yukon Region, Indian and Northern Affairs Canada, p. 165–174.

Mortensen, J.K., Hart, C.J.R., Tarswell, J., and Allan, M.M., 2016. U-Pb zircon age and Pb isotopic constraints on the age and origin of porphyry and epithermal vein mineralization in the eastern Dawson Range, Yukon; in Yukon Exploration Geology 2015, (ed.) K.E. MacFarlane and M.G. Nordling; Yukon Geological Survey, p. 165–185.

Renne, P.R., Mundil, R., Balco, G., Min, K. and Ludwig, K.R., 2010. Joint determination of 40K decay constants and $^{40}Ar*/^{40}K$ for the Fish Canyon sanidine standard, and improved accuracy for $^{40}Ar/^{39}Ar$ geochronology. Geochimica et Cosmochimica Acta, 74(18), 5349-5367.

Ryan, J.J., Zagorevski, A., Roots, C.F., and Joyce, N., 2014. Paleozoic tectonostratigraphy of the northern Stevenson Ridge area, Yukon; Geological Survey of Canada, Current Research 2014-4, 13 p. doi:10.4095/293924

Ryan, J.J., Westberg, E.E., Williams, S.P., and Chapman, J.B., 2016. Geology, Mount Nansen–Nisling River area, Yukon; Geological Survey of Canada, Canadian Geoscience Map 292 (preliminary), scale 1:100 000. doi:10.4095/298835

Ryan, J.J., Israel, S., Williams, S.P., Parsons, A.J., and Hayward, N, 2018. Geological Survey of Canada, Canadian Geoscience Map 376, 2018, 1 sheet, https://doi.org/10.4095/311301.

Schaen, A.J., Jicha, B.R., Hodges, K.V., Vermeesch, P., Stelten, M.E., Mercer, C.M., Phillips, D., Rivera, T.A., Jourdan, F., Matchan, E.L., Hemming, S.R., Morgan, L.E., Kelley, S.P., Cassata, W.S., Heizler, M.T., Vasconcelos, P.M., Benowitz, J.A., Koppers, A.A.P., Mark, D.F., Niespolo, E.M., Sprain, C.J., Hames, W.E., Kuiper, K.F., Turrin, B.D., Renne, P.R., Ross, J., Nomade, S., Guillou, H., Webb, L.E., Cohen, B.A., Calvert, A.T., Joyce, N., Ganerød, M., Wijbrans, J., Ishizuka, O., He, H., Ramirez, A., Pfänder, J.A., Lopez-Martínez, M., Qiu, H., and Singer, B.S. 2020. Interpreting and reporting $^{40}Ar/^{39}Ar$ geochronologic data. Geological Society of America Bulletin, doi: https://doi.org/10.1130/B35560.1

Steiger, R. and Jäger, E., 1977. Subcommission on geochronology: convention on the use of decay constants in geo-and cosmochronology. Earth and Planetary Science Letters, 36(3), 359-362.

Stern, R.A., 1997. The GSC Sensitive High Resolution Ion Microprobe (SHRIMP): analytical techniques of zircon U-Th-Pb age determinations and performance evaluation: in Radiogenic Age and Isotopic Studies, Report 10, Geological Survey of Canada, Current Research 1997-F, 1-31.

Stern, R.A., and Amelin, Y., 2003. Assessment of errors in SIMS zircon U-Pb geochronology using a natural zircon standard and NIST SRM 610 glass. Chemical Geology, 197, 111-146.

White, L.T., and Ireland, T.R., 2012. High-uranium matrix effect in zircon and its implications for SHRIMP U-Pb age determinations. Chemical Geology, 306-307, 78-91.